A compressed air cost savings identification model for deep-level mines

CJ Oosthuizen

orcid.org/0000-0001-6025-0157

Dissertation submitted in fulfilment of the requirements for the degree *Master of Engineering in Electric and Electronic Engineering* at the North-West University

Supervisor: Dr JF van Rensburg

Graduation ceremony: May 2019

Student number: 24576867

ABSTRACT

Title: A compressed air cost savings identification model for deep-level mines

Author: Christiaan Johannes Oosthuizen

Supervisor: Dr Johann van Rensburg

Degree: Master of Engineering (Electric and Electronic)

Keywords: Compressed air network, estimation model, cost-saving model, identification model, compressor power consumption, compressor power savings, compressed air benchmarking.

Eskom has requested a 15% electricity tariff increase over the next three years, which will put an increased burden on the South African mining sector. The cost of electricity directly influences the profitability of the mining industry. Energy efficiency and energy savings initiatives are becoming crucial, as many mines are implementing strategies to combat increasing electricity costs.

Compressed air systems are one of the top energy demand systems used by deep-level mines. These systems are also of the most inefficient systems. Therefore deep-level mines are driving awareness to optimise compressed air systems by implementing energy-savings initiatives, which require rigorous planning to launch and implement. Determining the scope for improvement on compressed air systems is also a complex and a time-consuming process which requires multiple personnel, capital and specialised equipment.

This study aims to develop a cost-saving identification model which will accurately predict the cost savings potential of a compressed air system on a deep level mine. Research regarding compressed air optimisation, management and demand predictions were conducted to establish a list of methods and tools to be used. No prediction methods were found which could accurately predict the power profile of a compressed air system using minimal input data. Multiple models were constructed to provide a possible solution to the problem using the tools found in research.

The models were constructed using statistical data from 29 deep level-mines scattered over South Africa. The data was used to evaluate the relationships between parameters used by previous researchers. The relationships were evaluated and used to construct a prediction model.

The cost savings identification model was validated by implementing it on two platinum mines in the Rustenburg area as case studies. Three months' data was used and averaged to evaluate the impact of the implemented initiatives. The estimation model used only the compressed air power baseline as input and produced optimised profile estimations which were 85% and 78% accurate respectively, compared to the actual measurements after optimisation. Due to the dynamic nature of the mining environment, some of the daily estimated results were 100% accurate. These accurate estimations proved that the developed model is capable of aiding in the management of compressed air projects by estimating the savings that can be achieved.

The use of the compressed air cost savings identification model decreased the total time to determine feasibility of compressed air energy savings initiatives by 86 weeks, using only two engineering personnel instead of eight. A potential of R 1.05 Million could also have been saved regarding personnel costs if the compressed air energy savings initiatives were not proven feasible.

The study aim and study objectives were successfully met while reducing the resources required by a deep-mine to identify the possible cost savings of a compressed air system.

ACKNOWLEDGEMENTS

Firstly, I would like to acknowledge the fact that all the elements that enabled me to complete this dissertation, were through the grace, love and sacrifice of Jesus Christ, the Name above all names. While this thesis is a representation of my journey towards the goal of a Master's in Engineering, I feel convicted to state that the much greater goal was to bring glory to the Son of God.

I would also like to thank the following people:

- Prof. E. H. Mathews and Prof. M. Kleingeld, who enabled me to grow in my pursuit of engineering excellence.
- Dr Johann van Rensburg, who assisted me in all the steps necessary for compiling this document.
- Dr Charl Cilliers and Dr Willem Schoeman, for their continued support and guidance.
- Dr Andries Nel and Dr Janco Vermeulen, for doing above and beyond that which is required as mentors and friends.
- A special thanks to my family and friends for their support and understanding during the write op of this dissertation. Without their continued support, I would not have been motivated to complete this study.

Finally, I would also like to thank TEMM International (Pty) Ltd and ETA Operations (Pty) Ltd, for the opportunity and assistance to complete this study.

TABLE OF CONTENTS

ABBREVIATIONS

Eskom	Electricity Supply Commission
DCC	Dynamic Compressor Controller
DCS	Dynamic Compressors Selector
DSM	Demand Side Management
DoE	South Africa's Department of Energy
ESCo	Energy Service Company
GDP	Gross Domestic Product
M&V	Measurement and Verification
POD	Point of Delivery
SCADA	Supervisory Control and Data Acquisition
TOU	Time of Use
IST	Integrators of Systems Technology
ERR	Energy Reduction Ratio
COLS	Corrected Ordinary Least Square
SFA	Stochastic Frontier Analysis
DEA	Data-envelopment Analysis

LIST OF EQUATIONS

LIST OF FIGURES

LIST OF TABLES

CHAPTER 1. INTRODUCTION & BACKGROUND

1.1 Challenges in the mining industry in South Africa

The South African mining industry is one of the largest import mineral producers of the global market[1], [2]. Underneath the surface, South Africa has the world's largest reserves of platinum, manganese, chrome and gold [1].

Although South Africa has vast mineral wealth, several socio-economic challenges have put the South African mining industry under severe pressure [1]. The most significant contributors are the increase in labour and electricity costs[2]. Figure 1 indicates that the price of electricity per kWh for the mining industry has increased by 403% over the last 12 years [3].

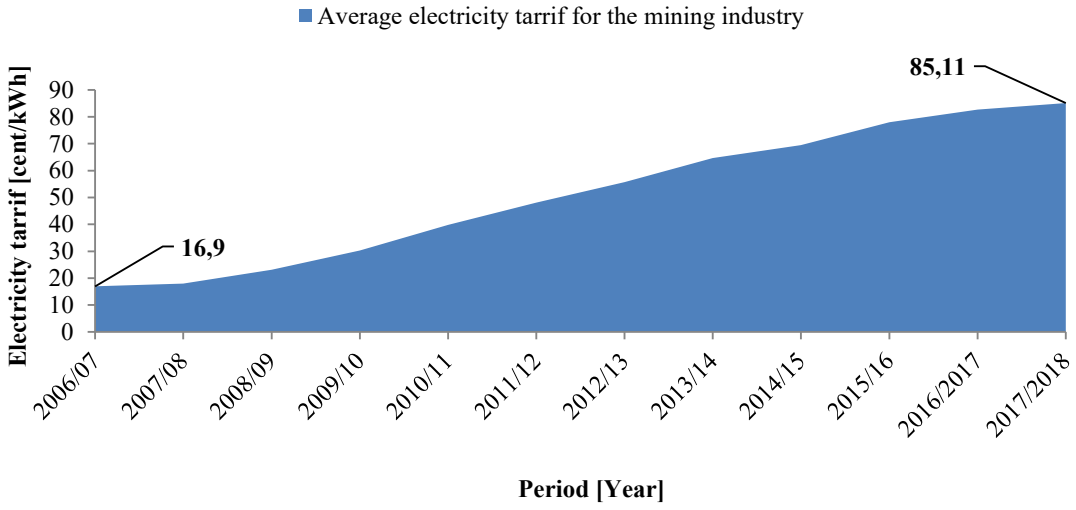

Figure 1 - Eskom power tariff increase

Mining operations in South Africa consume 14.3% of the national energy supply, with a usage of 30,559 GWh for the 2016/2017 financial year [4]. Due to this significant tariff increase, it is beneficial for mines to develop energy efficiency strategies [1].

Figure 2 compares the annual electricity tariff increase with the annual inflation rate. The electricity tariff increase percentage is much greater than the inflation rate percentage for each year from 2007 up until 2018 [5] .

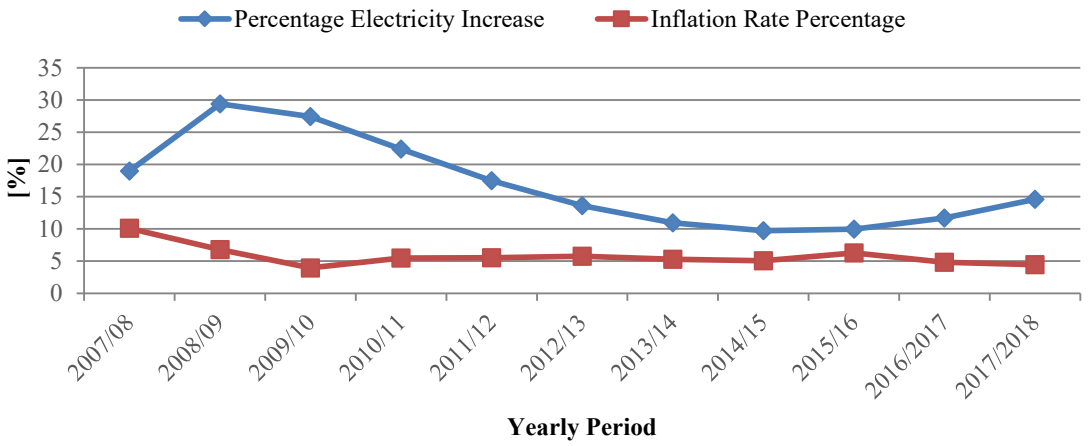

Figure 2 - Inflation vs electricity increase

1.2 Energy usage of mines in South Africa

The cost of energy, as well as the operational efficiency of mining systems, threaten the financial feasibility of the mining industry in South Africa. Utility costs such as electricity are one of the fastest growing expenditures increasing production costs of deep-level mines and contribute to 9% of total expenditure [6]. Figure 3 displays the expenditure breakdown of mines in South Africa.

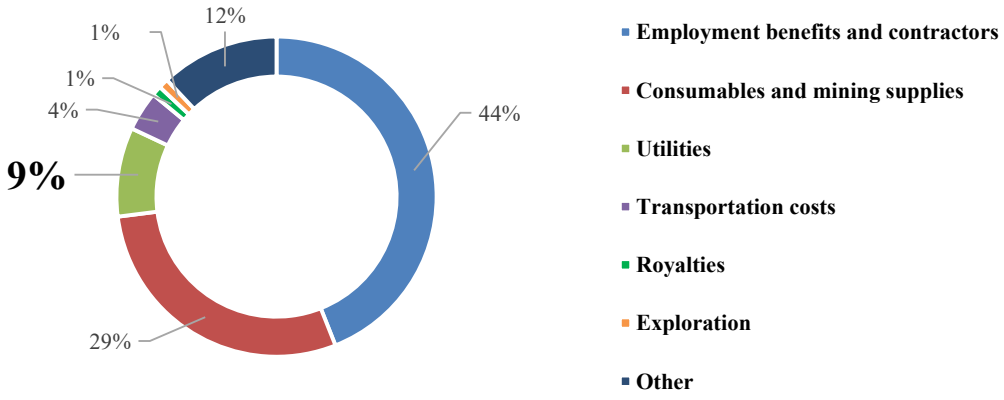

Figure 3 - Breakdown of total operating costs of mining in 2017 (adapted from [7])

Compressed air systems in South Africa and most European countries contribute an average of 10% of the total mining energy consumption [7], [8]. The energy breakdown of the South African mining sector, according to Eskom, shows that compressed air systems contribute 17% of mining energy expenses [9].

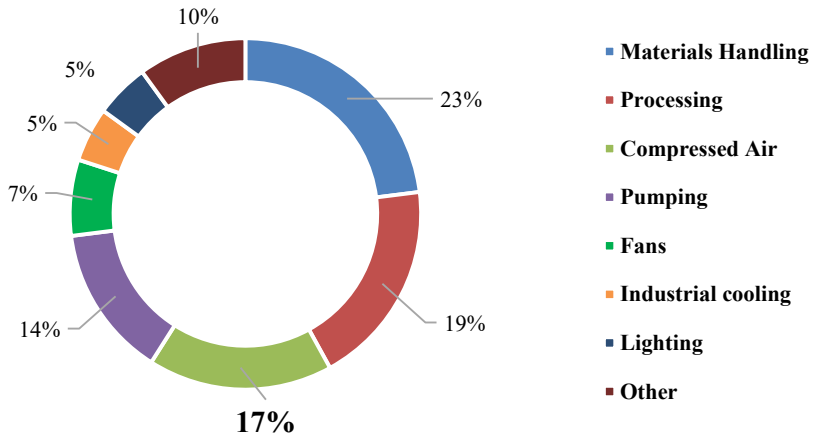

Figure 4 - Energy breakdown for mining services (adapted from [8])

Compressed air is used globally in mining due to its ease of use and relative safety, but this comes at the cost of increased energy losses compared to electricity distribution. Only 10-30% of the energy used to create compressed air reaches the consumer [8], [10],[11]. Not only are compressed air systems major energy consumers, but these systems are usually also inefficiently operated [10], [11],[12]. Therefore, energy efficiency and cost-saving initiatives require the attention of the mining industry by implementing and endorsing operational optimisation efforts.

1.3 Common compressed air practices on South African mines

1.3.1 Brief History

During the first decade of the 20th century, mining machinery was introduced to the Witwatersrand gold mining project, which required a vast amount of energy. As a result, one of the earliest mining compressed air networks in South Africa was developed by the Victoria Falls and Transvaal Power Company Limited (VFTPC), during 1906-1914 [13].

At present, mines in South Africa use compressed air on such a large scale that it is regarded as one of the top four mining utilities [14]. The use of compressed air as the energy supply to pneumatic tools has increased the ability of miners to extract, process and refine ore [14].

1.3.2 General mining compressed air systems

A mining compressed air ring consists of three operational sections [7], [15]:

1. Compressed air supply – compressed air generated by industrial compressors
2. Compressed air pipe networks – piping used to transport compressed air to surface and underground end users.
3. Compressed air consumers – mining equipment which uses compressed air.

Compressed air is mostly generated using statically mounted surface compressors, while pipes transport compressed air to underground consumers. Stationing static compressors on a surface separates it from the elements underground which could cause damage to the components of the compressor and the motor driving it. Enough clean and cold air for cooling the compressors down is available on the surface as opposed to underground, which avoids damage to the compressors and simplifies maintenance procedures [14].
Compressed air pipes vary in size between 150mm and 700mm in diameter, and are connected in segments to reach the point of delivery (POD) [7]. Pipelines can span over many kilometres, with some reaching 75 km [16]. At the end of the pipelines, multiple pneumatic machines are connected to the pipe segments.

The most common compressed air consumer equipment, located at mining shafts are loading boxes, Travis cars, butterfly valves, drills, dewatering pumps and pendulas [15]. Larger processing units like processing plants and mining workshops also require compressed air. These consumers are supplied with compressed air via surface pipelines [7].

Figure 5 displays a typical compressed air network seen from the surface. The distance is displayed in meters to indicate the span of the compressed air system, and the pipe diameter is displayed in NB (nominal bore), which is the equivalent of South African millimetres. The primary consumers, such as the shafts and concentrators, are indicated, while the supply compressors are located in respective compressor houses.

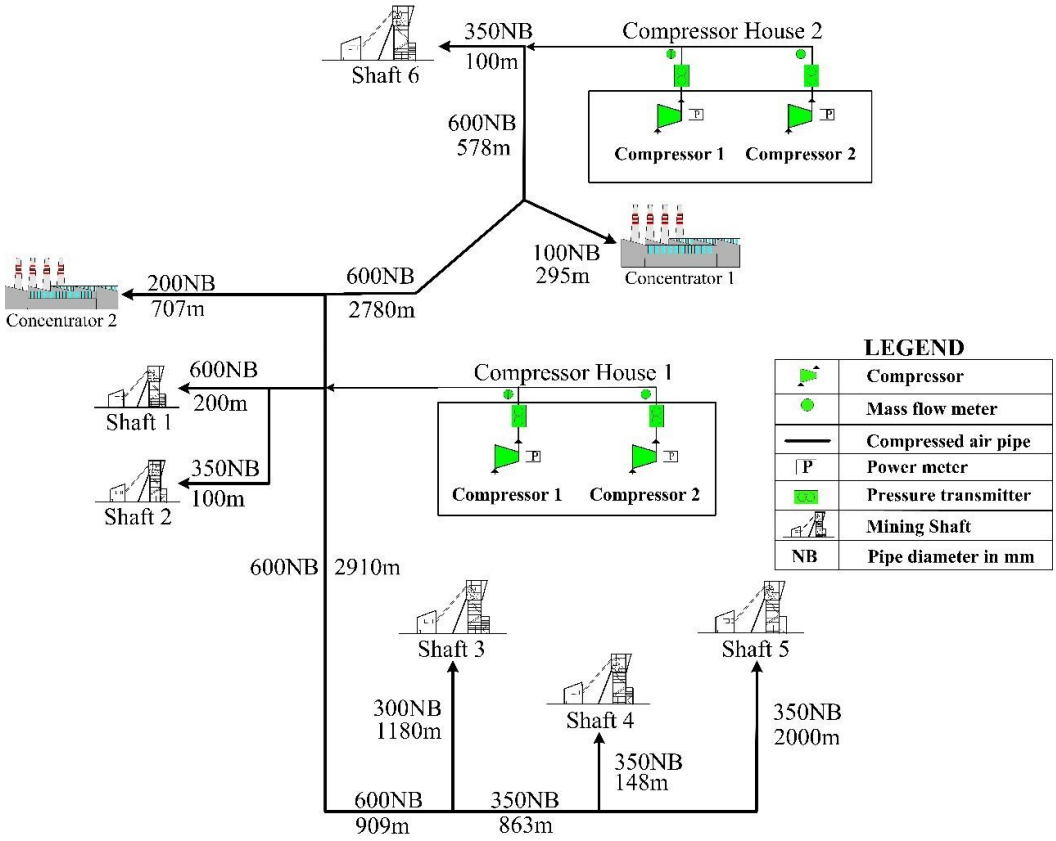

Figure 5 - Typical surface compressed air layout

Figure 6 displays a typical underground compressed air network. The supply compressors are situated on the surface, while the main compressed air pipe descends to below surface level.

Once underground, the main pipe splits into multiple branches of piping, which have a smaller diameter than the main pipe. The smaller branches of piping feed compressed air to the multiple working stations and equipment where compressed air end-users use pneumatic equipment for mining operations.

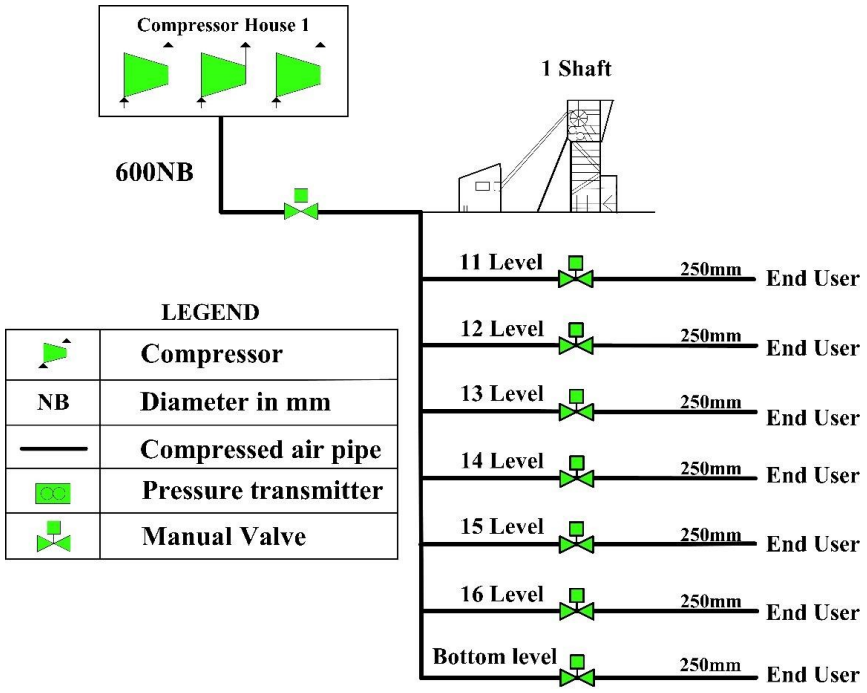

Figure 6 - Typical underground compressed air layout

1.3.3 Compressed air optimisation methods

Table 1 summarises the most common compressed air saving initiatives used by ESCo's in the mining industry (references supplied in Table 1). The initiatives in Table 1 are crucial in understanding the scope of this study.

The table gives a brief description of the initiatives and displays the complexity of the initiatives according to a South African Energy Savings Company (ESCo) survey summarised in Appendix A.

A survey was drafted and distributed at a company which boasts with more than 30 years of experience in energy optimisation, more than 100 consulting engineers, and a clientele that includes most of the South African gold and platinum mining industry.

An example survey is provided in Appendix A. The online platform Google Forms was used to construct and distribute the survey.

The survey was categorized into three sections. These three sections accumulate information to answer the questions :

- Who usually implements optimisation initiatives?
- How do they implement the optimisation initiatives?
- What resources do they use?

The qualification and experience of the individuals doing compressed air investigations greatly influences the cost of these investigations. According to PayScale.com an award winning international acclaimed big-data analysis company, the salary for an entry-level mechanical/project engineer is set at R 536 000.00 per annum. This increases by 59% for intermediate engineers, 126% for senior engineers and 150% for engineers more than 20 years of experience [17] .

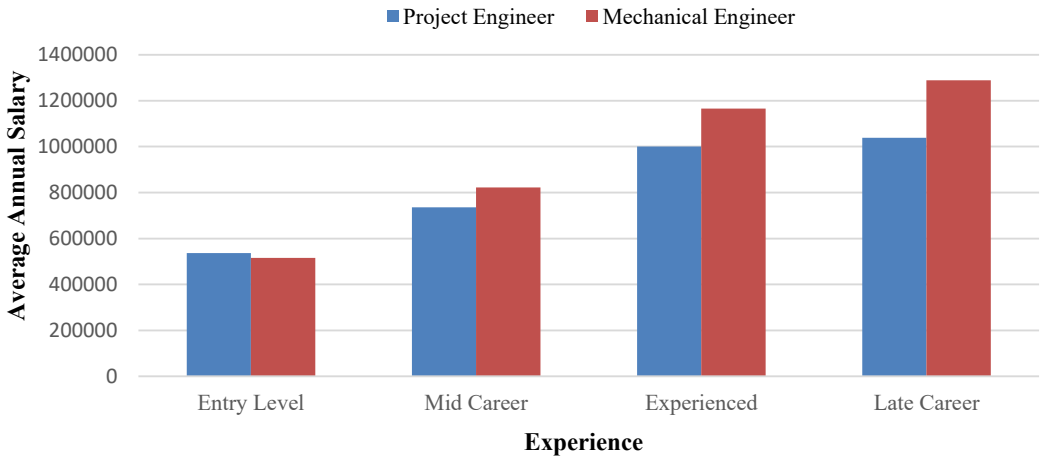

Figure 7 - Annual Salary

Section 2 of the survey contains questions regarding the resources used during projects conducted by the candidate in question. This sections is based on the methodology suggested by Joubert [18] . The third section is enquiring about the usage of the most common compressed air optimisation initiatives as presented in Table 1.

The purpose of these compressed air energy savings initiatives is to increase the efficiency of compressed air generation, distribution and implementation. By implementing these optimisation initiatives energy consumption of compressors can be reduced. This ensures that electrical and compressed air energy are not wasted while supplying equipment underground with the necessary energy.

Table 1 - Most common compressed air energy savings initiatives

Ref	**Initiatives**	**Description**	**Complexity**
[19]	Static Compressor Schedules	Create/update static compressor running schedules to ensure the most efficient compressors are operating at specific times.	5
[20]–[24], [25]	Dynamic Compressor Selection	Install control software which automatically uses the most efficient compressors at any given time to supply compressed air.	6
[26]	Manual Compressor Selection	Designated compressor operator controls compressor pressure setpoints and running statuses.	4
[21]	Master pressure setpoint reduction	Average pressure profile is used to control the total pressure of compressed air ring.	5
[27], [28], [29]	Leak Reduction	Repairs of damaged compressed air piping.	5
[30], [31]	Pipe Re-configuration	Reconfigure compressed air pipe segments to ensure less line losses.	6
[32]	Surface valve control	Control the pressure setpoint for each surface point of delivery (POD)/ shaft.	6
[21]	Peak-Clip Initiatives	Decrease pressure setpoints of compressed air control valves during ESKOM peak periods.	5
[19]	Stope-isolation valves	The closing of manual compressed air valves which connects the stopes to the main level pipelines.	5
[33]	Ring-feed clearance	Close ring feeds that bypass planned compressed air reticulation plans.	4
[34]	Close inactive sections	Close valves which lead to inactive mining sections.	4
[35]	Isolate compressed air components	Install dedicated compressors underground to isolate compressed air consumers from the main compressed air supply pipeline.	5

1.4 Resources required for compressed air investigations

Before a compressed air system can be optimised, a compressed air investigation needs to be conducted. Due to the multiple components and variables present in a compressed air network, investigations are resource-intensive. This section will focus on what resources are typically required during compressed air investigations.

1.4.1 Resource Survey results

A summary of the survey in Appendix A is shown in Table 2. The survey included a minimum and maximum table to display bandwidth of data. Eleven engineers took part in the survey ranging from 1 – 20+ years of experience. Collectively the survey group has more than 60 years of experience in compressed air systems while more than 165 compressed air investigations have been conducted.

Table 2 - Summary of ESCO survey results [Appendix A]

ESCO Action Item	**Required time [Weeks]**	**Required resources**	**Number of personnel**	**Complexity [0 - 10]**	**Project certainty [0 -10]**
Contact client	2 - 3	Senior Engineers	2 - 2	3 - 4	2
Obtain permission to investigate	1 - 4	Senior Engineers	2 - 2	3 - 5	3
Obtain data	2 - 7	Junior Engineers	2 - 3	4 - 6	4
Compressed air audits	5 - 15	Multiple Engineers	4 - 6	5 - 7	6
Simulate	6 - 9	Multiple Engineers	2 - 2	7 - 8	7
Determine Feasibility	2 - 3	Project Engineers	2 - 3	5 - 7	8
Compile Findings Report	2 - 3	Project Engineers	2 - 2	4 - 5	8
Compile Project Proposal	2 - 3	Project Engineers	2 - 2	5 - 6	8
Client Sign Off on Project Proposal	2 - 4	Senior Engineers	1 - 2	5 - 7	10
Total	**24-51**	**Multiple Senior and Junior Personnel**	**1-6**	**3-8**	**2-10**

From the 24-51 weeks that a typical air investigation takes to be completed, as indicated by Table 2, 13-31 weeks are spent on simulations and compressed air audits. This is more than half of the time spent on the entire project investigation. These audits and simulations increase the project certainty from a 4 to a 7 out of 10.

Data acquisition, audits and simulations are a crucial part of implementing compressed air saving initiatives, but also aid in understanding what impact these initiatives will have on compressed air systems.

Figure 8 displays the typical time breakdown for the compressed air investigations. If the information gathered from the compressed air audits and simulations can be determined at the beginning of the process, significant time can be saved. This can lead to better management of the compressed air optimisation initiatives.

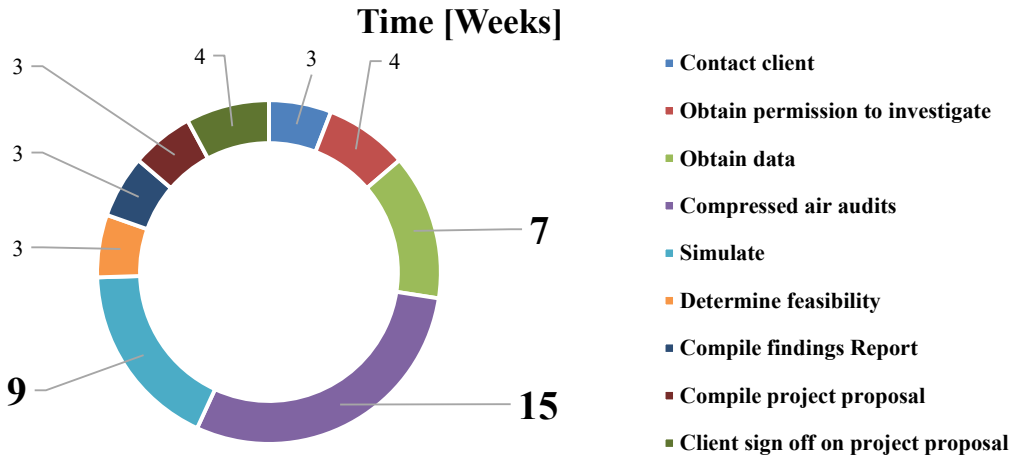

Figure 8 - Compressed air investigation time distribution [Appendix A]

1.5 Problem statement

Eskom's tariffs have increased by 403% over the last 12 years. This puts a lot of pressure on industries to reduce their energy consumption in order to save costs. Compressed air networks have been identified as a significant energy consumer in the mining sector. Therefore, the energy consumption of mining operations can possibly be reduced by optimising their compressed air networks [10][12]. Numerous studies have been done regarding strategies to improve compressed air systems. However, the identification and implementation of these strategies take a significant amount of time and engineering resources.

1.6 Need for study

A need exists to reduce resources used to identify feasible energy savings initiatives on compressed air systems.

Third-party investigators, focussing on energy saving initiatives have the greatest need for this study. An effective method of assessing feasiblity of energy-savings initiatives without the need of detailed investigation would possibly save time, fast-tracking feasible initiatives. The increased incentive to optimise energy consumers, and the vast amount of time that it takes to do the relevant investigations, are the most significant contributors to the identified need.

1.7 Study aim and objectives

The primary objective of this study is to investigate the feasibility of a cost-saving identification model to determine the cost-saving potential of a mine's compressed air system before any initiatives have been implemented. This will be done by developing a model to determine the cost-saving possibility of deep-level gold and platinum mines. The primary objective will be met by achieving the following objectives:

1. Complete research on compressed air power profiles, operating schedules and compressed air management techniques.
2. Developing a cost-saving identification model which aims to:
    - Decrease the time required to obtain the energy saving potential of a compressed air system at a deep-level mine
    - Achieve accurate predictions compared to calibrated simulations
    - Decrease the resources required to determine the energy saving potential of a compressed air system at a deep-level mine
    - Provide an acceptable level of certainty to ensure energy savings can be realised
    - Provide a benchmark for mines to determine the efficiency of their compressed air systems
3. Verify the cost-saving identification model by applying it to actual case studies.

1.8 Study overview

Chapter 1 provides a brief background on the current challenges that the national mining sector is facing. Mining compressed air networks, and the limitations of previous studies are also briefly discussed. Finally, the problem statement and deliverables are formulated and discussed.

Chapter 2 investigates the previous research conducted on compressed air benchmarking, compressed air investigation procedures, prediction tools and statistical methods of developing a prediction model.

Chapter 3 develops a proposed cost-saving identification model by implementing the necessary techniques and lessons learned from the literature study in chapter 2. The proposed model will take inputs such as the existing compressed air power baselines of a given mining business unit (shaft) and produce a potential compressed air power profile. This new power profile can be achieved after successful implementation of the most compressed air energy saving initiatives.

Chapter 4 displays the results of applying the cost-saving identification model to two different platinum business units. The results of the cost savings identification model are validated by actual recorded results and calibrated simulations.

Chapter 5 concludes the study by summarising the method used to predict the cost saving potential of compressed air optimisation initiatives, and the accuracy thereof. This chapter also states how the objectives of the study were met. Future recommendations for further studies are stated, as well as some errors that should be avoided.

CHAPTER 2. LITERATURE REVIEW OF COMPRESSED AIR ESTIMATION METHODS

2.1 Preamble

Chapter 2 is divided into four major sections. The first section displays the complexity of compressed air systems. The second section describes the contribution of previous researchers in predicting energy savings on compressed air systems. The third section describes the specific methods and tools that previous researchers have implemented to estimate energy savings on compressed air networks. The final section describes the M&V (Measurement and Verification) process and how it can be used in future studies.

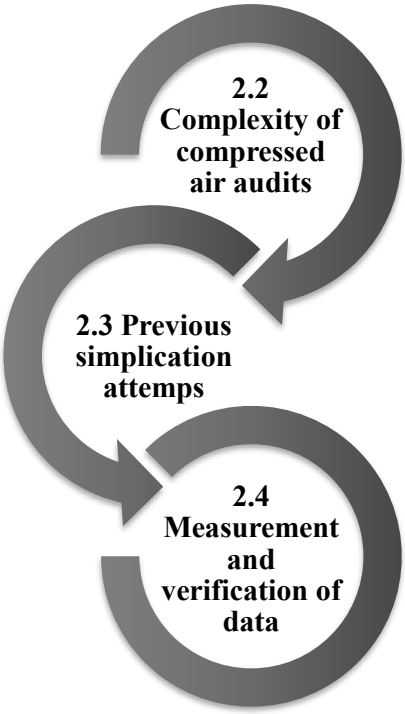

Figure 9 - Chapter 2 literature review process

A simplified compressed air network is shown in Figure 10 as an introduction to the first section of this chapter. It will aid in interpreting other figures later in the document. Compressed air networks consist of multiple components and sectors that can be divided into sub-categories such as supply, distribution and consumers (demand)[30], [36]. The supply is the primary reference point of any compressed air system. Therefore, the compressors are investigated first.

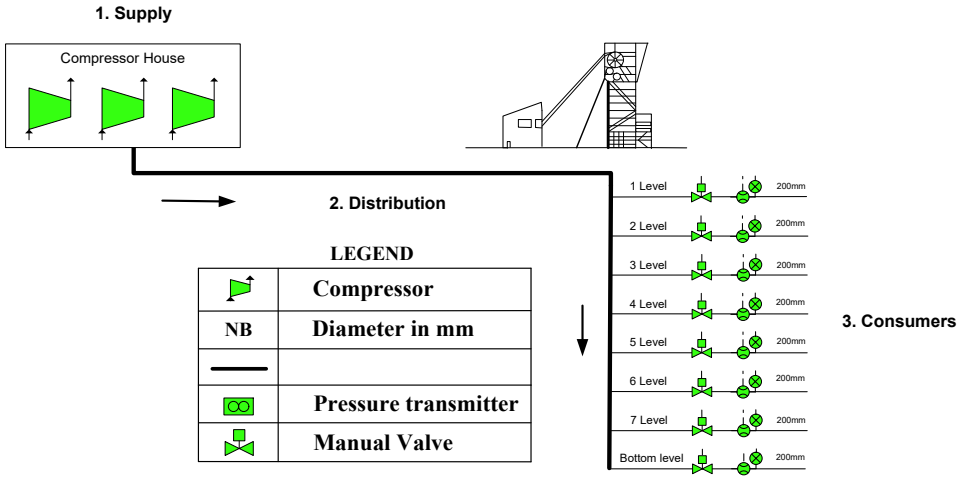

Figure 10 - Simplified compressed air network categories

2.2 The complexity of compressed air audits

2.2.1 Compressed air supply variables

The aim of compressed air investigations it to determine where the generated compressed air is distributed to, how effectively it is distributed, what impact it has on the mining process, etc. A detailed compressed air investigation helps to establish the cost of compressed air at the end at user-level. The cost of compressed air is determined by the amount of power that a compressor consumes to generate the necessary volume and pressure of compressed air.

Bredendkamp [30], Jonker [21] and Van Heerden [22], [37] conducted compressed air and compressor analysis studies on multiple mines and compressed air networks, which suggested that there are multiple compressor types that consist of two main groups: continuous and intermittent flow compressors [22], [38],[39]. Due to the compressed air configurations of deep-level mines, most gold and platinum mines use centrifugal compressors. Figure 11 displays the categorisation of compressor types.

This breakdown shows the diversity of compressors, as well as the diverse set of techniques required to characterise compressors on compressed air networks.

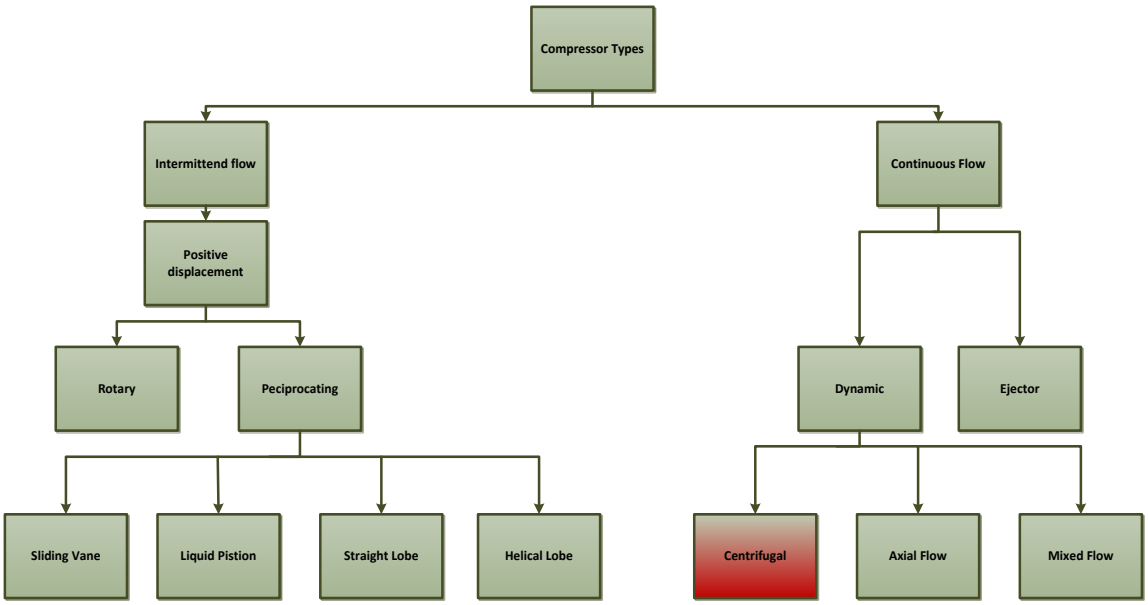

Figure 11 - Typical compressor types (Adapted from [21])

Figure 12 shows the simplified functioning of a typical centrifugal compressor. The atmospheric air is sucked in at the inlet pipe, controlled by the guide vane. The impeller of the compressor then forces the available air into the next stage(s) contained in the compressor housing. The increased compressed air is discharged through the discharge pipe [39]. The inlet guide vane angle is also an active parameter in the performance of centrifugal compressors[40].

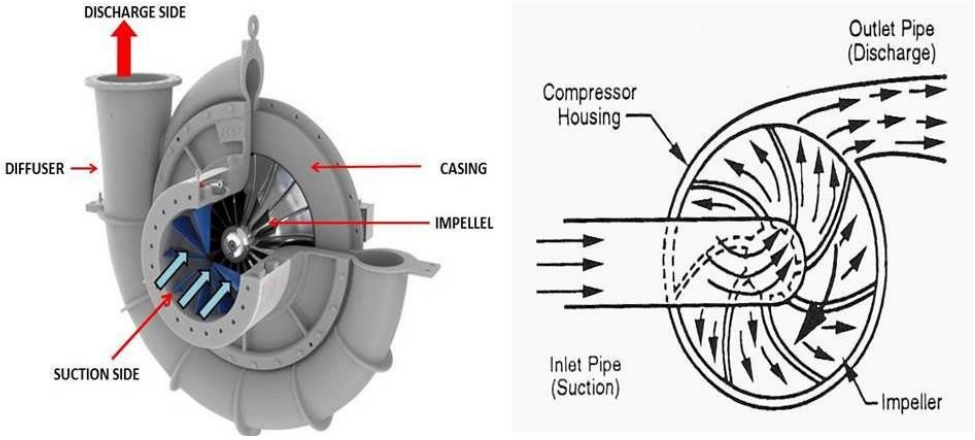

Figure 12 - Centrifugal compressor simplified operation diagram[1]

[1] M. Bairwa, 'Centrifugal Compressor: Principle, Construction, Working, Types, Advantages, Disadvantages with its Application', 2017. Available: http://www.mech4study.com/2017/11/centrifugal-compressor.html. [Accessed: 11-Oct-2018].

Bredenkamp[30] conducted a study regarding the reconfiguration of compressors in mining compressed air systems, while Jonker [21] conducted a study regarding how to control compressors efficiently during dynamic demand conditions. Bredenkamp and Jonker described the dynamic variables that influence the power consumption of a compressor. These variables are displayed in Equation 1 and Equation 2, which are later used in the construction of the simulations which verify the results in chapter 4.

Equation 1 and 2 show the different variables that influence the performance ability of compressors. Bredenkamp noted in his study that multiple compressors are put in place to supply compressed air rings. Jonker described how the interaction between the independent and dependent variables in a compressed air ring become more complicated with the addition of multiple compressors with various characteristics.

Equation 1 –Theoretical required the electrical energy of a compressor

$$\mathbf{P_{Comp}} = \dot{m}_{air} W_{comp}$$

$\mathbf{P_{comp}}$	= Required electrical power	[kW], [kJ/s]
$\dot{m}$	= Mass flow	[kg/s]
W_{comp}	= Compressor mechanical energy	[kJ/kg]

Equation 2 - Theoretical required mechanical energy of a compressor

$$\mathbf{W_{comp}} = \frac{nRT_{in}\left(\left(\frac{p_{out}}{p_{in}}\right)^{\frac{n-1}{n}} - 1\right)}{\eta_{comp}(n-1)}$$

$\mathbf{W_{comp}}$	= Compressor mechanical energy	[kJ/kg]
R	= Gas constant for air taken as 0.278	[J/kg•K]
T_{in}	= Inlet air temperature	[K]
p_{out}	= Compressor discharge pressure	[kPa]
p_{in}	= Atmospheric inlet pressure	[kPa]
n	= Polytropic constant for isentropic compression taken as 1.4	[-]
η_{comp}	= Compressor efficiency	[-]

Heyns [31] discussed the compressed air ring-feed system, indicating that multiple compressors can be connected to a centralised compressed air piping network, as shown in Figure 5 at section 1.3.2. Centralising compressors increases the complexity of determining operational inefficiencies within the ring, as well as individual compressors.

It is evident that on the supply side of a compressed air network, the investigation of all these variables can become a complex and time-consuming process, especially if the infrastructure is outdated or not installed.

2.2.2 Compressed air distribution network parameters

Multiple factors contribute to the characteristics of compressed air-flow throughout distribution piping. The age and condition of piping, as well as the relative moisture in the compressed air systems, pipe friction and turbulence can lead to increased compressed air distribution inefficacies [41], [42], [35]. The degradation of a pipe (due to time and multiple other conditions) can lead to an increased pressure drop due to a change in the pipe friction coefficient. Figure 13 displays the standard compressed air distribution pipes, as well as an inspection of the pipe wall.

Figure 13 - Standard galvanised compressed air distribution pipes[2]

[2] C.J Oosthuizen, Personal photograph. “Compressed air pipes”, Marikana, 2018.

The pressure drop of a compressed air distribution pipe can be determined by the Darcy-Weisbach equation [41], [30], [21]. Equation 3, Equation 4 and Equation 5 illustrate the parameters used to determine compressed air losses over distribution lines.

The simulation software will use the equations in Chapter 4 and aid in showing the complexity of compressed air distribution investigations.

Equation 3 - Darcy-Weisbach pressure loss in compressed air distribution

$$\mathbf{\Delta P} = \frac{f\rho LQ^2}{82.76D^5}$$

$\Delta\mathbf{P}$	= Pressure loss	[kPa]
f	= Friction factor	[-]
ρ	= Density of compressed air	[kg/m^3]
L	= Pipe Length	[m]
Q	= Volume flow rate	[m^3/s]
D	= Inside diameter of pipe	[m]

To determine the friction, the flow characteristic factors of the compressed air must also be considered. In 2012, Joubert et al. [35] stated that airflow could be assumed as turbulent due to high flow and airspeeds. Van Heerden [22] and Bredenkamp [7] used the Reynolds number to determine the friction factor of turbulent compressed air flows.

Equation 4 - Reynolds number calculation

$$\mathbf{Re} = \frac{\rho vD}{\mu}$$

Re	= Reynolds number	[-]
ρ	= Density of compressed air	[kg/m^3]
v	= Airflow velocity	[m/s]
D	= Inside diameter of pipe	[m]
μ	= Dynamic viscosity of air	[kg/m·s]

Once the Reynolds number has been determined, the Colebrook-White friction factor can be determined.

Equation 5 - Colebrook - White friction factor

$$\frac{1}{f} = -2\log_{10}\left(\frac{e}{3.7D} + \frac{2.51}{Re\sqrt{f}}\right)$$

f	= Friction factor	[-]
Re	= Reynolds number	[-]
e	= Pipe roughness	[m]
D	= Inside diameter of pipe	[m]

Distribution losses also include compressed air leaks along the distribution piping. Bredenkamp's thesis states that deep-level gold mine distribution networks can span 40 km [30], [43]. This increases the time and effort that mining personnel and ESCO's need to spend auditing compressed air distribution lines effectively.

Bredenkamp also states that water and compressed air leaks can account for up to 50% of compressed air usage [43], [9]. The U.S Department of Energy's advanced manufacturing office stated that 20 – 30% of compressed air losses could be a result of air leaks in distribution lines [44].

Locating compressed air leaks and quantifying the effect of compressed air leaks is a resource-intensive task. Some mine compressed air systems lack suitable compressed air measurement infrastructure and accurate equipment, which makes it difficult for even known leak-quantification methods. A lack of measuring points contributes to the inefficiency of quantifying the compressed air leaks.

Due to the tedious task of compressed air leak identification, new methods to identify leaks are continually being developed [45]. These methods are not error-proof, as even ultrasonic leak quantification proves problematic on steel pipes due to the noise levels caused by the shape of the orifices [45]. The result is that compressed air line losses are tedious to locate and difficult to quantify, even with modern technologies.

2.2.3 Demand-side variables

The demand side of the compressed air network consists mainly of underground levels where mining activities are taking place. Figure 14 and Table 3 mention the typical underground compressed air users in a simplified schematic [7], [14], [21], [22], [46]. The variety of equipment, components and piping configurations that are found underground dramatically increase the complexity of the compressed audits. The audits of the compressed air distribution lines underground are conducted similarly to on surface, stated in section 2.2.2. Therefore, similar challenges are also faced. Figure 14 shows an underground compressed air consumer and where it is typically located in the mining level.

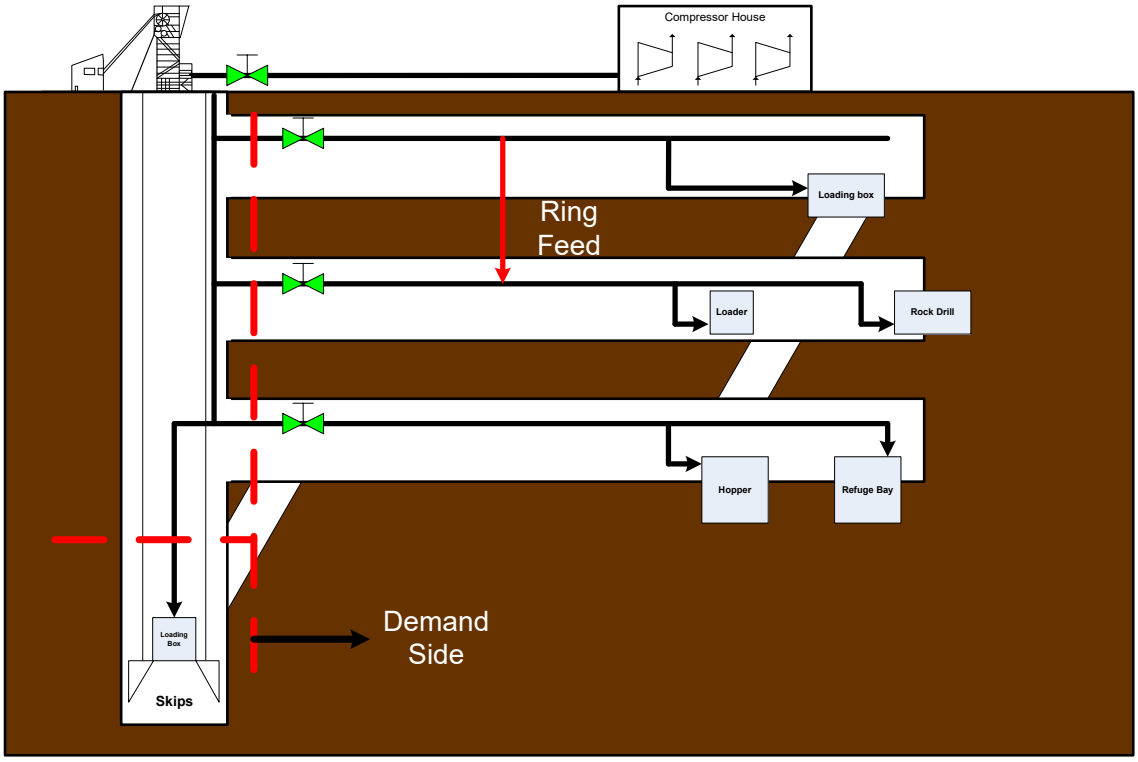

Figure 14 - Underground compressed air users (Adapted from [31])

Table 3 summarises the function of the compressed air users in Figure 14 and describes the typical periods that the consumers are active and what the normal compressed air operating requirements are. These parameters are essential for understanding compressed air energy saving initiatives. Infrastructure restrictions and schedules are key factors used to optimise compressed air systems, but can also act as limitations [21], [36].

Table 3 - Underground compressed air consumers (Adapted from [6])

Item	Mining Application	Normalized Operating Hours	Flow Requirement [m^3/s]	Pressure Requirement [kPa]
Rock Breakers	Reduces the size of rock segments	00:00-24:00	0.28	450
Rock Drills	Produces blasting holes for explosives	09:00-15:00	0.06-0.42	400-620
Diamond Drills	Development on active levels	00:00-24:00	0.14	500
Pneumatic cylinders	Opens doors and chutes throughout the mine	00:00-24:00	0.0006-0.14	350-600
Loading Boxes	Transfer accumulated ore to skips	00:00-24:00	0.0006-0.14	350-600
Mechanical Loaders	Transport ore to loading boxes	00:00-24:00	0.12-0.3	450-860
Water Agitators	Agitation of water dams	00:00-24:00	0.47	400
Venturi Blowers	Aids in cooling active areas	00:00-24:00	0.019-0.091	350-620
Open-ended Pipes	Cleaning active areas / wasted air	09:00-15:00	0.2-1.6	100-650
Valve Control Actuators	Opens and closes valves	00:00-24:00	Negligible	350-600

To better understand how the schedules of different consumers impact the compressed air supply, Heyns [31] has summarised the daily operations schedule into five distinct periods, as shown in Figure 15. Although a mining schedule can be determined by the ventilation officer on the specific shaft, multiple factors cause different levels of mine to deviate from the proposed schedule.

Figure 15 displays the typical flow demand profile of a compressed air system. The timeline is broken into five periods, which indicate what the major mining activities are during that period. Drilling shift is the period where the most compressed air is consumed due to many compressed air drills that are operated throughout the mine at the same time [30],[22], [37].

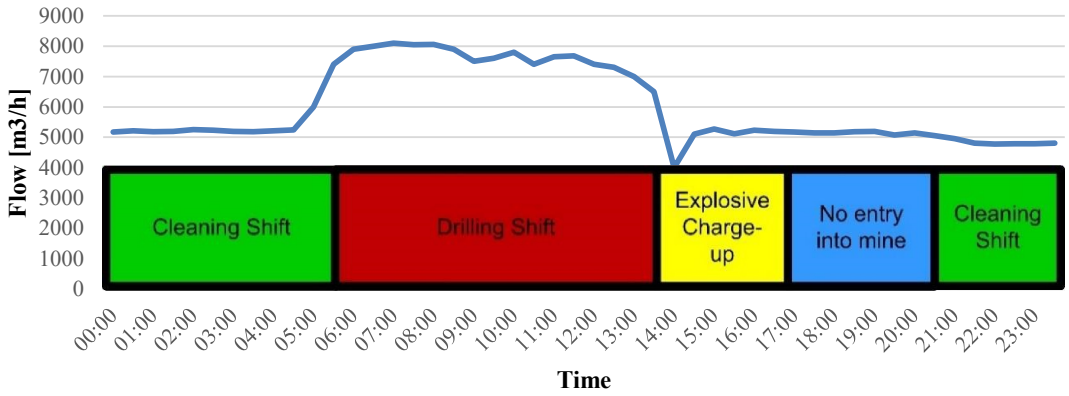

Figure 15 - Daily summarised mining schedule (Adapted from [22])

Specific levels may have different profiles other than the profile in Figure 15. Different schedules combined with multiple ring feeds cause micro-anomalies during level-specific compressed air audits. These ring feeds are compressed air connections that link multiple levels, usually downstream of the level-specific flow and pressure instrumentation and produces flow measurements shown in Figure 16. A non-typical profile is displayed in blue. Such occurrences increase the effort and skill level required to complete compressed air investigations.

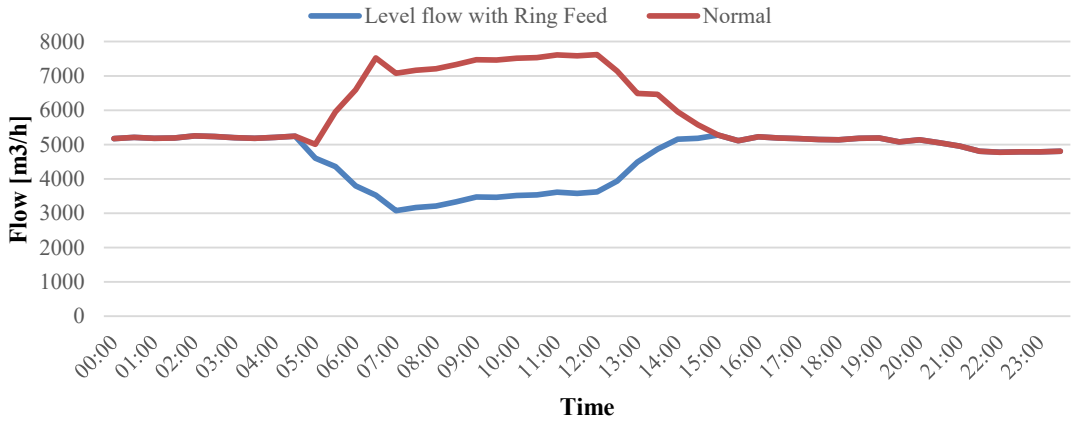

Figure 16 - Level flow during ring-feed

The discussion on the complexity of compressed air audits underground concludes the literature review regarding compressed air networks, audits and the variables used to calculate compressed air consumption. The next section will discuss how previous researchers have attempted to decrease the time required for air audits to be completed, but also to estimate and predict energy consumption of mining utilities.

2.3 Previous simplification attempts

2.3.1 Preamble

Due to the complexity of compressed air systems and the dynamic design of different compressed air rings as discussed in section 2.2, multiple methods for fast-tracking audits and predicting and calculating compressed air savings have been developed. This section is divided into four categories of previous studies which present the successes and failures to verify the need for estimating the scope of compressed air energy saving initiatives.

2.3.2 Studies on optimisation of compressed air auditing processes

Energy Audits - Abdelaziz, 2011 [47]

Abdelaziz developed a methodology for a typical air audit used to create a model of a compressed air system. Abdelaziz states that there are three types of energy audits – preliminary, general and detailed. The general audit expands from the preliminary audit and takes historic data into account. The detailed audit further expands on the general audit by developing a model for energy characteristics which is calibrated with actual utility data.

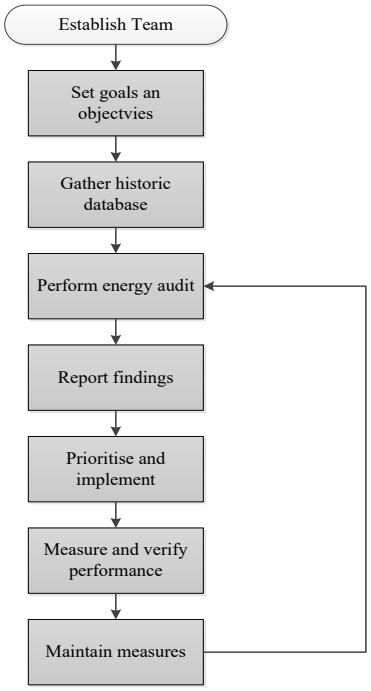

Figure 17 - Preliminary audit methodology (adapted from [14])

ESCo Compressed Air Investigation Methodology - Joubert, 2012 [35]

Joubert developed an improved methodology to determine the compressed air savings opportunity for a specific compressed air system.

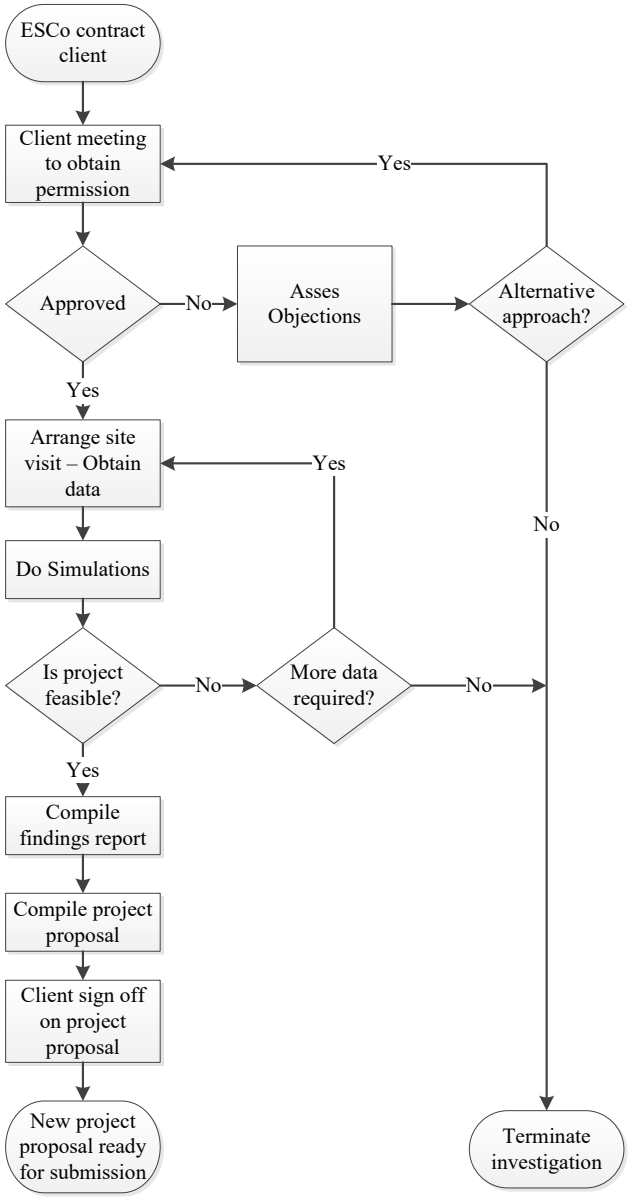

Figure 18 - Compressed air investigation procedure (adapted from [18])

Figure 16 indicates that there are multiple complex functions that need to be completed before the feasibility of a compressed air optimisation project can be determined. The optimisation of the compressed air investigation protocol reduces the time expenditure of compressed air audits but does not address the issue of mines/systems which may lack infrastructure or data. Additional studies need to be consulted.

2.3.3 Studies on energy prediction and scope identification

Rule of Thumb - Marais, 2012 [36]

Marais developed a simplified estimation model which predicts the change in power used to generate compressed air flow by looking at the change in absolute pressure of the compressed air system. The model suggests that for every X% change in absolute system pressure, there will be a 1.6X% – 1.8X% change in compressor power consumption.

This model was derived by using theoretical calculations, as well as practical measurements used after optimisation methods have been implemented. Although the model predicts the change in power consumed, a predicted change in pressure is required.

A model is required which will estimate the power decrease without the need to first conduct an investigation. The rule of thumb suggested by Marias requires an estimated pressure decrease, which will only be obtained after a complete compressed air investigation.

Artificial Neural Networks - Cox, 2013 [48]

In 2013, Cox developed an artificial neural network to help predict the electricity consumption of deep-level mines based on monthly electricity data extracted from ESKOM bills. The neural network used 48 (monthly) data points to calibrate the prediction algorithm. Monthly results were produced which were within a 10% error range.

Historical data forms a crucial part of the site-specific model, which might pose a problem for mines with insufficient instrumentation or data storage systems. The prediction model is also limited to the overall electricity expenditure and was not tested on subsystems such as compressed air. The complexity of sub-systems such as compressed air was discussed in section 2.2.

Benchmarking - Cilliers, 2016 [41]

In 2016, Cilliers developed a mathematical benchmarking model for determining the efficiency of large energy usage systems on deep-level mines. One of the contributions in the PhD thesis was a best-practice benchmarking method for compressed air systems. The efficiency of the compressed air system required the depth of a specific mining shaft and the tonnes of ore mined by that shaft.

Equation 6 - Best practice compressed air benchmarking model (Winter)

$$E_{bp_{comp}} = -1507.45+1.51(Z)+33.36(T)$$

Equation 7 - Best practice compressed air benchmarking model (Summer)

$$E_{bp_{comp}} = 737.21+1.31(Z)+30.33(T)$$

$E_{bp_{comp}}$	= Best practice benchmark for compressed air energy consumption	[MWh]
Z	= Mine Depth	[m]
T	= Kilo tonnes of ore mined	[kT]

In the development of benchmarking techniques, Cilliers used multiple statistical methods to equate benchmark parameters, which are summarised in Table 4

Table 4 - Cilliers' regression methods summary [49]–[52]

Statistical Regression Method	**Appendix Reference**	**Purpose**
Standard regression models (R^2)	C.2	Determine best-fit regression of any order polynomials
Ordinary least square regression (OLS)	C.3	Determine best fit linear regression line.
Corrected ordinary least square (COLS)	C.4	Determine minimum and maximum regression boundaries
Stochastic frontier analysis (SFA)	C.5	Determine most probable occurrence of random data
Data envelopment analysis (DEA)	C.6	Dynamic regression line constructed for special purposes.

Using Cilliers' model, the scope for compressed air optimisation can be determined by looking at the mining output variables. The restriction with this model is that it only benchmarks the total power consumption of compressed air systems over a period (day, month, year), and doesn't provide an hourly power profile benchmark.

An hourly power profile is considered essential for ESCo's and energy saving initiatives because it allows for optimisation of systems during specific times.

This section 2.3.3 attempts to address the need for an estimation model with a variety of innovative calculations and benchmarking, but these methods require high-level data and produce high-level results such as monthly or yearly estimation. Low-level or daily/hourly estimations are required to realise the full potential of energy-saving initiatives.

2.3.4 A specific study on 24-hour profiles

This section discusses the results from a study that attempted to estimate the performance of a particular period within a 24-hour day. This study focuses on a unique statistical method to potentially predict the effect of compressed air saving initiatives on the energy consumption profile of compressors.

A practical tool for quantifying potential energy savings - Vermeulen, 2018 [53]

Vermeulen developed multiple tools to determine the expected power savings on compressed air systems during a specific period. These tools are based on the concept of the Energy Reduction Ratio (ERR). The Energy Reduction Ratio is the relationship between the peak power usage recorded by the compressed air system (red) and the power usage of the system at any other given time (green), as seen in Equation 8.

Equation 8 –Energy Reduction Ratio

$$\mathbf{ERR_i} = 1 - \left(P_{no\text{-}Peak_i} / P_{Peak} \right)$$

$\mathbf{ERR_i}$	= i^{th} Energy reduction ratio of a 24-hour profile	[-]
P_{peak}	= Maximum / reference period in a 24-hour profile	[kW]
$P_{non\text{-}peak_i}$	= i^{th} non-peak power in a 24-hour profile	[kW]
i	= Airflow velocity	[-]

Figure 19 shows an example of a mine's compressed air power consumption profile before energy-saving initiatives have been implemented. It also shows what parameters are used in Equation 8.

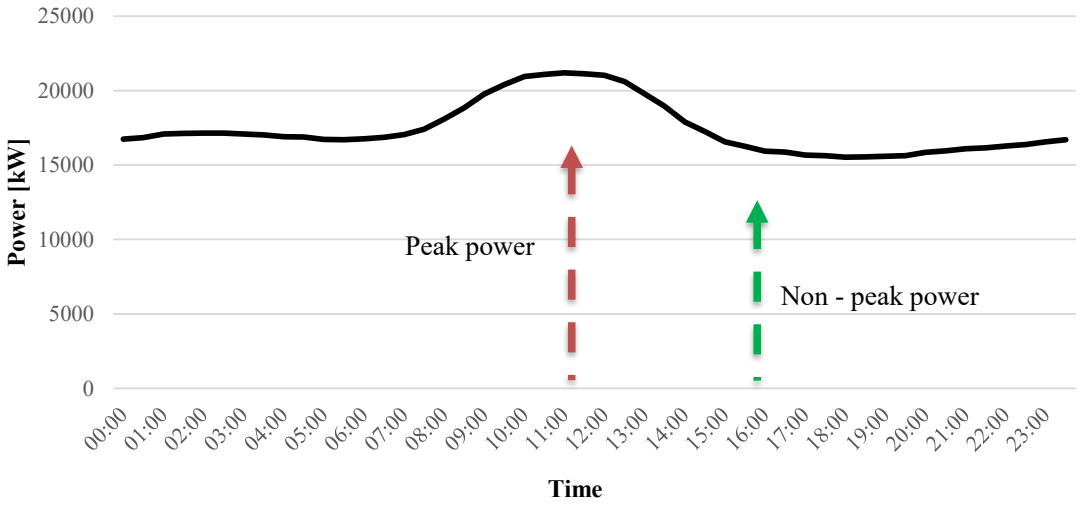

Figure 19 - Typical power baseline for deep-level mines

Figure 20 displays the ERR of the example mine's compressed air system's power profile after energy saving initiatives have been implemented.

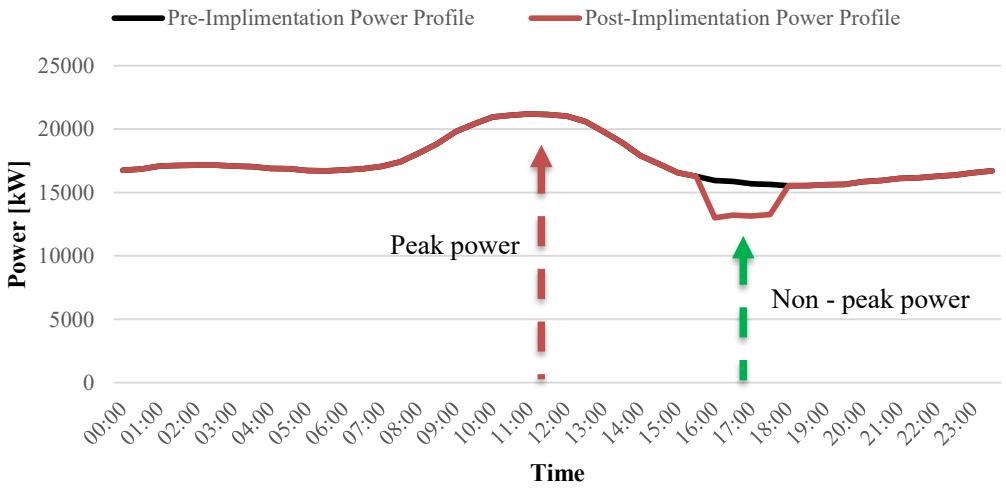

Figure 20 - Pre-ERR vs post-ERR power profiles

Vermeulen discovered that a linear relationship exists between the ERR of mines before and after energy saving initiatives were implemented.

Using this relation, Vermeulen constructed a prediction model which predicted the potential success of energy-saving initiatives during the 16:00-18:00 blasting period.

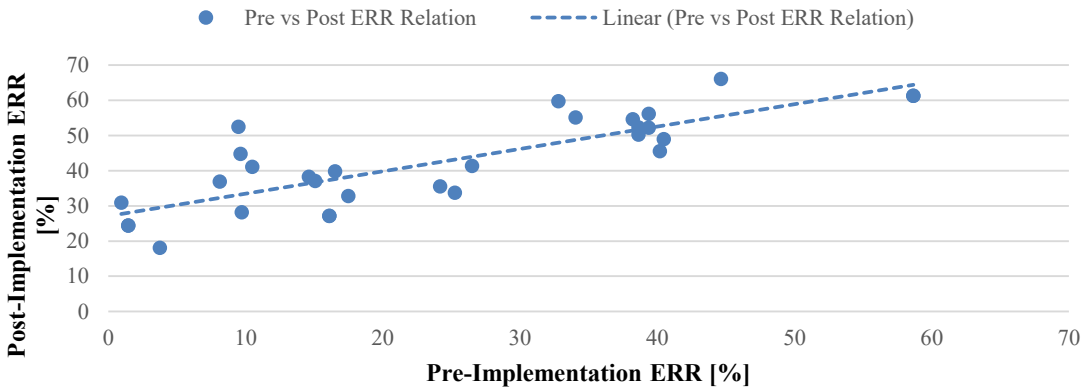

Figure 21 – Pre vs post- ERR datasets

After determining the relation between the pre-implementation ERR and post-implementation ERR, Vermeulen categorised the relational dataset to indicate which ERR relations yielded the most promise/gain from energy saving initiatives. Vermeulen found that mines with a lower pre-implementation ERR had a broader scope for energy-saving initiatives than mines with a higher pre-implementation ERR relationship. Figure 22 displays the pre- and post-implementation ERR relations arranged from low pre-ERR to high pre-ERR value. This indicates a decrease in the impact of energy saving initiatives.

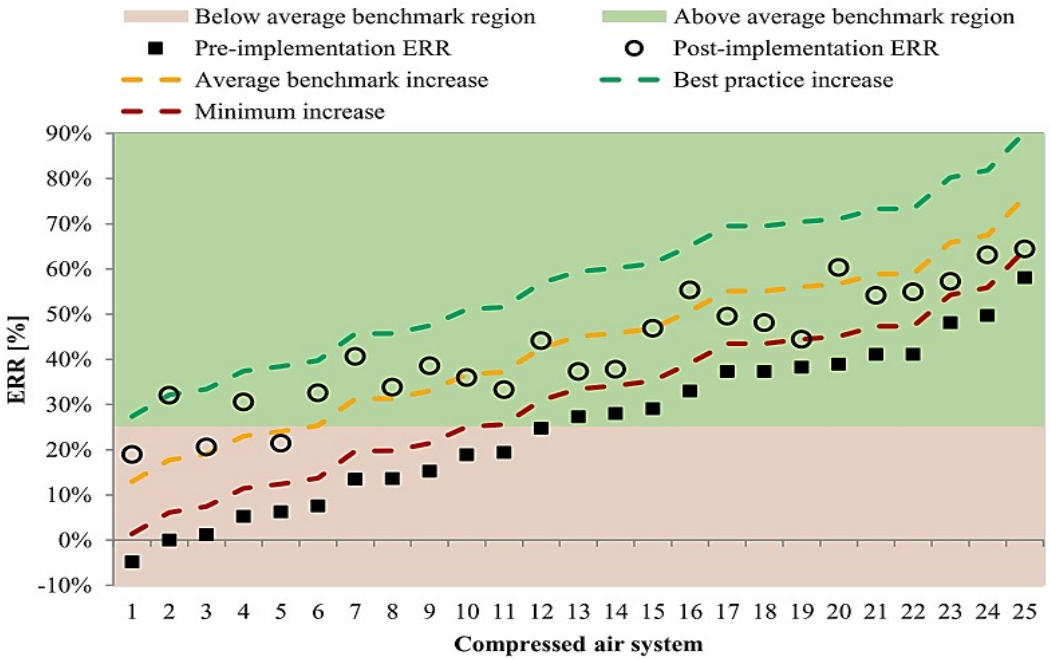

Figure 22 - ERR categories (Adapted from [32])

Using the ERR as a benchmarking method allows for benchmarking and statistical investigation to be done based on the cumulative characteristics of a compressed air system, rather than specific variables. Vermeulen predicted the impact of energy saving initiatives on a compressed air system for the period 16:00 to 18:00 using this prediction model, based on the EER relationship of a compressed air system.

Equation 9 - Regression equation for post-implementation ERR

$$\textbf{Predicted ERR after savings project} = 0.7105 \cdot (\text{Baseline ERR}) + 0.2439$$

The regression equation yielded a coefficient of determination (R^2) of 0.87. Vermeulen validated his model using:

1. Simulations of compressed air systems before and after energy initiatives were implemented.
2. Novel benchmarking techniques.

The limitation of this study is that it only focused on a single period and not a 24-hour profile. The correlation and relations of ERR were only investigated for the peak period 09:00-12:00 and blasting period 16:00 – 18:00. Further investigation into this method is required.

Table 5 summarises the contributions made by the studies discussed in sections 2.3.1 – 2. 3 4. The limitations of the studies were mentioned and indicated why the specific individual study alone would not solve the problem statement. The contributions that each study present can be used together or in a different context. The most prominent contributors are Cilliers and Vermeulen.

Table 5 - Summary of contributions by previous studies

Study Contributor	Shortcoming	Contribution
Abdelaziz [47]	Requires intensive labour	Optimisation of the compressed air audit process
Joubert [35]	Requires mining infrastructure	Further optimisation of the process to identify, implement and report on compressed air initiatives
Marais [36]	Requires variables which are not always known.	Statistically determined rule of thumb which simplifies the process of determining the impact of pressure change on a system
Cox [48]	Requires in monthly data – period too long.	Neural network model which predicts the power usage of a mine with limited inputs
Cilliers [41]	Does not provide a 24-hour profile prediction/evaluation.	The use of regression statistics to create a benchmarking model (bandwidth) for compressed air systems
Vermeulen [53]	Does not provide a 24-hour profile prediction/evaluation.	The use of the ERR parameter to estimate the future potential compressed air savings for a specific time zone

2.3.5 Statistical data analysis techniques

The use of benchmarking and statistical analysis techniques depend on the type, size and frequency of data sets that will be investigated [41], [49]. It is, therefore, necessary to consider multiple statistical methods for benchmarking and analysing information [54].

These different methods can be used to construct different models which can be assessed using the criteria that Botes [54] prosed. Xie et al., [55] published an article regarding the assessment of energy demand of machining systems in 2017.

It was stated that the machine process and energy consumption could be dissected using a breakdown structure, as indicated by Figure 23. On the left of Figure 23, the breakdown of a typical machine process is displayed. On the right end of Figure 23, the breakdown of energy consumption from the total value to the base value is indicated.

This visual breakdown applies not only to the actual consumption of energy but also to the benchmarking of energy [55]. Therefore, both the real total energy consumption and total benchmarked energy consumption of a system can be derived by using equations 27-29 in Appendix B.

By using the method indicated by Figure 23, any machine (energy consuming) process can be transposed to a mathematical model for evaluation. Therefore, it will also be suitable to apply to mine compressed air systems, which have base energy consumers (end users) and machine plants (compressors).

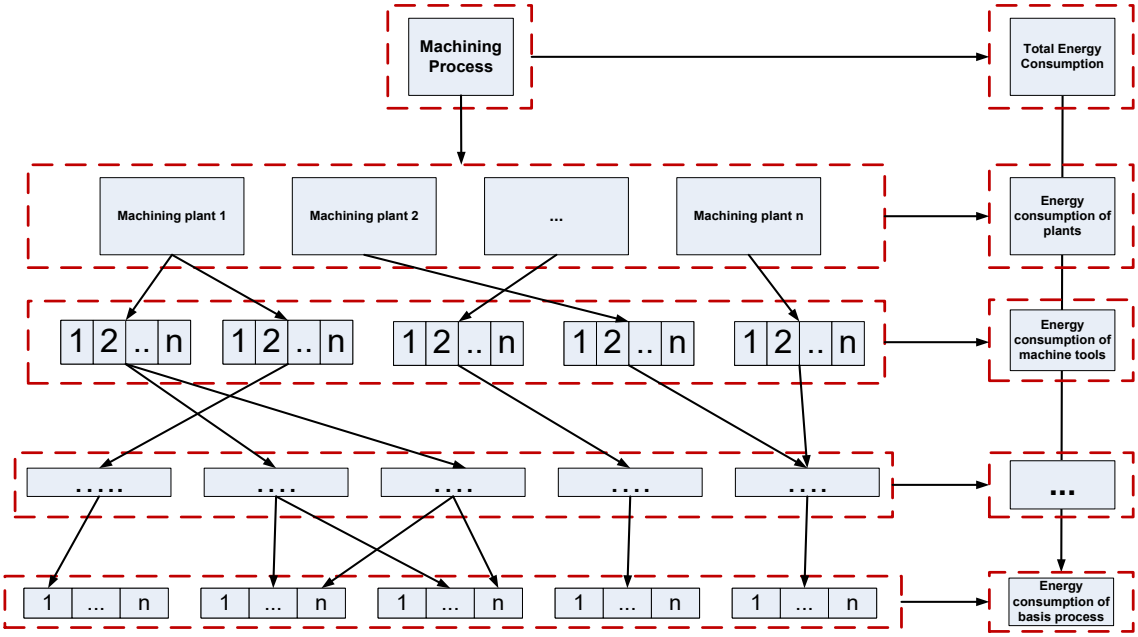

Figure 23 - Decomposition of machine processes and energy consumption (Adapted from [35])

This study concludes this section of the literature review by stating that a statistical approach to the detailed working of energy consuming systems can be useful if mathematical modelling methods can be used to analyse and predict specific outputs.

2.4 Measurement and verification of data

The data that is used in studies play a vital role in the results that studies produce. Therefore, the next section explains the validity of M&V (Measurement and Verification) results as trusted data sets.

2.4.1 Purpose of M&V

Meek [56] describes the M&V process as utilising measurements to determine the actual savings achieved in a single energy consuming system, by an energy management program. This definition is supported by the International Performance Measurement and Verification Protocol of 1997, which was revised int 2012 [57]. The M&V process plays a crucial role in energy service companies (ESCo's) operating procedures, as it validates the performance indicators that ESCo's provide to clients[18]. The M&V process of validating measurements is conducted by third-party assigned M&V teams which conduct independent measurements, audits and investigations [53],[18]. The work conducted by the M&V teams are governed by the South African National Standard (SANS) 50010 document [18], [53], [56], [58]. The M&V teams oversee the ESCo's IDM project phases listed below [53].

1. Investigations
2. Proposal approval
3. Implementation
4. Performance assessment

The independent M&V teams audit the performance assessment phase for three months. These audits are necessary because of ESCo's need to deliver at least 90% of the proposed savings [53]. Therefore, it can be concluded that the three-month, energy-saving performance baselines, and actual profiles which were validated by third-party auditors, can be viewed as valid and accurate.

2.4.2 Statistical tools used by M&V teams

Booysen [50] and Botes [54] listed the most commonly used statistical parameters used by ESCo's and by M&V teams in South Africa.

1. The coefficient of determination (R^2)
2. Root mean squared error (RMSE)
3. Standard Error
4. F-statistic

5. T-statistic
6. Average Error
7. Mean bias error
8. Degrees of freedom (df)

The statistical parameters mentioned can be readily determined by software packages such as Microsoft Excel, and the statistical formulas are listed in Appendix D [59]. Table 6 shows the summary of statistical parameters calculated by the Microsoft Excel Linest function. The statistical formulas are given in Appendix D.

Table 6 - LINEST parameter array (Adapted from [41])

	A	B	C	D	E	F
1	m_n	m_{n-1}	. . .	m_2	m_1	b
2	se_n	se_{n-1}	. . .	se_2	se_1	se_b
3	R^2	se_y				
4	F	d_f				
5	ss_{reg}	ss_{resid}				

The coefficient of determination (R^2) determines the strength of the relationship between variables and ranges from 0 – 1, where 0 is no correlation and 1 a linear relationship between variables[41], [54],[50]. The R^2 value should be higher than 0.75 in order to be considered as valuable, according to Botes [54].

RMSE is the error between the predicted value and the actual value, and should typically be below 15%[54].

The standard error (se) represents the standard deviation of a sampling distribution[49]. This parameter is used to determine the error of the y-estimate found as a result of the regression model of choice.

The F-statistic is used in conjunction with the degrees of freedom to test the significance of a regression model, also aiding in the decision-making process of accepting or rejecting a null hypothesis [41], [50].

The residual sum of squares is a measure of the discrepancies between the estimated values determined by the regression model and the real y-values[50], [54].

2.5 Summary

Chapter 2 summarises the fundamentals that will be required to construct a compressed air cost savings identification model for deep-level mines. Firstly, the vast number of variables required for accurate compressed air network auditing and energy-saving scope identification was described (Section 2.2). It also indicated that the complexity level of these audits varies due to multiple factors specific to each mine.

Secondly, previous studies which were conducted were categorised in four segments (Section 2.3). While all studies lacked a clear resolution for the problem statement, Vermeulen's study [53] produced a valuable tool known as the ERR (Energy reduction ration). This tool can aid in the development of an energy-saving estimation model.

The third and final section described the function of M&V teams, and how the M&V performance assessment reports are audited and validated by third-party companies; increasing the validity of the performance data sets (Section 2.4).

CHAPTER 3. DEVELOPMENT OF POWER ESTIMATION MODEL

3.1 Preamble

The focus of chapter three will be on developing a model which will be able to estimate the potential cost saving on compressed air systems located in deep-level mines. The model will be developed to adhere to the objectives stated in section 1.5. The expected result of the model is an output that closely resembles the output of advanced and complex engineering and mathematical equations, which are obtained using statistical analysis. Particular attention will be given to Vermeulen's estimation tool. Chapter three will progress through multiple stages, from data acquisition to the evaluation and comparison of multiple models. Figure 24 indicates the flow of the five stages of this chapter.

Stage 1 of this chapter will differentiate between what data sets and subsets are required to construct a statistical model. Stage 2 will evaluate the parameters identified in section 2.3 and 2.4. Stage 3 will determine the relationship between the necessary parameters. Stage 4 will construct a mathematical estimation model by combining the subsets of data to form a 24-hour profile data processing model. Stage 5 will aim to evaluate the base model and apply the necessary statistical filters to ensure the accuracy of the model.

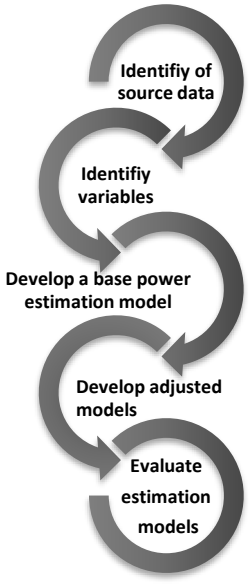

Figure 24 - Methodology flow

The primary hypothesis is that compressed air demand varies through a 24-hour profile on a normal deep-level mine. Therefore the greater the demand of mining personnel and equipment, the greater the power consumption of the motors [12], [18], [25], [32],[48]. It is expected that the results produced by the estimation model will also adhere to this relation between air demand and power consumption, proving the hypothesis is true for all cases.

Equation 1 - Equation 4 conveys theoretically how the air demand of a system contributes to the power required by the compressor motors. A key parameter in the development of an estimation model is thus the relation between when consumption is high and when consumption is low. Time as a parameter is thus of importance.

The secondary hypothesis is that the varying compressed air demand, which is linked to a specific time, is also linked to the mining activity occurring at that given period. Investigation into mining activities displayed in Table 3 dictates that a key variable in the estimation of a model should be which activities are active during specific periods.

The third hypothesis is that more efficient mines have larger power consumption differences between the peak mining activities and non-peak mining activities [30], [53].

The fourth hypothesis is by knowing the peak power consumption, a prediction of a non-peak power consumption period can be made if the compressed air supply (power consumption) is scaled to meet the (lower) demand [53].

The fifth hypothesis is that an accurate estimated power consumption decrease can be made if tested compressed air savings initiatives are implemented.

These five hypotheses are proven in the literature study and will be consulted in the development of the cost-savings identification model.

Figure 25 displays the flow of the development of the estimation model. The sections contained within Chapter 3 are also indicated. Evaluations were done on a continuous basis to ensure that errors were eliminated before continuing the development of the estimation model.

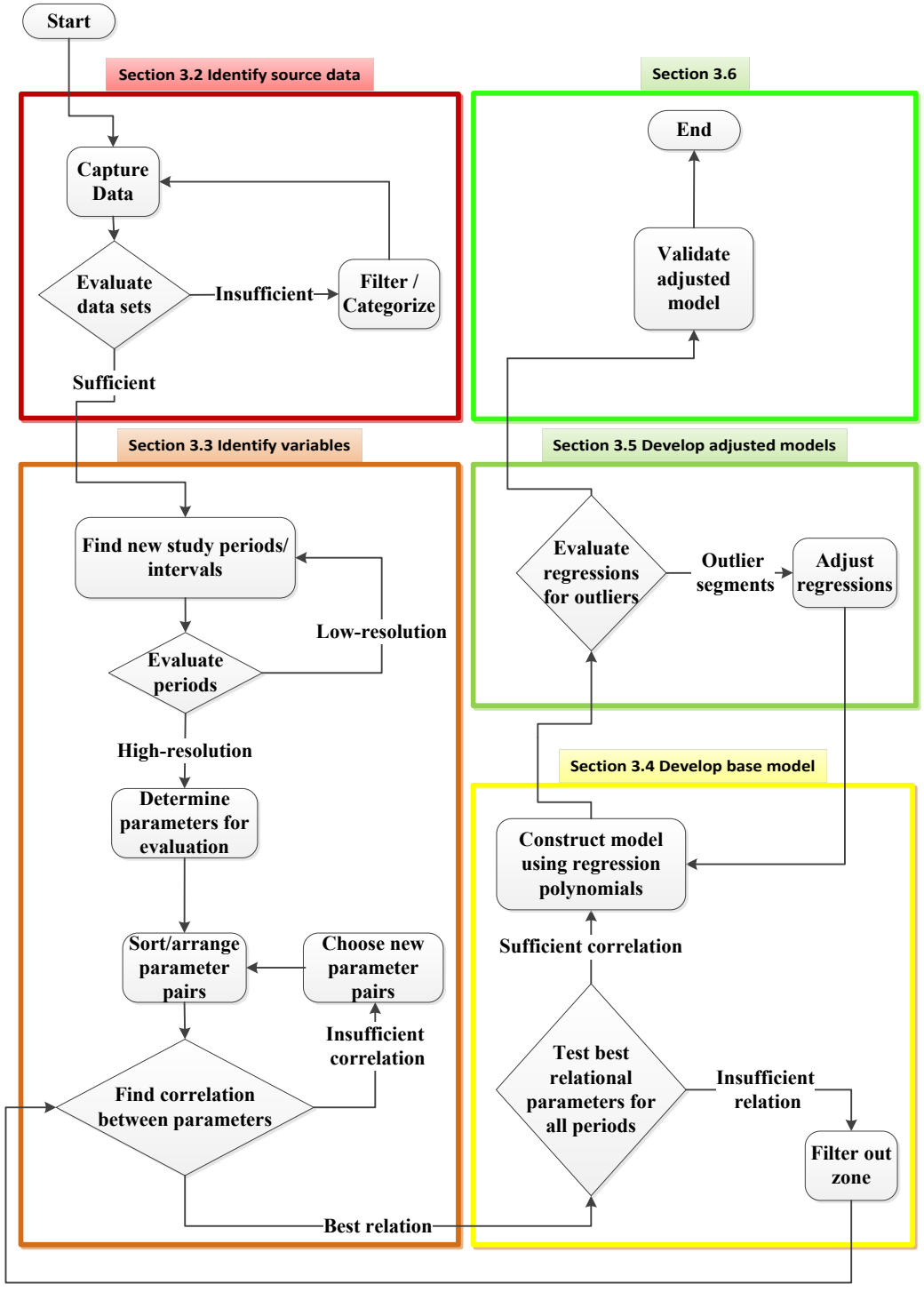

Figure 25 - Functional diagram of the model construction

3.2 Identification of source data

The objective stated in section 1.5 is to develop a statistical model that is robust enough to be implemented on any compressed air system on deep-level mines, yet accurate enough to ensure credibility. The use of data sets that are M&V verified, like baselines and results, ensure the credibility of the data sets.

It is of utmost importance to ensure that the foundation of a statistical investigation is credible, as starting from an incorrect premise leads to an unsure conclusion.

3.2.1 Processing M&V data-tables as sample space

The purpose of this section is to describe how the M&V data can be organised to be used in mathematical and statistical analysis. Figure 71 in Appendix E displays an excerpt example M&V performance assessment report drafted after a compressed air project was implemented. The structure of the excerpt is as follows:

Three baselines and measured profiles are drafted for the respective months of the performance assessment period, each containing a summarised 24-hour performance table. Each table is divided into three sections

- Weekly (Baseline vs Actual)
- Saturday (Baseline vs Actual)
- Sunday (Baseline vs Actual)

The separation of this data is due to the ESKOM tariff structure that differs for weekdays and weekend days. The baseline power usage is determined by the ESCo's and M&V teams. The third-party M&V team then measures and audits the actual power consumption and produces a monthly average 24-hour profile. The total population proportion of M&V results, in this case, various mining shafts and multiple power profiles, is noted as ***P***. Equation 10 displays the breakdown of data that will be used as a case study.

Equation 10 - Test data breakdown equation

$$P = \{ P_1, P_2, \ldots, P_n \}; \quad P_i = \{p_1, p_2, p_3\} \quad ; \quad p_k = \{x_1(t), y_1(t), x_2(t), y_2(t), x_3(t), y_3(t)\}$$

P	= Total population proportion	[kW]
$P_{1\text{-}n}$	= Population proportion for each mine	[kW]
$p_{1\text{-}k}$	= Monthly performance assessment data	[kW]

x_{1-3}	= Baseline vector for weekdays, Saturday *and* Sunday as a function of t	[kW]
y_{1-3}	= Measured Power vector for weekdays, Saturday and Sunday as a function of t	[kW]
t	= 24-hour daily profile containing 48 half hour segments as independent variables	[-]
k	= 3 = Number of months in performance assessment period	[-]
n	= Number of mines in the study (number of population elements)	[-]

Ideally, the population size n would be the number of all deep-level compressed air systems in South Africa. Realistically, access to all mines' M&V reports could not be achieved. Some of the reports had incomplete data or references, and therefore the most complete 29 M&V audited compressed air project reports were included in the total population. The M&V team differentiates between weekdays and non-weekdays due to the difference in mining operations during these days. Non-weekdays are typically used for maintenance related operations. This causes the non-weekday profiles to fluctuate more than the weekday profiles, as Figure 26 indicates. Only the weekdays will be included in the statistical scope due to limited information regarding weekend operations of the sampled mines.

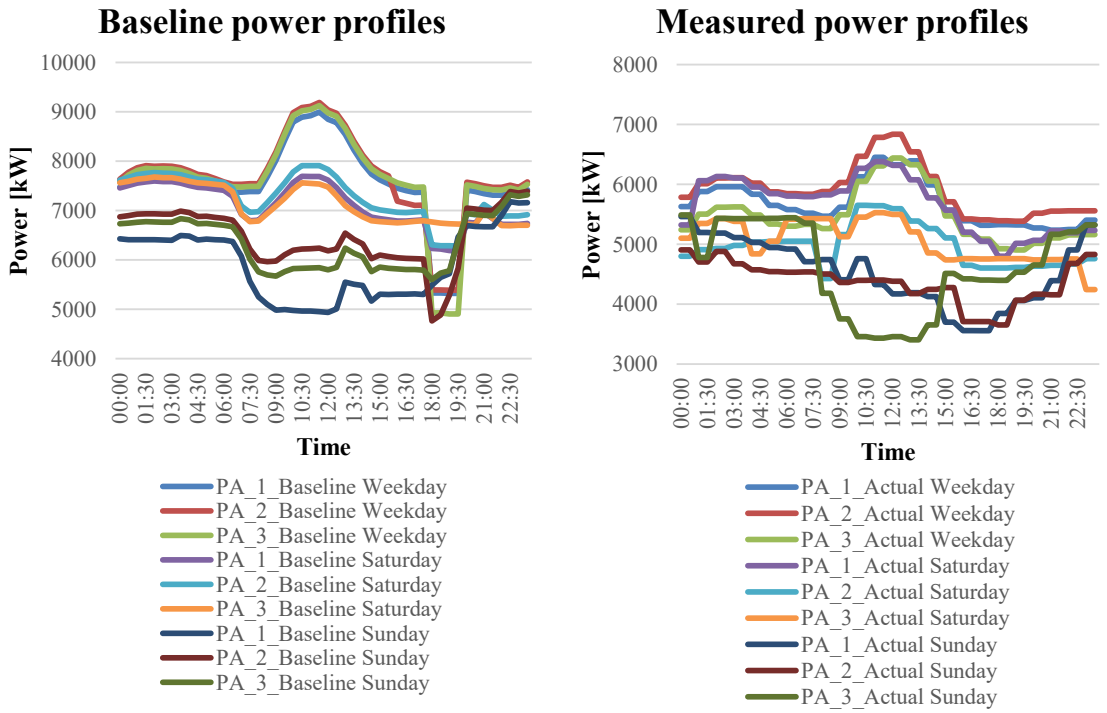

Figure 26 - Difference between weekday and weekend profiles

The filtering of the weekend days from the M&V data sets transforms Equation 10 into the equations summarised in Table 7. Table 7 splits the baseline and measured results, as these data sets will be processed independently.

Table 7 - Sample Space Differentiation

Baseline Sample Space	*Measured Sample Space*	*Total Population Proportion*
$P=\{P_{B1},P_{B2}, \ldots, P_{B29}\}$	$P=\{P_{M1},P_{M2}, \ldots, P_{M29}\}$	$P=\{P_1,P_2, \ldots, P_{29}\}$
$P_{Bi}=\{p_{B1},p_{B2},p_{B3}\}$	$P_{Mi}=\{p_{M1},p_{M2},p_{M3}\}$	$P_i=\{p_1,p_2,p_3\}$
$p_{Bk}=\{x_1(t)\}$	$p_{Mk}=\{y_1(t)\}$	$p_k=\{x_1(t),y_1(t)\}$

3.2.2 Investigating mining schedules

After filtering the days of the week to be included in the population, attention also needs to be given to how each weekday will be deconstructed and modelled. A 24-hour mining weekday can be deconstructed into multiple periods where specific operations are completed, as stated in section 2.2. Yet, different mines and third-party investigators use different deconstructions of a 24-hour daily profile. This section will summarise the different ways that investigators deconstruct and categorise a 24-hour profile. The first being the schedules that regulatory bodies use, the second normal mining schedules, and the third the numerical investigation result.

Regulatory bodies

The M&V reports approved by Eskom deconstructs the 24-hour weekday profile in 7 segments as indicated by the M&V excerpt in Figure 27. The red block indicates the Eskom periods.

1. Morning Off-peak
2. Morning Standard
3. Morning Peak
4. Midday Standard
5. Evening Peak
6. Evening Standard
7. Evening Off-peak

2. Performance assessment: March 2012

Table 2 Actual vs. Contracted Weekday Impact Mar-12

	Weekday (MW)						
	Morning Off-peak	Morning Standard	Morning Peak	Midday Standard	Evening Peak	Evening Standard	Evening Off-peak
Baseline Demand	6.32	6.12	6.379	6.745	6.144	6.091	6.08
Actual Demand	5.819	5.578	5.535	5.946	5.325	5.255	5.324
Actual Impact	0.501	0.542	0.844	0.799	0.712	0.836	0.756
Contractual Impact	1.5	1.5	1.5	1.5	1.5	1.5	1.5
Over/ Under performance	-66.60%	-63.80%	-43.70%	-46.80%	-52.60%	-44.30%	-49.60%

Figure 27 - M&V report weekday periods

Mining Operations

Heyns [31] determined a time-variant operational deconstruction, according to the mine's activities in section 2.2.3. Heyns concluded that the mine has five distinct periods of operation in a 24-hour profile, as indicated by Figure 13.

Mathematical investigations

The mathematical analysis of the data shows that a typical/average power profile can be divided into many distinct periods/zones. The inflection points were used to determine the zones. An inflection point is a point of a curve at which a change in the direction of curvature occurs. The red curve in Figure 28 is the average power profile, while the purple curve (D6) is the sixth differential of the average power profile curve. The inflection points are rounded to periods where the differential curve intersects the secondary y-axis at 0 (green arrows). The secondary axis is to the right of Figure 28.

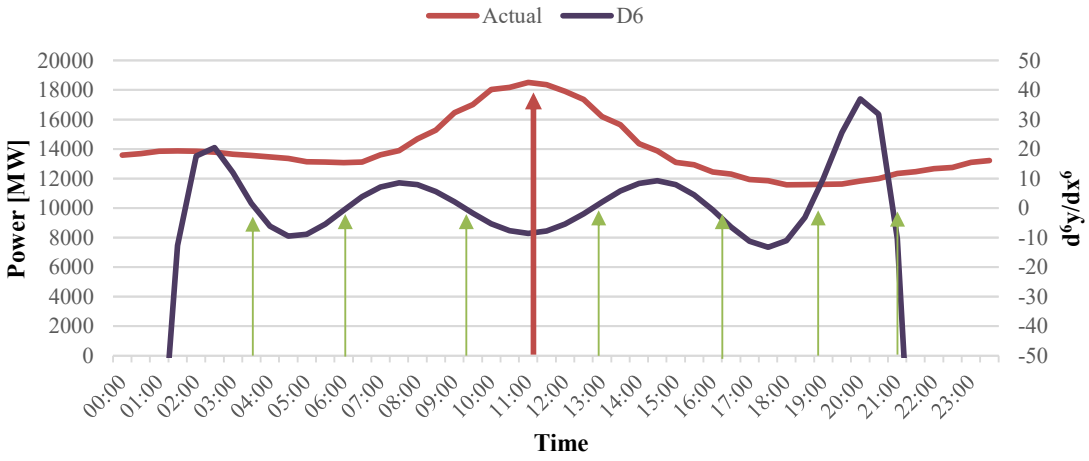

Figure 28 - Inflection points

Appendix F describes how the M&V data is averaged, processed and used to reconstruct the data into distinct time zones. A summary of Appendix F is shown in Table 8.

Table 8 - Appendix F summary regarding the evaluation of mean profiles

Appendix Reference	**Purpose**
F.1	Construction of mean profiles
F.2	Transformation of statistical profiles to polynomials equations
F.3	Derivation of inflection points from polynomials

Summary

Table 9 summarises the different scheduling methods used by the mines, ESKOM and the mathematical evaluation. The ESKOM schedules do not correlate with the mining operations and provide inadequate periods to differentiate the operations on the mine and the influence these operations have on the power consumption.

Heyns' [31] typical mining schedule also produces a low-resolution approach to group the change in power profile into district periods. The mathematical derivate oscillating periods correlate with Heyns' grouping while providing a higher resolution differentiation of the power profile.

Table 9 - Summary of scheduling approaches

Schedule Times	Zones	Z1	Z2	Z3	Z4	Z5	Z6	Z7	Z8	Z9
	ESKOM Low Demand Period	06:00	07:00	10:00	18:00	20:00	22:00	23:59		
	ESKOM High Demand Period	06:00	09:00	17:00	19:00	22:00	23:59			
	Heyns Breakdown	06:00	14:00	16:30	21:00	23:59				
	Baseline Inflection	03:30	05:30	09:00	11:00	13:00	16:30	19:00	21:00	23:59
	PA Measured Inflection	03:30	05:30	09:00	11:00	13:00	16:30	19:00	21:00	23:59

3.2.3 Section Summary

This first statistical evaluation correlates with the first hypothesis stated in section 3.1. The baselines and performance-assessed measured profiles were divided into 9 time periods /zones. This decision was made based on the scheduling of mines provided in the literature, as well as a mathematical derivation which indicated the most suitable distinct periods.

The total available data set for the investigation consisted of 29 M&V reports (consisting of 89 columns) signed by ESKOM, the involved ESCo responsible for the implementation of energy saving initiatives, and the third-party M&V teams.

These reports were filtered by excluding the weekend periods, as too much operational variation existed to derive proper relations. The baseline and measured performance assessment profile were separated and regarded as mutually exclusive to ensure that no relational bias occurred during calculations.

3.3 Identification of variables

This section focuses on finding the best variables to include in the construction of a mathematical model which will best predict the effect that energy-saving initiatives will have on the power baselines of compressed air systems. Hypothesis two can only be determined by means of power consumption – as mining activities are not always well documented. Therefore, by comparing consumed power parameters, indirectly the compressed air consumer/mining-activities parameters are being compared.

The available parameters from the M&V reports are:

1. Baseline power per half hour
2. Performance-assessment measured power per half hour

The calculated parameters from the literature for the baseline and measured power are:

1. Mean power
2. Maximum power
3. Minimum power
4. 24-hour profile
5. Energy reduction ratio (ERR)

The identification of parameters which will aid in the development of a model which will be able to estimate energy savings is not always obvious. Therefore, relationships between the mentioned parameters must be investigated to choose the most suitable parameters for a statistical estimation model.

The parameters and variables for the relationships shown in section 3.3.1 include the entire population of 29 compressed air systems. Section 3.2 concluded that nine distinct periods exist in a 24-hour compressed air profile. Therefore, these same periods will be used to evaluate the same parameters in 9 periods/zones that occur in a 24-hour profile.

3.3.1 Common statistical parameters

The most commonly used statistical parameters are the maximum, minimum and average parameters. The sample data discussed in section 3.2 was divided into the baseline sample and performance-measured sample. This was done to ensure that the change in performance can always be correlated to the baseline as an independent variable.

The power profiles in Figure 29 are sorted from the smallest to the largest maximum power of the sampled power profiles. The sorting of data provides structure to the data patterns to ensure correlations are visible in graphical diagrams. Figure 29 indicates the scope of the power profiles within the investigated 29 compressed air systems.

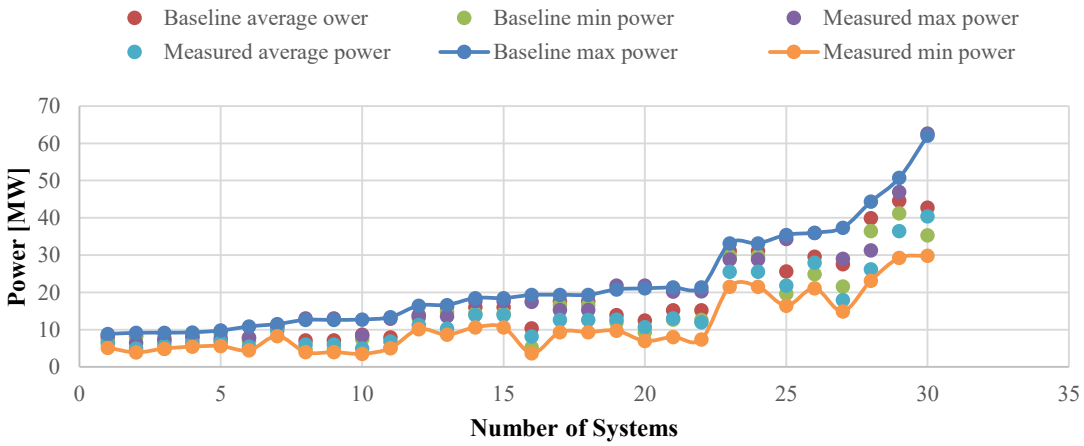

Figure 29 – Scope bandwidth

The correlation between the parameters of the baseline sample and the performance measured sample, the maximum, minimum and average parameters, will be compared individually. Figure 30 compares the baseline's maximum power data points with the performance measured sample space's maximum power data points.

The calculated coefficient of correlation (R^2) indicates that there exists a strong linear correlation between the two data sets. R^2 is calculated using Equation 24 in Appendix D. R^2 (for the maximum power data) is calculated at 0.95 (calculated using Microsoft Excel® 2016).

The correlation between the maximum baseline profiles and the maximum measured profiles is displayed in Figure 30.

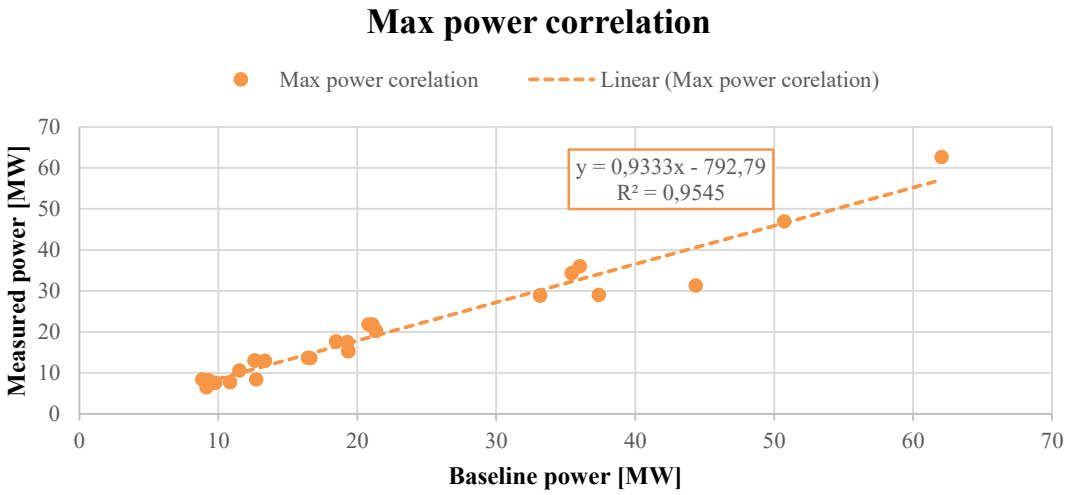

Figure 30 - Maximum power correlation

Appendix G contains figures like Figure 30 but using the average and minimum power profile data. The results are summarised in Table 10. The results in Table 10 show that as the baseline power profile increases, so the measured power profile also increases. Therefore, a strong correlation for the average and minimum power values are also present.

Table 10 - Appendix G summary of max, average and min power regression

Appendix G Reference	Correlation Coefficient (R^2)
Figure 30	0.954
Figure 78	0.949
Figure 79	0.953

3.3.2 Uncommon statistical parameters

The Energy Reduction Ratio (ERR) was developed by Vermeulen [53] and is an uncommon parameter which showed promise for a specific period in a 24-hour profile. Section 3.2 identified that there exist nine periods which can be best divided into a 24-hour profile.

Therefore, the ERR will be applied for these nine periods. While determining the ERR of the specific periods, the other parameters will also be compared to the ERR to investigate if any relevant correlations are evident. The ERR parameter compares the compressed air power consumption of a system to a static point (usually the maximum power point) unique to the

system under investigation. This parameter can be used to assess if there exists a noticeable correlation between compressed air systems and how they react to energy efficiency initiatives.

A complete result set will be displayed for one of the periods as an example. An example of a compressed air power dataset will be used to illustrate the development of the ERR parameter.

Determining the ERR parameter for a **single compressed air system** is broken down in the following steps. Examples of each step is given in chronological order.

1. Acquire baseline and performance assessed data (Table 7)
2. Determine the reference power and variable power
3. Average the power in identified periods
4. Use Equation 8 to determine ERR for each time zone (period) before and after energy initiatives were conducted, using the data obtained from step 3
5. Tabulate results

Five-step ERR development

1. Figure 31 displays the **first step** by displaying the 24-hour profile of the baseline and performance assessed data sets. The equation used to calculate the input profiles of Figure 31 can be found in Appendix F.1, Equation 25 and Equation 26. These equations only average the 3-month M&V data for the baseline and the measured results. Therefore, Figure 31 displays the 3-month average M&V data.

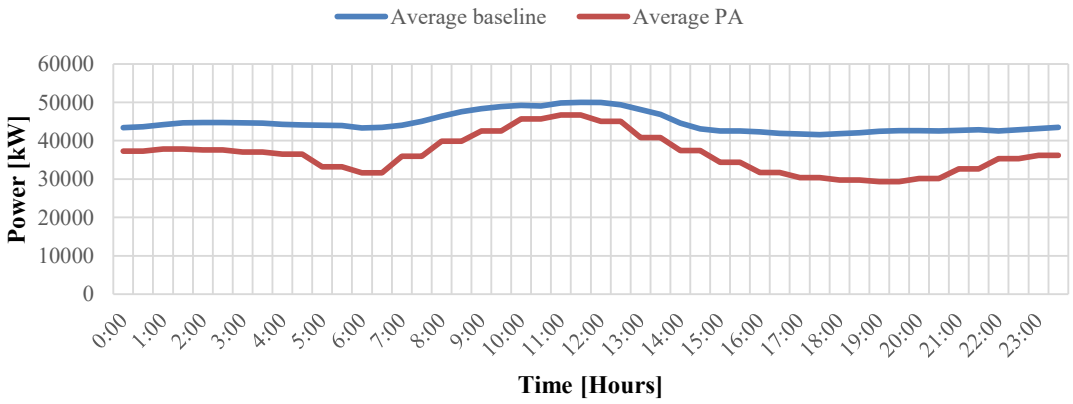

Figure 31 - Example compressed air system investigation data

2. Figure 32 displays the **second step** by identifying the reference power magnitude (red arrow) and variable power variables (green arrow). The yellow lines display the areas where power is averaged to a single value, as shown in step 3. The power values are averaged for the baseline (blue) and measured (red) profiles.

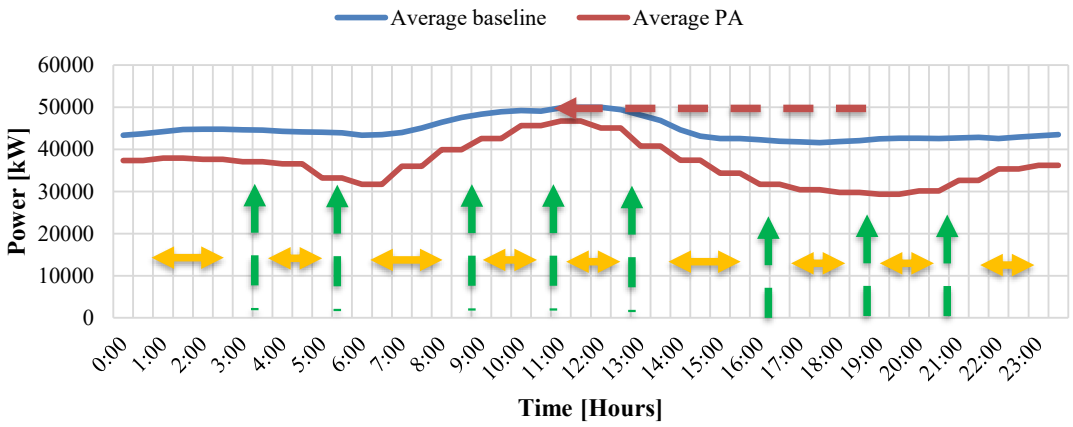

Figure 32 - Reference and variable power identification

3. **Step three** is shown by Table 11, which summarises the average power for the different time periods shown in Figure 32. The variable time zones are marked in colour, while the reference power is left without colour.

Table 11 - Average power for 9 zones in 24-hour profile

Baseline Average Power [MW]									
Drilling peak	**Z1**	**Z2**	**Z3**	**Z4**	**Z5**	**Z6**	**Z7**	**Z8**	**Z9**
49,4	44,7	44,2	44,8	48,8	49,7	44,3	41,8	42,5	42,9
Average Performance Assessed Power [MW]									
Drilling peak	**Z1**	**Z2**	**Z3**	**Z4**	**Z5**	**Z6**	**Z7**	**Z8**	**Z9**
46,1	37,5	35,8	35,4	44,1	45,8	36,6	30,3	29,7	34,7

4. The **fourth step** is to calculate the ERR of each zone using the peak and non-peak data from the baseline dataset. Nine iterations of Equation 8 will be required for a total profile.

5. The **fifth step** is to tabulate these results to be used as variables in a new ERR data set. Appendix H contains the full mathematical expressions for the results which are shown in Table 12.

Table 12 - Pre- and post-implementation ERR data results

Pre-implementation ERR									
Drilling peak	**Z1**	**Z2**	**Z3**	**Z4**	**Z5**	**Z6**	**Z7**	**Z8**	**Z9**
0	0.104	0.105	0.093	0.011	-0.006	0.104	0.154	0.139	0.131
Post-implementation ERR									
Drilling peak	**Z1**	**Z2**	**Z3**	**Z4**	**Z5**	**Z6**	**Z7**	**Z8**	**Z9**
0.066	0.241	0.275	0.282	0.108	0.071	0.258	0.385	0.398	0.297

The total results for 9 zones for all 29 compressed air systems/mines are tabulated in Table 26 of Appendix I.1. This table is the result of using the five-point method discussed in this section. Table 27 in Appendix I.2 shows the statistical expression for the data.

3.3.3 Comparison of data relationships

The different parameters and correlations identified in (section 3.3) need to be compared to ensure that the best statistical parameters are used for the proposed model. This section compares the identified parameters and is divided into four sub-sections. These sections will indicate which relations are acceptable and which are not.

The relationships between the ERR parameters are determined individually for each period. An example graphical expression of each relationship will be displayed, followed by a table summarising the results for the nine distinct periods. The total results can be found in the assigned appendices.

Pre-implementation Sorted Relations

Figure 33 displays the pre-implementation ERR parameter for all the systems in the original population proportion. Included in Figure 33 are the minimum positive increase in the post-implementation ERR, the average increase in post-implementation ERR and the maximum increase in post-implementation ERR, which is added to the pre-implementation ERR (this is to create a bandwidth of operation for all the systems). The light blue line is the actual performance (post-implementation ERR) parameter, displayed in relationship to the bandwidth of the system.

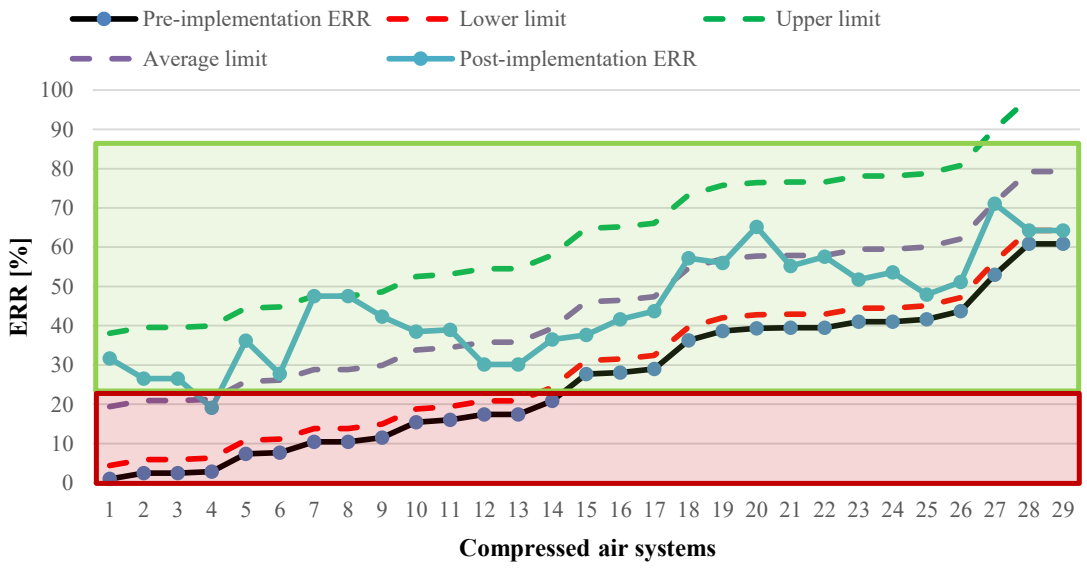

Figure 33 - Bandwidth of ERR parameters for systems sorted by pre-ERR

The results for the nine different zones are displayed in Appendix J. The average pre-implementation ERR of the entire Zone 1 population proportion is 0.2635 (shown where the red block and green block meet). Systems with a pre-implementation ERR which is lower than 0.2635 show an above-average post-implementation ERR.

Systems with a pre-implementation ERR which is higher than the average has a lower post-implementation. This is in agreement with the findings of Vermeulen [53]. 14 systems had below-average pre-implementation ERR values (shown by the red block). The average pre-implementation ERR for all zones were determined and displayed in Appendix J. The results of Appendix J are summarised in Table 13. The table shows that the lower 3rd of the sample produces higher post-implementation ERR values. Thus, indicating that profiles with a low pre-implementation ERR have higher potential savings than those with higher pre-implementation ERR. The ERR relationship thus agrees with hypothesis three and four.

Table 13 - ERR Sorted bandwidth results

Zones	Average pre-implementation ERR	Average difference	Nr of under average pre-implementation ERR values	Turning point
Z1	20.35	15.82	16	12
Z2	20.75	17.46	16	19
Z3	18.72	17.47	16	11
Z4	3.28	16.28	16	3
Z5	0.35	14.75	15	22
Z6	16.17	17.24	15	13
Z7	26.32	18.42	14	11
Z8	26.11	19.14	14	11
Z9	23.40	17.18	16	12

Power consumption vs ERR

The relationship between the maximum, average and minimum power has been discussed in section 3.3. Strong linear relationships were found between these parameters, yet the parameters are confined to daily values and do not have relationships on a half-hour basis. The comparison of maximum, average and minimum values to the ERR's parameter can identify power relations within the 24-hour profile. An increased data resolution will be the result.

Figure 34 displays the maximum power correlations to the pre- and post-implementation ERR parameters. Linear regressions have been added to evaluate the relationships. An example zone has been chosen to display the data graphically. The correlation coefficient (R^2) for the other zones will be tabulated as a summary of the total results. Graphical examples related to Table 14 can be found in Appendix K.

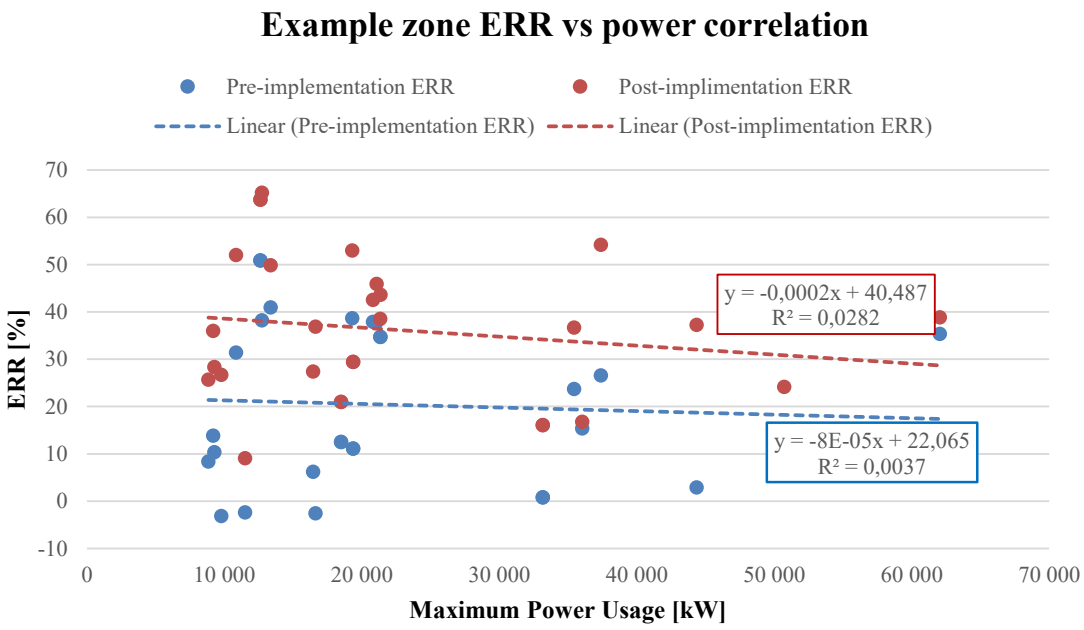

Figure 34 - Maximum power vs zone ERR parameters

The summary of correlations of the power parameters (maximum, average and minimum) and the ERR parameters (pre-implementation and post-implementation) is summarised in Table 14. The maximum correlation coefficient (R^2) is 0.194, and the average is 0.0735.

This is clear evidence that the maximum, average and minimum power **do not** have a high-resolution correlation with the 24-hour profile of a compressed air system. Table 14 displays the insufficient correlation strength between the maximum, minimum and average parameters. Therefore, other relationships must be considered.

Table 14 - Power parameter vs ERR correlation summary

Power parameter vs ERR correlation coefficient (R^2)						
Zones	**Maximum Pre**	**Maximum Post**	**Average Pre**	**Average Post**	**Minimum Pre**	**Minimum Post**
Z1	0.0037	0.0282	0.0819	0.1183	0.1454	0.1784
Z2	0.004	0.031	0.0861	0.1247	0.1521	0.1856
Z3	0.008	0.0386	0.0993	0.1303	0.1695	0.1904
Z4	0.033	0.0888	0.1005	0.078	0.1374	0.0769
Z5	0.0308	0.0073	0.0037	0.00006	0.00001	0.0021
Z6	0.0173	0.0008	0.0119	0.0304	0.051	0.0583
Z7	0.0031	0.007	0.08	0.0729	0.1533	0.1274
Z8	0.0044	0.0135	0.0825	0.0858	0.156	0.1418
Z9	0.0036	0.0242	0.0774	0.1144	0.14	0.1797
Maximum	**0.1904**					
Average	**0.073533**					

Power consumption difference in Pre -and post-implementation ERR

The power parameters were compared to the ERR parameters producing no distinct correlation. The power parameters (maximum, average and minimum) are compared to the difference in pre-implementation and post-implementation ERR in Figure 35. Linear regressions have been added to evaluate the relationships.

An example zone has been chosen to display the data graphically. The correlation coefficient (R^2) for the other zones will be tabulated as a summary of the total results. Complete graphical illustrations are shown in Appendix L

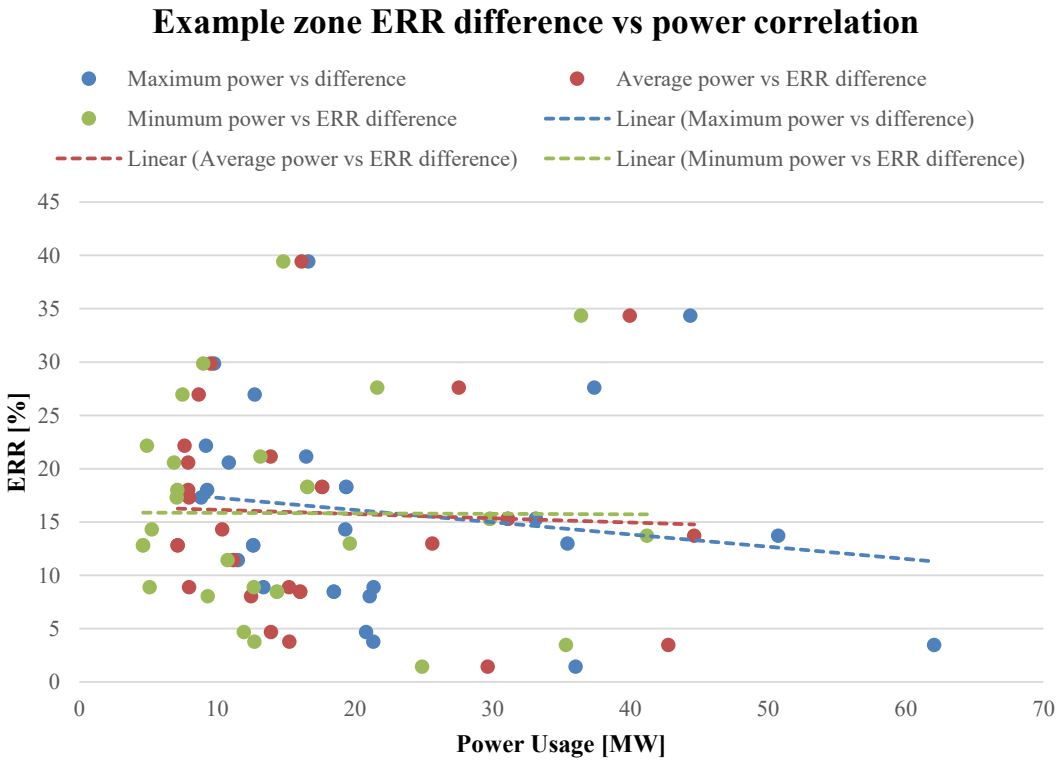

Figure 35 - Power parameter vs difference in ERR

No significant correlations are visible, as summarised in Table 15. The best correlation coefficient was 0.0663, while the average correlation coefficient is 0.016729. The evidence in Table 14 and Table 15 indicate that a correlation between the power parameters and the ERR of a compressed air system does not exist.

Table 15 - Power parameters vs ERR difference summary

Power Parameter vs ERR Difference Correlation Coefficient (R^2)			
Zones	Maximum Power	Average Power	Minimum Power
Z1	0.0278	0.0023	0.00002
Z2	0.0273	0.0012	0.0003
Z3	0.0302	0.0029	0.0001
Z4	0.0663	0.0348	0.027
Z5	0.0153	0.00003	0.0021
Z6	0.0278	0.0023	0.00002
Z7	0.0002	0.025	0.0596
Z8	0.0017	0.0195	0.0537
Z9	0.0168	0.0006	0.0068
Maximum	**0.0663**		
Average	**0.016729**		

Pre-implementation ERR vs Post-implementation ERR

The novel correlation that Vermeulen [53] used was based on determining the correlation that the pre-implementation ERR had with the post-implementation ERR. This correlation was also investigated for the systems in the original population proportion. An example zone has been chosen to display the data graphically. The correlation coefficient (R^2) for the other zones will be tabulated as a summary of the total results. Complete graphical illustrations are shown in Appendix I.

Figure 36 displays a scatter plot diagram presenting the correlation between the pre- and post-implementation ERR parameters. The x-axis represents the pre-implementation ERR, while the primary y-axis represents the post-implementation of the specific zone under investigation. The linear regression line and the correlation coefficient are calculated using Microsoft Excel ® 2016 built-in LINEST function.

The secondary y-axis displays the number of data points that are found within a 5% ERR interval. The secondary y-axis displays the frequency distribution of the ERR parameters.
The correlation coefficient displays the strength of the linear relationship, while the frequency distribution displays how the data is distributed over the entire pre-implementation ERR interval.

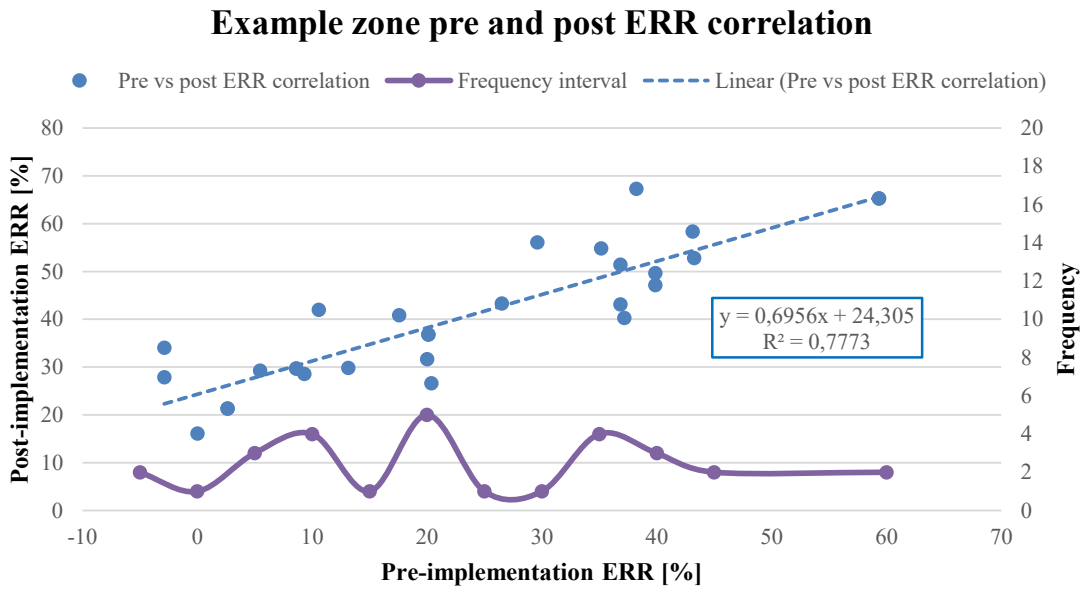

Figure 36 - Example Zone pre-implementation ERR vs post-implementation ERR

Figure 37 displays the ERR correlation coefficient for each zone. Zone 4, 5 and 6 can be considered as having insufficient correlations, according to Botes [54]. Zone 4, 5 and 6 is within the peak drilling shift schedules of deep-level mines. The primary focus of the drilling shift is production, and therefore not all mines allow for energy optimisation to be implemented during this time. Appendix N.1 summarises the linear regression results for all zones, while Appendix N.2 summarises the effect that not considering zone 4, 5 and 6 has on the data distribution.

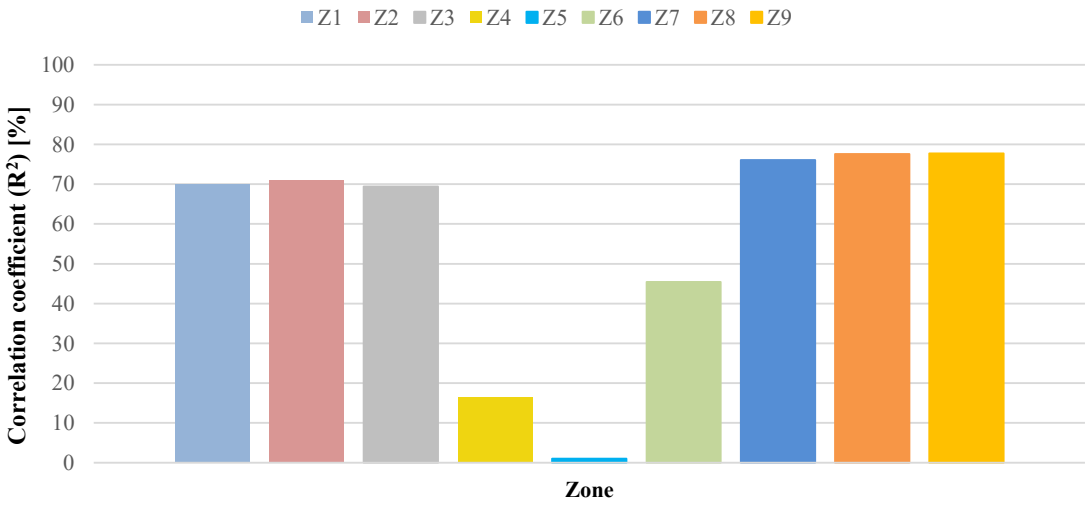

Figure 37 - Comparison of zone correlation coefficients

3.3.4 Section Summary

This section investigated which parameters and relations were most suited to construct a 24-hour estimation model. The power consumption parameters showed no significant correlations. The correlation coefficient describing the relationship between the pre-implementation ERR and post-implementation ERR showed significant correlations, according to Botes [54].

3.4 Development of a base power estimation model

The estimation model will focus mainly on the ERR implementation method, due to the high correlation between the 29 systems which were used in the initial statistical investigation. The purpose of the estimation model is to estimate the most probable energy saving impact that energy-saving initiatives will produce. Therefore, the input of the proposed model will consist of mainly two inputs:

1. 24-hour baseline profile
2. Time and duration of drilling shifts.

The output of the estimation model is a 24-hour adjusted profile which consists of 48 distinctly calculated data points.

3.4.1 Input Quantification

A 24-hour hour profile with 48 distinct data elements must be provided or translated into an input data array.

Equation 11 - Model input

$$\text{Power Baseline} = \overline{x} = \{ x_1, x_2, x_3 \ldots x_{48} \}$$

Power Baseline	= Vector of power elements	[kW]
$\overline{x}$	= Vector of power elements	[kW]

3.4.2 Calculation of Parameters

The equation to transform the input vector to a pre-implementation ERR vector is given below.

Equation 12 - Input to pre-ERR transformation (Adapted from Equation 8)

$$\overline{ERR_{pre}} = \overline{y} = A\overline{x} + b$$

$$\overline{ERR_{pre}} = \overline{y} = \left(\frac{-1}{P_{Max\text{-}ref}}\right)\overline{x} + 1$$

$\overline{ERR_{pre}}$	= Pre-implementation Vector	[-]
$\overline{x}$	= Vector of baseline power elements	[kW]
A	= parameter	[kW^{-1}]
b	= Constants vector	[-]
$P_{Max\text{-}ref}$	= Maximum peak drilling shift power	[kW]

3.4.3 Transformation of calculated parameters

The equation to transform the pre-implementation ERR vector to a post-implementation ERR vector is given below. The ERR-vectors were determined by the ERR regression models.

Equation 13 - Post Implementation Vector

$$\overline{ERR_{post}} = \overline{y} = \overline{C} \cdot \overline{ERR_{pre}} + \overline{d}$$

$$\overline{ERR_{post}} = \overline{y} = \begin{bmatrix} 0.7612 \\ 0.7443 \\ 0.7972 \\ 1.1887 \\ 0.4663 \\ 0.5915 \\ 0.6563 \\ 0.6569 \\ 0.6956 \end{bmatrix} \overline{ERR_{pre}} + \begin{bmatrix} 0.2069 \\ 0.2277 \\ 0.2127 \\ 0.1566 \\ 0.1494 \\ 0.2385 \\ 0.2747 \\ 0.2811 \\ 0.2430 \end{bmatrix}$$

$\overline{ERR_{post}}$	= Post-implementation vector	[-]
$\overline{x}$	= Vector of pre-implementation ERR	[-]
$\overline{C}$	= Gradient vector	[-]
$\overline{d}$	= Constants vector	[-]

3.4.4 Transformation to output vector

Equation 14 displays the transformation of the post-implementation ERR vector to an usable 24-hour estimated power profile.

Equation 14 - Output vector

$$\overline{x_{output}} = \left(P_{Max\text{-}ref} - P_{Max\text{-}ref} \cdot \overline{ERR_{post}}\right)$$

$\overline{x_{output}}$	= Power estimation vector	[kW]
$P_{Max\text{-}ref}$	= Maximum peak drilling shift power	[kW]
$\overline{ERR_{post}}$	= Post-implementation vector	[-]

3.4.5 Section Summary

This section displayed how the statistical parameters which were determined in sections 3.1 – 3.3 were used to construct a base model for estimating the cost savings of a typical mining compressed air system. Figure 38 summarises the mathematical process of determining a power estimation profile using a baseline power profile as input.

Figure 38 - Estimation model flow

3.5 Development of adjusted estimation models

After further inspection of the base model, certain outliers (which will be discussed in Figure 39 and Figure 40) were identified which influenced the base estimation model.Two alternative models were developed to mitigate the influence of these outliers on the model.

Error Identification

Figure 39 shows the linear regression (blue) for the base model compared to an averaged interval grouping of the same data sets (red). The lowest percentile pre-implementation ERR does not correlate with physical events. Section 3.3.3 showed that the lowest pre-implementation ERR segments have the highest potential for an ERR increase after implementation of energy-saving initiatives.

Possible Solution Model #1 (Green)

The blue dots indicate the normal pre-implementation and post-implementation correlation. The regression is shown by a dotted blue line. At the zero pre-implementation ERR mark, the post-implementation ERR is only 15%. The red line indicates the grouping data method which indicates that at zero pre-implementation ERR, most of the data is very low, pulling down the regression line (dotted blue line). This suggests that data sets contained data where energy efficiency projects were not the focus of the ESCo. The green line is used to mitigate this error by implementing the statement of Vermeulen that zero levels of pre-implementation ERR have the highest potential for increase.

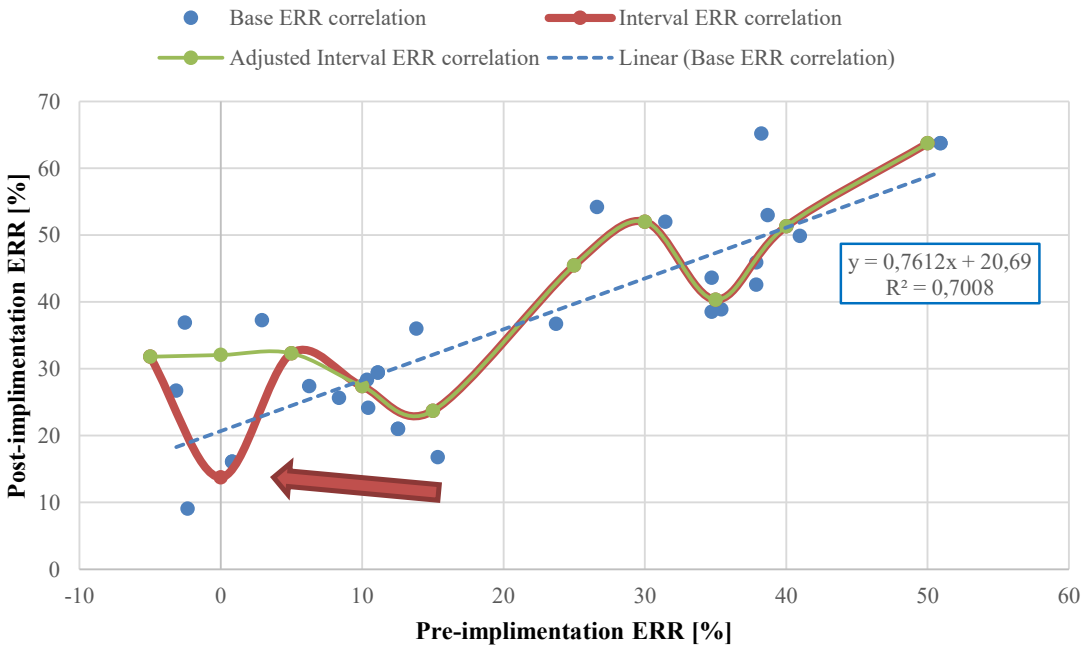

Figure 39 - Base estimation outlier identification and adjustment #1

The outliers have been averaged to produce a more linear expectable function (green). The displayed regression is an example of the adjustment to the original ERR regression. Adjusted model #1 regressions for all zones are included in Appendix O.

Error Identification

Figure 40 displays the difference between the pre-implementation ERR and the post-implementation ERR (blue). The outlier data dramatically decreases the regression line formula predicting the effect of energy-saving initiatives on mines with zero optimised profiles. This again does not correlate with industry results.

Possible Solution Model #2 (Green)

The outlier data has been averaged to present a proposed regression model (green). The frequency distribution for the data elements is presented at the bottom and on the secondary axis (purple). The adjustment curves for all zones are shown in Appendix P.

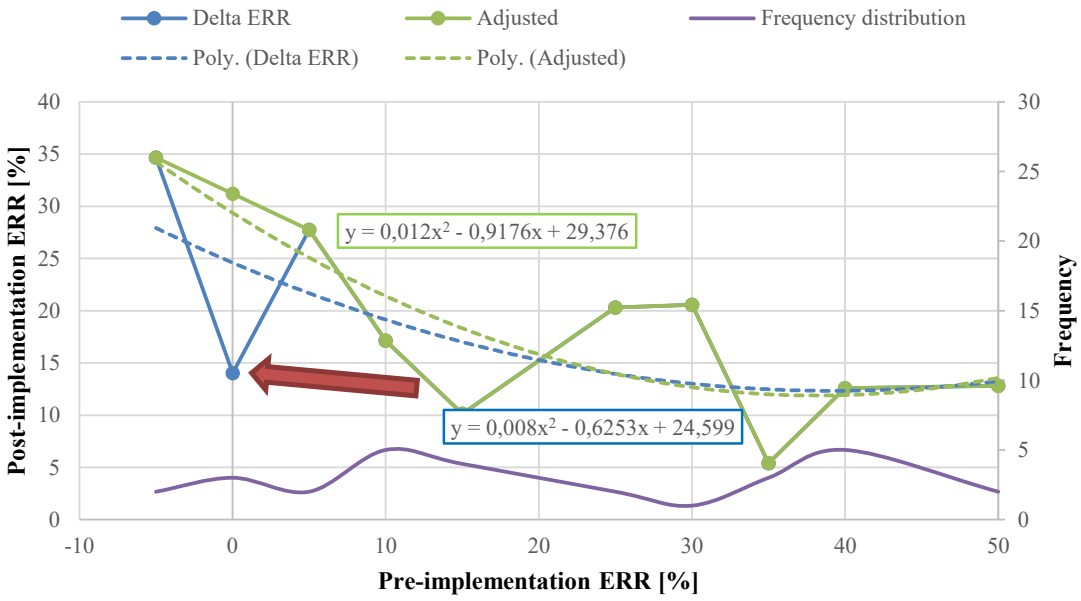

Figure 40 – Base estimation model adjustment #2

The two adjusted regressions are shown in Figure 39 and Figure 40 can be used instead of the ordinary linear regressions. By using the method shown in section 3.4 (base model development), the alternative regressions can be used to construct two adjusted estimation models. As a result of this, guidance regression can also be used to help predict what post-implementation ERR values future systems can have.

Using guidance parameters to create ERR bandwidth

Regression models are tools used for historical analysis, and thus have shortcomings when it comes to predicting future values. Additional guidance is required for the user of this model to make decisions regarding the probability of an event occurring. Therefore, the SFA (Stochastic Fortier Analysis) and COLS (Corrected Ordinary Least Square) models have been calculated to indicate where the most probable results will be located. These methods have been discussed in Appendix C.2-6.

Figure 41 displays the guidance regression models which display where the densest operating band of data is located. More than 50% of the data is located between the upper SFA (purple) and lower SFA (green).

Figure 41 is an example diagram, and all the zones' guidance parameters can be found in Appendix Q.1. As the parameters can be used to construct a bandwidth of data probability for linear regression, the same bandwidth can be translated into the ERR domain by using the linear regression in Figure 41 and using equations in section 3.4. The calculation results for the two adjusted models can be found in Appendix Q.4

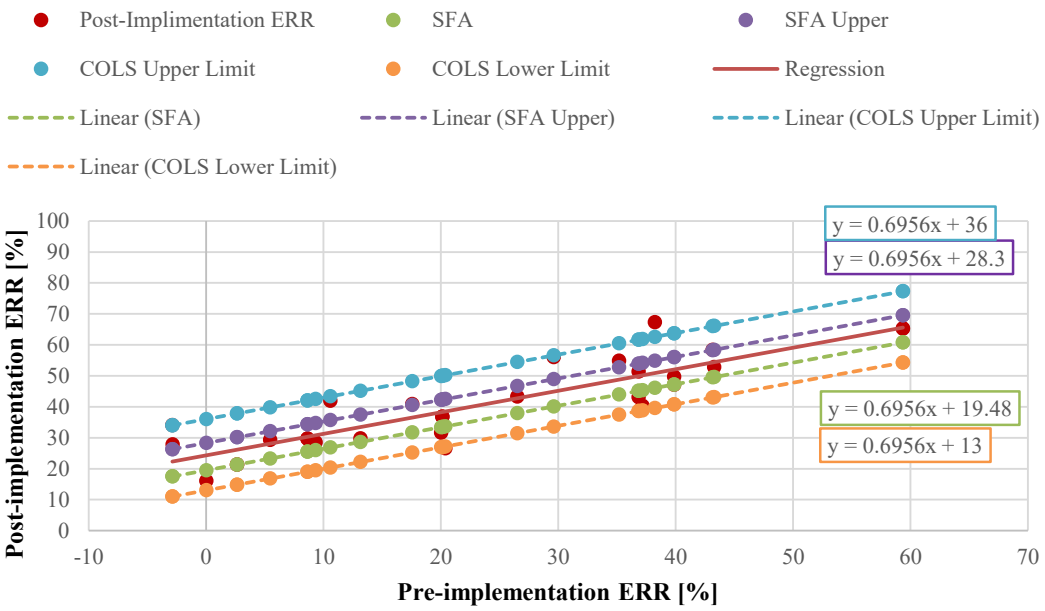

Figure 41 - Guidance parameters

This section summarises the changes made to the base model with all calculations and filtering processes added in Appendix O - Q. The same methods and calculations that were used in section 3.4 to calculate the base model were used to calculate the adjusted models. With all the models successfully constructed, the next section will evaluate which model is the most suitable for the practical application.

3.6 *Evaluation and verification of estimation models*

The proposed models will be evaluated against the findings of Vermeulen and Cilliers to determine if it is a valid model. The three proposed models (one base model and two adjusted models) will also be evaluated to determine which model is best suited for the practical application.

The first step in the verification process is to determine the scope of the statistical sample space, to ensure that the model is not implemented outside of the intended environments.

As all three estimation models are based on the ERR relationships, the pre-implementation ERR parameter is thus used as the independent variable in most cases. The scope of the predictive outcomes then relies on the scope of the pre-implementation ERR.

Figure 42 displays the scope for the dependent variable for all zones. The maximum scope permitted is set at 50% pre-implementation ERR. The green line indicates the 50% mark, whereas the red line indicates that a 60% ERR can be used in the afternoon periods. Zones 4-6 have shown little or no correlation, as discussed in section 3.3. Therefore, these zones' maximum pre-implementation ERR will be ignored.

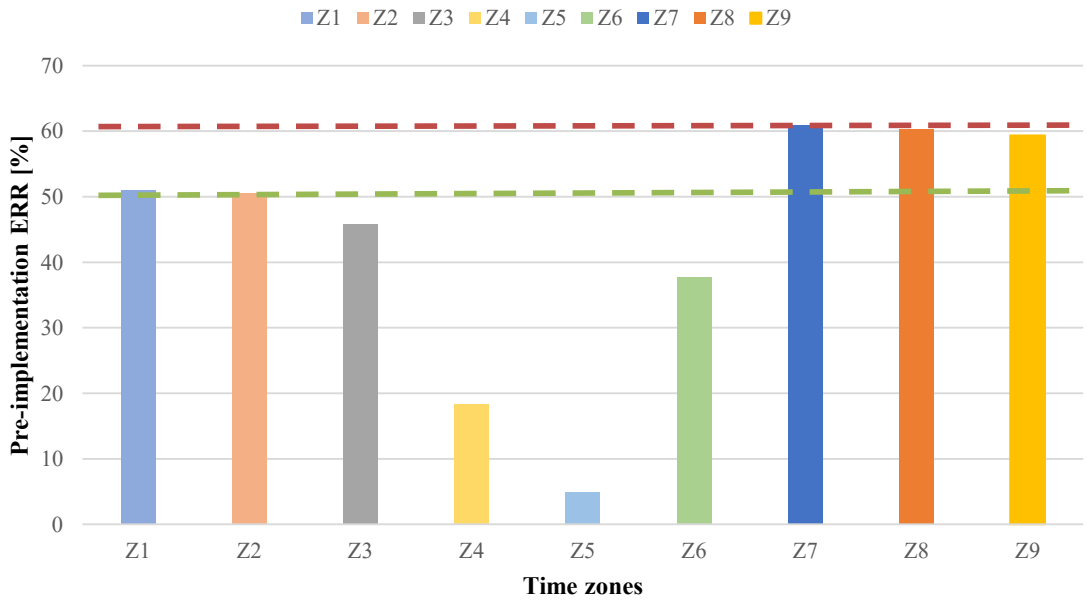

Figure 42 - Independent variable scope

Some mines are reluctant to implement energy-saving initiatives during peak drilling shifts. Therefore, the scope of the prediction model lies outside of the drilling shift. The drilling shift for most mines is located between zone 4-6. These are also the zones with the lowest correlation in ERR data.

3.6.1 Verification of ERR parameters

Vermeulen [53] used the ERR comparison mechanism to create a novel methodology for the identification of energy-saving opportunities. His study only focused on the peak blasting shift – which in this case is a similar period to Zone 7. The reason for this is the Eskom DSM projects mainly focused on the Eskom evening peak period. Figure 43 displays the similarities in the results obtained from Vermeulen and the data set defined in 3.2.

The initial constant of Vermeulen's study is lower, accounting for the difference in gradient. The maximum difference between the two regressions is 3.1 %. This indicates that although different data sets were used, the correlation is very similar. This verifies the strong correlation that the ERR parameters have in compressed air systems of deep-level mines.

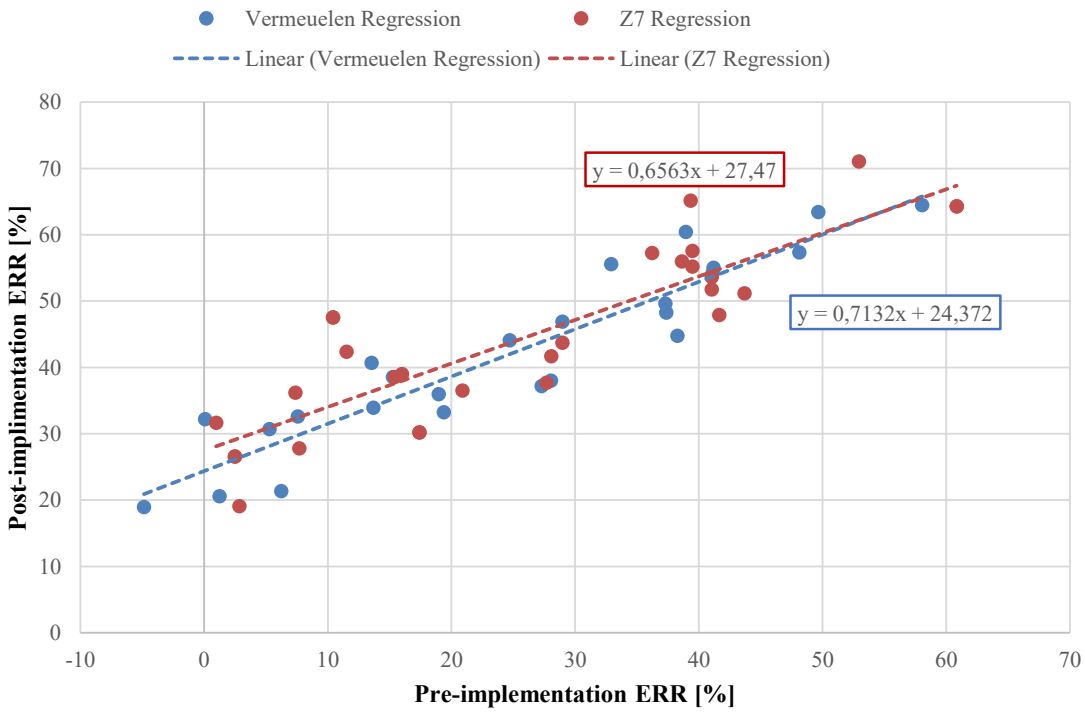

Figure 43 - ERR calculation verification

3.6.2 Verification of ERR method as opposed to traditional averaging

The ERR correlation method is independent from the normal averaging of data method. The main difference is that the averaged data only shows the average baseline vs average performance assessed measurement, while the ERR gives a relation for a range of baselines vs a range of measurements.

The average can still be used to increase confidence in the performance of the ERR method. Figure 44 shows the average baseline (blue) vs the average performance assessed results (red). The three ERR methods are then also plotted to display the similarities. 09:00 to 12:00 is excluded, due to insufficient ERR correlations during the mentioned period. The adjusted methods were 3% more accurate over a 24-hour period than the base ERR model discussed in section 3.4. The total difference between the adjusted model and the statistical average is 3.04%.

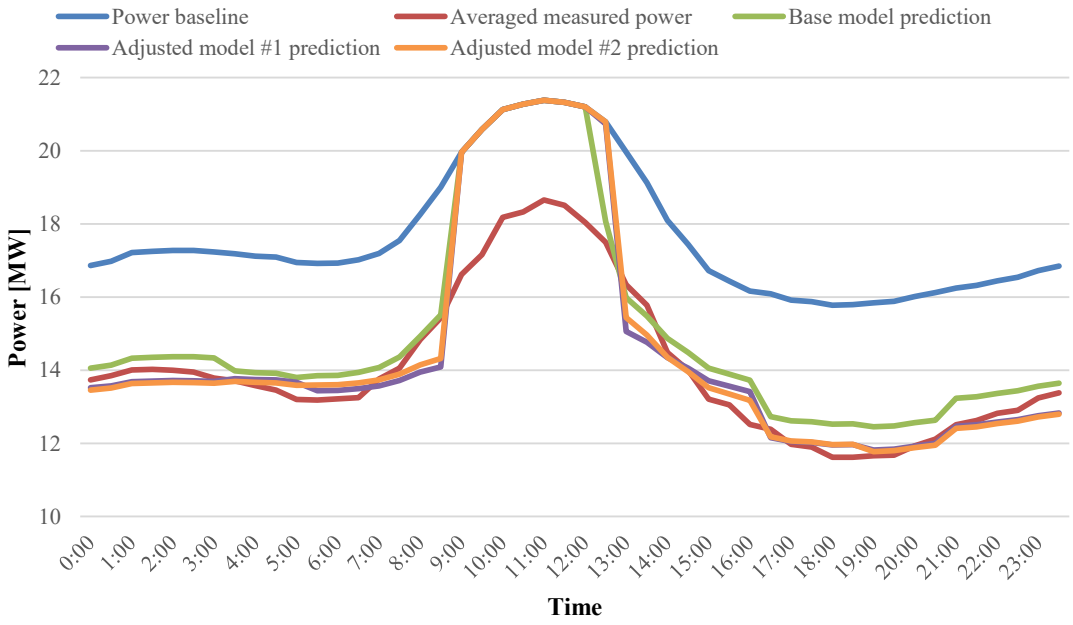

Figure 44 - Data average vs ERR method

3.6.3 Verification of ERR method zero percent optimisation

If a compressed air system has no implemented optimisation strategies, and all compressors are running on full load, the 24-hour profile will be a straight (constant) line. The power baseline for a compressed air system constantly under full load will consume the maximum

rated power indicated by the motors (disregarding minor fluctuations). This case will act as a worse case (un-optimized) compressed air network. The prediction capability of the models must be tested against this scenario to ensure applicability.

Figure 45 shows the prediction of the ERR models concerning a single reference power (peak power), which is calculated by averaging the power values of the drilling shift. The Stochastic Frontier Analysis (SFA) and Corrected Ordinary Least Square (COLS) methods have also been included to show within which quartile the profile is performing.

The original ERR model is the most underperforming model, which estimates a lower optimisation opportunity than the average or adjusted models. This is due to the irregularity where the post-implementation ERR is low at low percentages of pre-implementation ERR, which was discussed in section 3.5. The adjusted models correlate with the average value for zones 1-3, while the minimum boundary (COLS) of the prediction models correlate with the average value for zones 7-9. Figure 45 shows that the adjusted method is within 13.3% of the average value, the SFA method shows a 7% difference and the COLS method shows a 3.4 % difference. The highest's probability occurs between the adjusted method and the SFA method, with an average of 10% accuracy.

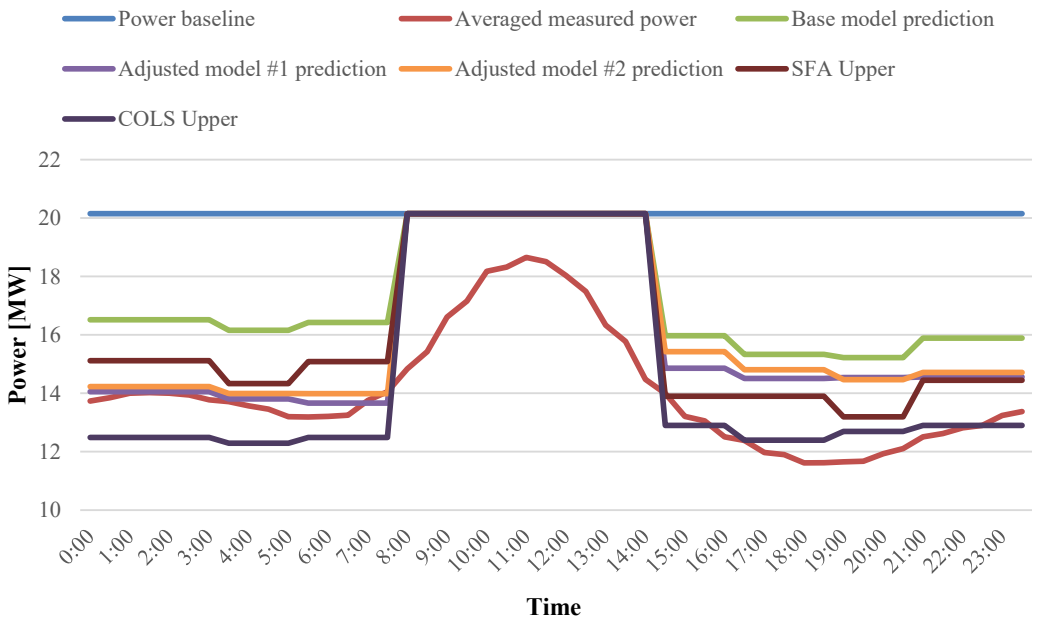

Figure 45 - Zero optimisation reference prediction

Prediction model 2 (purple) has shown the best overall performance with regard to statistical derivation in comparison with previous models, the average profile and the zero % estimation test. Therefore, this model will be used to estimate the cost savings potential of deep-level mines in South Africa.

Table 16 shows the summary of the verification tests done in this section. Adjusted model #1 has the best results in three out of the four categories indicated in green. The green blocks display the best performance, and the red blocks display unavailable data or the lowest performance.

Table 16 - Model evaluation summary

Verification Test	**Vermeulen**	**Base model (adapted from Vermeulen)**	**Adjusted model #1**	**Adjusted model #2**
Maximum ERR Range	50-60%	50-60%	50-60%	50-60%
Post-implementation ERR Offset	24.372	27.47	28.02	26.58
Comparison to statistical average (difference) *(0 is best)*		3.70%	0.90%	0.80%
Comparison to statistical average from a zero optimized profile *(100% is best)*		77.65%	89.02%	87.51%

3.7 Summary

This chapter described how statistical parameters were used to construct an estimation model which can aid in the estimation of energy savings on deep-level mine compressed air systems.

Section 3.2 described how M&V data for 29 compressed air systems could be collected, analysed and arranged in order to be used for future studies. The first hypothesis was tested and is in agreement with the estimation model. Section 3.3 provided multiple relational parameters, which concluded that the ERR parameters showed the most promise. The first primary objective was achieved by successfully conducting a study on the power profiles of compressed air systems on deep-level mines. Correlations do exist which can be used to

estimate the performance of other compressed air systems. The second hypothesis was tested and found in agreement with the methods used to determine the parameters.

Section 3.4 tested the parameters in section 3.3 to determine the most suitable parameters for a base model. The ERR parameters were used for 9 individual zones. The unique regression lines for each zone was used to construct the base estimation model. This model used 24-hour compressed air baseline information and produced a 24-hour profile estimation curve using the regression models of all 9 zones. The third and fourth hypotheses were tested and founded to be true for the ERR relationships which are calculated.

Section 3.5 evaluated the base model and identified some data shortcomings. This was because the data at around zero pre-implementation ERR was not physically possible. To mitigate this error, two adjusted models were created, based on the base model of section 3.4

Section 3.6 evaluated all models against previous research and normal averaging methods. The fifth hypothesis was tested, and the estimation model agreed with the literature findings. The correlation between known energy savings initiatives and the ERR parameters are evident in literature as well in the statistical analysis. The second objective was achieved by developing a model which can estimate the compressed air energy saving potential of a compressed air system on a deep-level mine. The final model can be expressed by Equation 15. The full expression is shown in Appendix Q.4, Equation 33.

Equation 15 - Final model expression

$$\overline{ERR_{post}} = \overline{y} = \overline{C} \cdot \overline{ERR_{pre}}^{2} + \overline{D} \cdot \overline{ERR_{pre}} + \overline{e}$$

$\overline{ERR_{post}}$	= Post-implementation ERR vector	[-]
$\overline{ERR_{pre}}$	= Pre-implementation ERR vector	[-]
$\overline{C}$	= Second order gradient vector	[-]
$\overline{D}$	= First order gradient vector	[-]
$\overline{e}$	= Constants vector	[-]

CHAPTER 4. IMPLEMENTATION & VALIDATION

4.1 Preamble

In this chapter, the adjusted model developed in Chapter 3.5 will be applied to real-life case studies. Chapter 4 has four main sections. The first and second sections display the results of the actual energy savings achieved vs the estimated energy savings for two case studies. The third section lists the irregularities and shortcomings found in the case studies. The last section concludes what the overall results were.

Two case studies were chosen which differed in initial maximum power usage: total shafts connect to the ring, compressor combinations, geographical location and different mining schedules. This aids in determining how robust the estimation model is for mines which have many operational differences.

This chapter will focus on the results obtained from the implementation of energy-saving initiatives, as well as complete compressed air simulations constructed to determine the effect of energy-saving initiatives. This chapter aims to indicate that the real-world results obtained correlate with the estimation model. The methodology used in each case study to achieve the results is displayed in Figure 46.

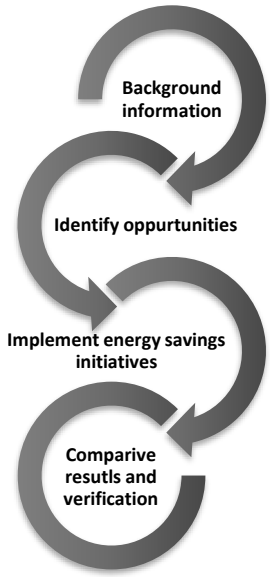

Figure 46 - Case study investigation methodology

4.2 Case study #1

4.2.1 Background information

The first case study is a platinum mining group near Rustenburg, South Africa. Most mining groups have multiple mines/shafts which are connected to an interconnected compressed air ring. The compressed air ring is a closed loop piping system that connects all the mines/shafts. Ordinary compressor houses supply the entire ring with compressed air, while the air is distributed to the shafts according to the demand on each shaft. Figure 47 displays the surface layout of the compressed air ring with all shafts interconnected. All suppliers and consumers have been indicated with function blocks.

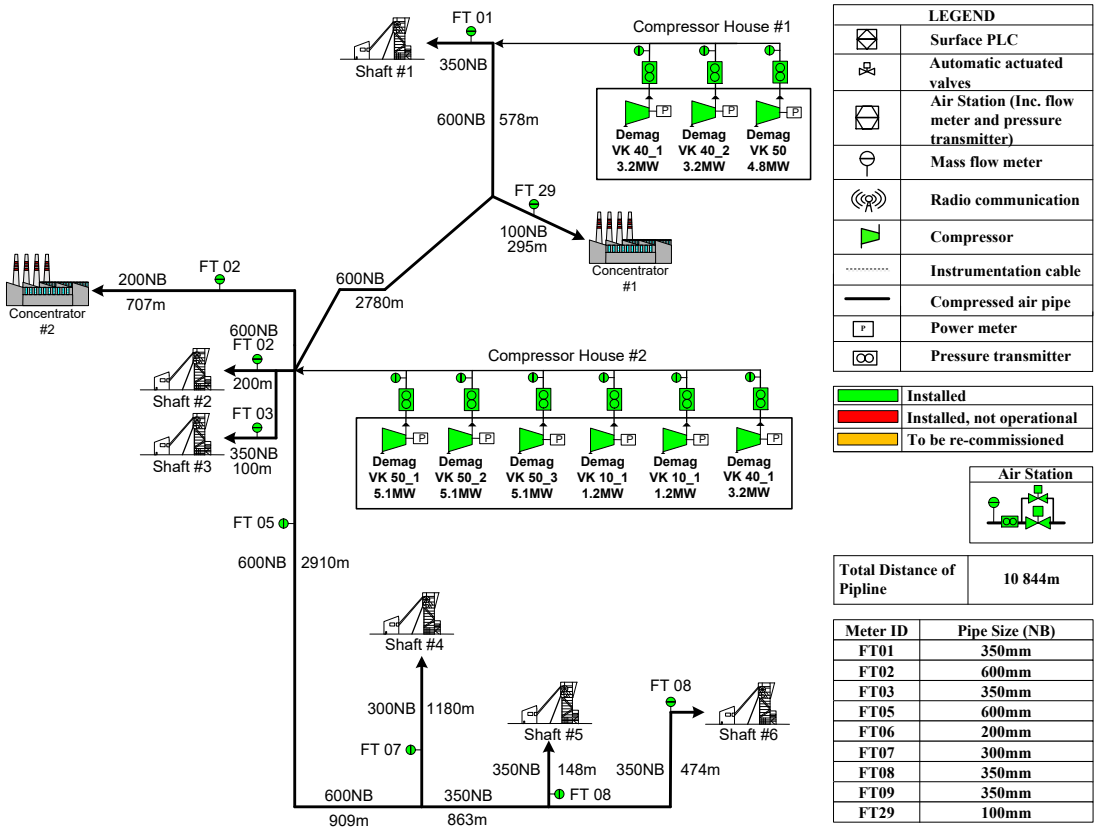

Figure 47 - Study case #1 surface layout

The compressed air ring can be categorised into three function blocks:

- Supply
- Distribution
- Demand units

A summary of the categorised infrastructure is given below.

Table 17 - Case study #1 surface summary

Supply	Distribution	Demand
VK50 - 5.1 MW	10.8 km of galvanised piping	Shaft #1 - Care and Maintenance
VK50 - 5.1 MW		Shaft #2 – Primary Shaft
VK50 - 5.1 MW		Shaft #3 – Linked to Shaft #2
VK10 - 1.2 MW		Shaft #4 – Care and Maintenance
VK10 - 1.2 MW		Shaft #5 – Secondary Shaft
VK40 – 3.2 MW		Shaft #6 – Care and Maintenance
VK50 - 4.8 MW		
VK40 - 3.2 MW		
VK40 - 3.2 MW		
32.1 MW	10.8km	2 Production Shafts

Figure 48 displays the primary production shaft connected to the compressed air ring of case study 1. 11 levels are connected to the vertical shaft, while eight levels are part of the decline shaft.

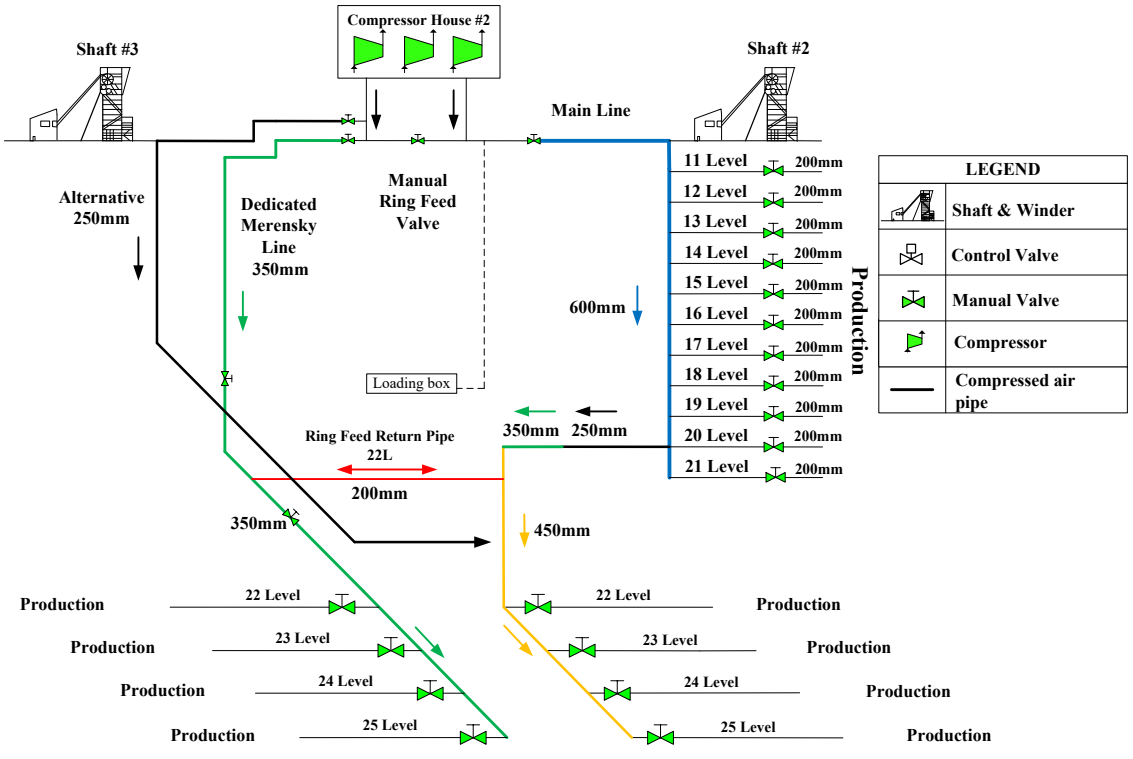

Figure 48 - Shaft #2 & #3 basic underground layout

Figure 49 displays the secondary production shaft connected to the compressed air ring of case study 1.

Eight levels are connected to the decline shaft. The highest production level is level 9. Therefore, a dedicated compressed air pipeline is connected from the surface of shaft #4 to shaft #5's level 9.

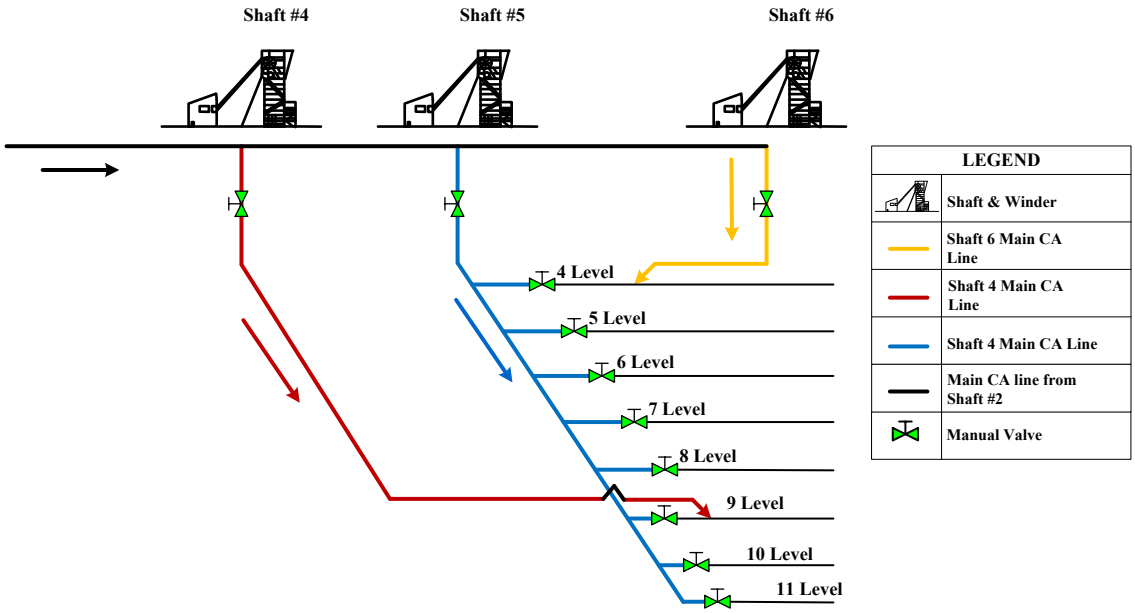

Figure 49 - Underground layout of secondary production shaft #5

4.2.2 Identified Opportunities

The first step in the identification of energy savings on the compressed air system of case #1 was to determine a baseline for weekly energy consumption. IST power loggers were used to capture data at the incomer providing the power to the compressor. Figure 50 indicates the power baseline (blue) constructed using the previous financial year (Sept 2015 – Sept 2016) values of case #1. The months of December and January were excluded in the construction of the baseline as these months have irregular workday patterns. The baseline report is attached in Appendix R.

The dark blue and dark green lines in Figure 50 indicate the most probable bandwidth of potential energy savings according to the proposed estimation model. The light blue line indicates the estimated optimised energy profile after the most common energy-savings initiative have been implemented. The light green is based on the regressions discussed in chapter 3.4.

Figure 50 indicates that an 11.25% energy saving opportunity exists over a 24-hour period, which amounts to a 2.070 MWh of energy saving. The estimated savings thus amount to R 9.37 Million per annum. The upper SFA prediction and lower SFA prediction generated a savings estimation bandwidth of 1.422 MWh to 3.018 MWh. This results in an annual cost savings bandwidth of R6.44 Million to R13.66 Million.

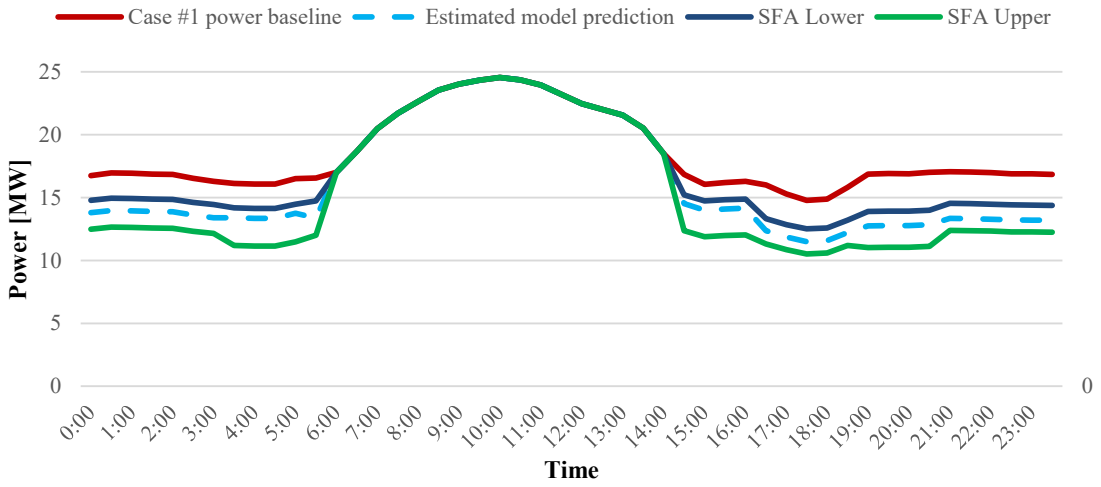

Figure 50 - Case #1 compressed air power baseline

4.2.3 Implementation of energy savings initiatives

After determining the estimated scope that existed on the compressed air network, a complete compressed air audit of the compressed air system was conducted. The compressed air audit included:

1. Characterisation of compressors
2. Inspection of distribution pipes that connected all five shafts
3. Stock-taking of control instrumentation on the surface and underground
4. Individual-level inspections of all active shafts
5. Inspection of underground distribution pipes on shaft #2 and #4
6. Measuring of compressed air flow and pressure for all levels and pipe branches
7. Construction of a compressed air simulation using the necessary parameters.

Process ToolboxTM (PTB) is a powerful simulation package for thermal-hydraulic systems. It can be used to simulate the compressed air, cooling and dewatering systems [41],[21],[37], [53]. The simulation package considers all the complex parameters and equations from section 2.2 to calculate the power consumed by the compressors. By comparing the estimation results with the simulation results, the relationship between fundamental engineering calculations and statistical analysis can be determined.

Figure 51 displays the thermodynamic and power parameters used in the simulations. The complete simulation layout can be found in Appendix S.

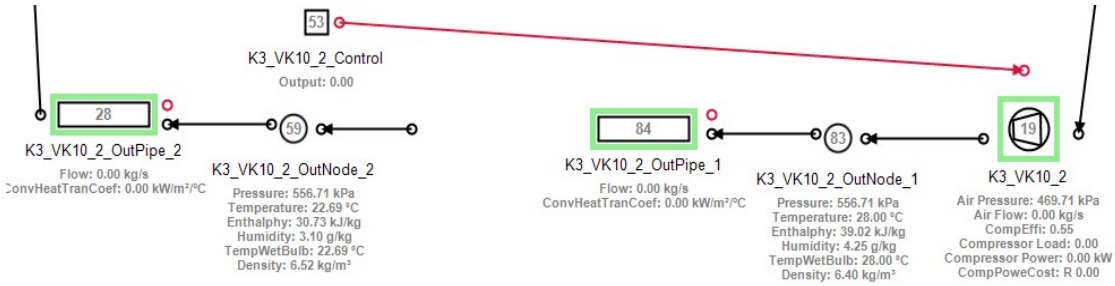

Figure 51 - Typical simulation configuration for a compressor

The simulation can be constructed because of the instrumentation installed on the compressed air ring. The compressed air measuring instrumentation consists of power loggers connected to the compressor motors, flow and pressure loggers connected at specific nodes and valve-positioners installed with the compressed air control valves. The compressed air simulation for case #1 was constructed using the measurement data provided by the Information Management System (SCADA) of case study #1. Figure 52 shows the simulation results vs the actual measured power from the motor of the compressors. The average positive difference in power is 1.66%, and the average negative difference is 2.9 %. Therefore, the difference bandwidth is smaller than 4%. Due to the accuracy of the simulation results, the simulations were used to determine the impact of specific energy-saving initiatives on the system, regarding power consumption, flow and pressure.

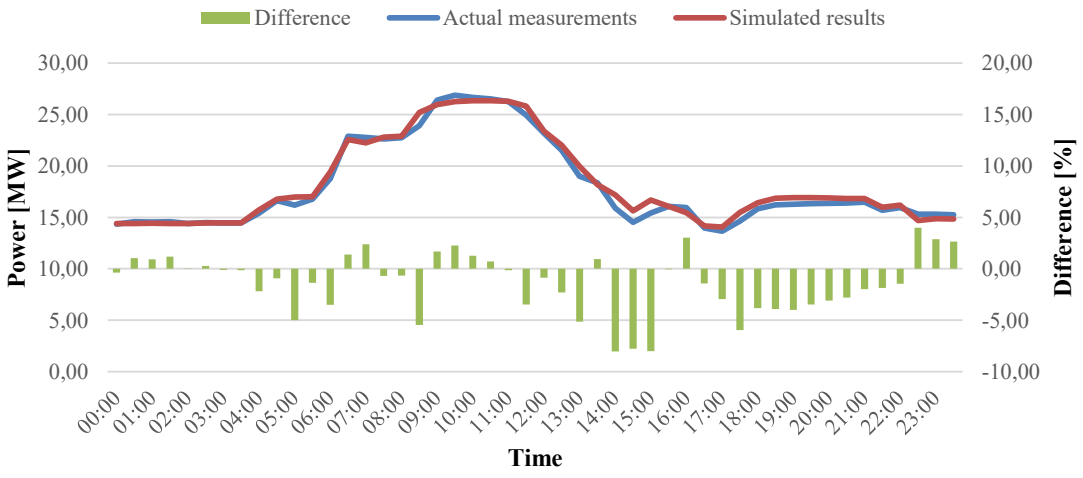

Figure 52 – Case study #1 compressor power simulation results

During the compressed air investigation process and after the simulations were constructed, specific projects were identified, simulated and implemented. These projects were all according to the most common compressed air initiatives discussed in section 1.4.

Table 18 shows a summary of the energy-saving initiatives that were implemented on case study #1. The specific area where an initiative was implemented is shown in green, and an initiative was not implemented due to the scope or other logistical reason, given in red.

Table 18 – Case study #1 implemented energy savings initiatives summary

Energy Saving Initiative	**Reference**	**Compressors**	**Shaft #1**	**Shaft #2**	**Shaft #3**	**Shaft #4**	**Shaft #5**	**Shaft #6**
Compressor setpoint control (reduction)	[21]	X	X	X				
Compressed air pipe leak identification and repair	[27]	X	X	X	X	X	X	X
Surface main control valve scheduling	[32]	X	X	X	X	X	X	X
Underground compressed air valve installation and scheduling	[21]			X	X		X	
Temporary closure of inactive mining levels and sub-levels	[34]		X	X	X	X	X	X
Optimisation of compressed air pipe configurations and pipe sizing.	[30]			X	X		X	

An investigation work breakdown analysis for case study #1 is given in Table 19. Project certainty, project complexity and the resources used are the most critical variables.

Table 19 shows the total implementation time for each subsection, yet the total amount of time is not equal to the total amount of time of the project due to specific tasks that coincided. A total of 39 weeks (sum of the red numbers) spent obtaining data, doing audits and simulating the effect of energy savings initiatives.

Table 19 – Case study #1 compressed air investigation work breakdown

ESCO Action Item	Required Time	Required Resources	Number of Personnel	Complexity [0 - 10]	Project Certainty [0 -10]
Contact client	**4 Week**	**Senior Engineering Personnel**	**2**	**4**	**0**
Obtain permission to investigate	**6 Weeks**	**Multiple Engineering Personnel**	**2**	**5**	**1**
Access objections	2 Week	Senior Engineering Personnel	2	4	1
Propose alternative solutions	1 Week	Senior Engineering Personnel	2	5	1
Arrange site visits	1 Week	Junior Engineer	2	2	1
Obtain layouts	2 Weeks	Junior Engineer	2	2	1
Obtain data	**14 Weeks**	**Junior Engineering Personnel**	**4**	**4**	**4**
Compressor data	5 Weeks	Junior Engineering Personnel	4	4	3
Valve data	6 Week	Junior Engineering Personnel	4	3	3
Mining level compressed air data	3 Week	Junior Engineering Personnel	4	4	4
Compressed air audits	**18 Weeks**	**Junior Engineering Personnel**	**3**	**4**	**5**
Level investigations	15 Weeks	Junior Engineering Personnel	3	4	5
Surface investigations	3	Junior Engineering Personnel	2	3	4
Simulate	**7 Weeks**	**Multiple Engineering Personnel**	**2**	**8**	**8**
Formulate a baseline simulation model	3 Weeks	Senior Simulation Personnel	1	7	6
Validate the baseline simulation model	1 Week	Simulation Personnel/ Project Engineer	2	4	6
Implement simulation scenarios	1 Week	Simulation Personnel & Project Engineer	2	7	7
Annalise simulation scenario results	1 Week	Simulation Personnel & Project Engineer	2	8	8
Verify simulation scenario results	1 Week	Simulation and Project Engineers	2	4	9
Summary	**49 Weeks**	**Multiple Engineering Personnel**	4	8	9

4.2.4 Comparative results and validation

The weekday profiles of the three months were taken and averaged to determine the effect that the energy-saving initiatives had on the power consumption of the compressors' motors.

Figure 53 shows that the peak drilling shift of case study #1 is from 06:00 to 14:00. Due to production targets, the mine only allowed for projects that did not affect the peak drilling shift.

During the early morning period from 0:00 – 06:00, the average difference between the estimated value and the actual performance result is 1.03%. During the evening period, the average difference between the estimation model and performance results is 9.21%. The difference between the SFA boundary and the performance results are 2.45%. The total estimated daily profile energy savings was **2.07 MWh,** and the total actual energy savings was **1.722 MWh**. Thus an **83.18 %** accuracy was achieved by the estimation model.

The prediction was 83.18% accurate, and it took only a few minutes to implement. This significantly reduces the amount of time to achieve the project certainty, as discussed in Table 19. A junior engineer acquired the baseline data and implemented the estimation model. This shows that only a basic understanding of the system is required. This model also provided a practical way of benchmarking the power profile of a compressed air network. The mining group can implement the same model to determine if the saving potential exists on other shafts.

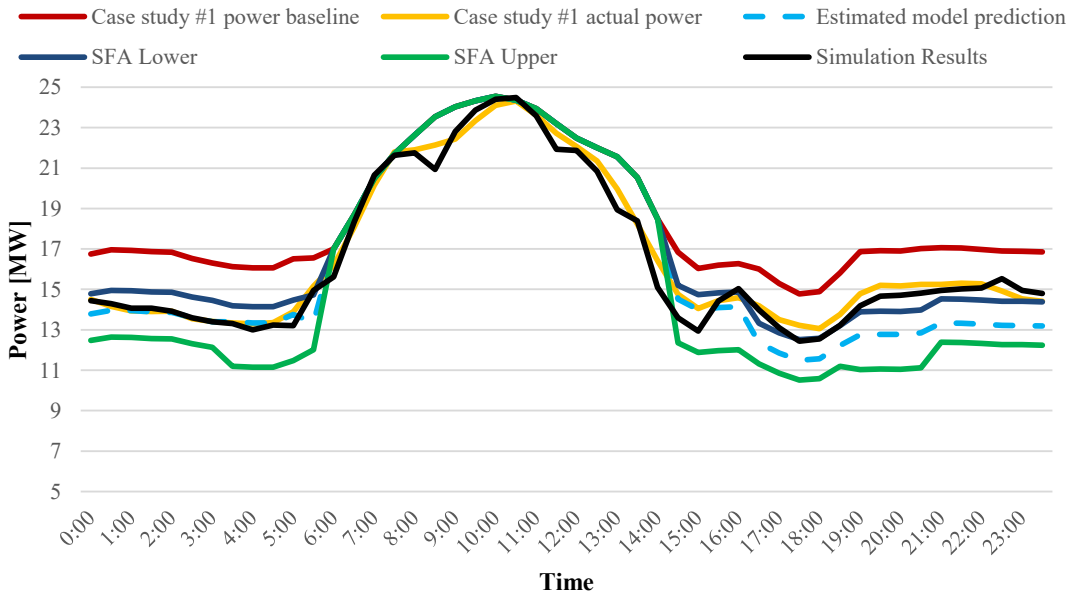

Figure 53 - Case #1 performance measurement results vs model estimation

The day-to-day results differ slightly. Figure 54 indicates the profile of a day when the energy-saving initiatives had the most significant impact. The estimated energy savings was set at **2.07 MWh,** and the energy savings achieved was **2.1 MWh.** Therefore, 100% of the estimated energy saving potential was achieved.

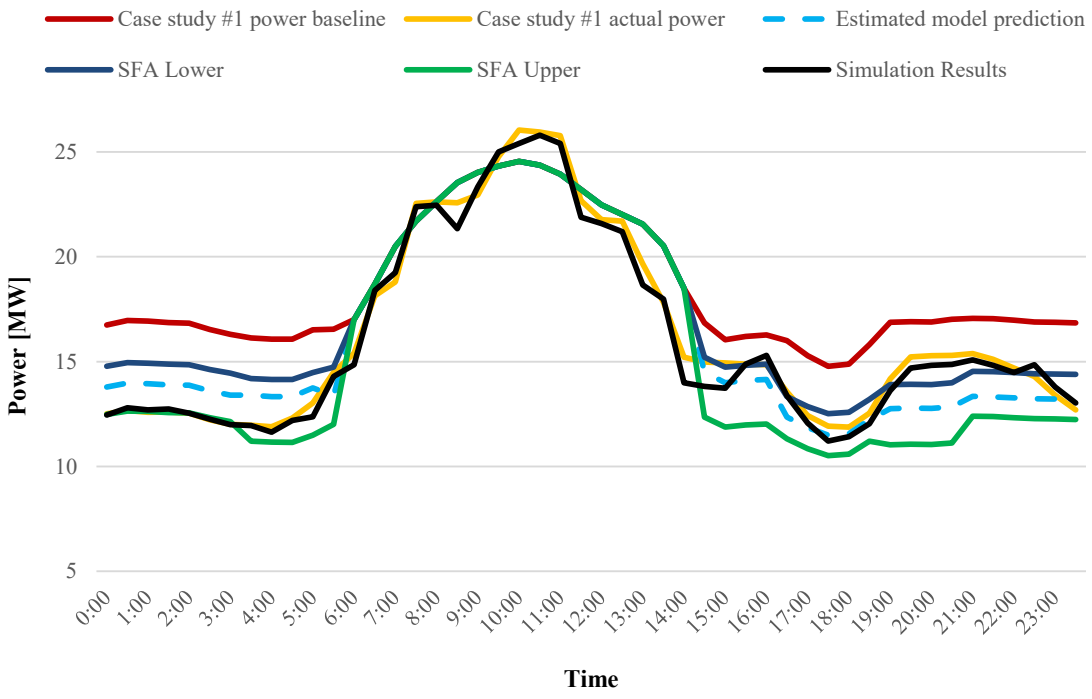

Figure 54 – Case study #1 maximum impact

4.3 Case study #2

4.3.1 Layout and description of compressed air network

The second case study is also a platinum mining group (business unit) near Rustenburg, South Africa. The configuration of this business unit closely resembles the previous case study where more than one operational unit is connected to a compressor house which supplies all the compressed air.

Figure 55 displays the surface layout of the compressed air ring present in case study #2. The legend to the right explains the use of specific schematic icons. The segment highlighted in red is infrastructure still present, but not connected to, the central compressed air ring. These operational units are also not managed by the mining group but are sub-contracted.

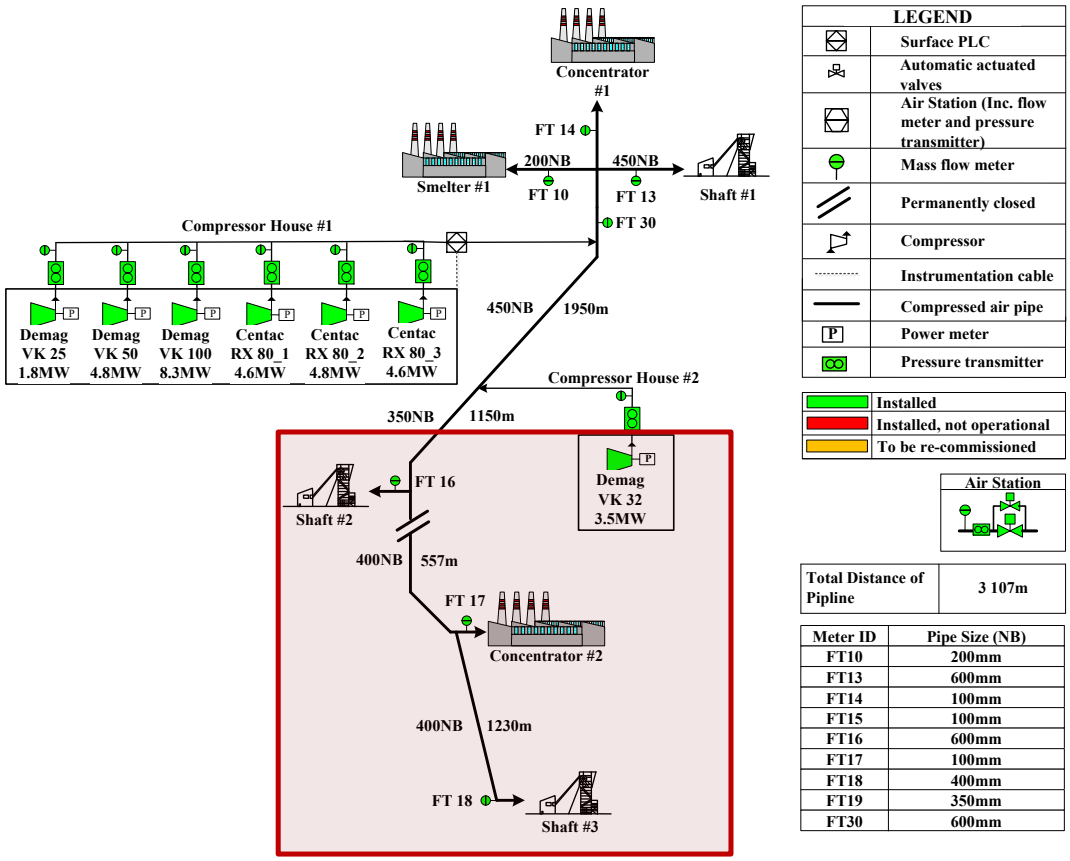

Figure 55 - Case study #2 compressed air ring surface layout

The compressed air ring can also be categorised into three function blocks - supply, distribution and demand units. A summary of the categorised infrastructure is given in Table 20. The VK32 compressor is installed but not in working condition and is displayed in red.

Table 20 – Case study #2 surface summary

Supply	Distribution	Demand
VK100 – 8.3 MW	3.1 km of galvanised piping	Shaft #1 - Primary Shaft
VK50 – 4.8 MW		Shaft #2 – Contractors Shaft
VK25 – 1.8 MW		
Centac_1- 4.6 MW		
Centac_2- 4.6 MW		
Centac_3- 4.6 MW		
VK32 – 2.8 MW		
28.7 MW	3.1 km	2 Production Shafts

Figure 56 displays the underground compressed air network of shaft #1 in study case #2 The shaft is divided into two parts, a vertical shaft and decline shaft shown at the bottom right. The configuration of the compressed air pipes and the different compressed air requirements of each mining level contributes to the overall compressed air demand and relating power consumption of the compressors' motors.

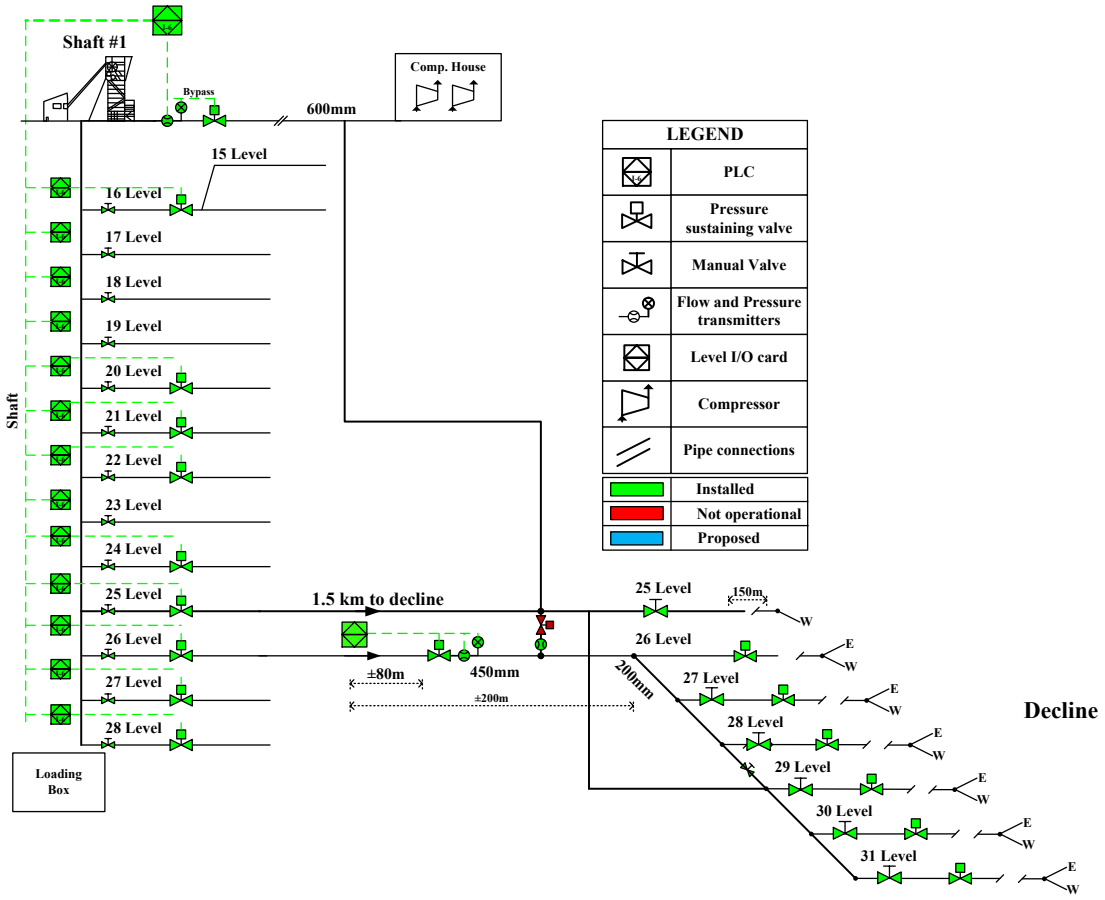

Figure 56 - Shaft #1 underground compressed air layout

4.3.2 Identified Opportunities

The first step in the identification of energy savings on the compressed air system of case #2 was to determine a baseline for weekly energy consumption. IST (Integrators of Systems Technology) power loggers were used to capture data at the incomer providing the compressor motors with electrical power. Figure 57 displays the power baseline for case #2 (red) constructed using the values from the previous financial year (Sept 2015 – Sept 2016). The months of December and January were excluded in the construction of the baseline as these months have irregular workday patterns.

The upper and lower SFA (Stochastic Frontier Analysis) curves are the boundary lines which indicate the most likely area where results will occur. The estimated prediction model is indicated in light blue.

The baseline report is attached in Appendix T. Figure 57 indicates that an 11.9% energy saving opportunity exists over a 24-hour period, which amounts to 1.287 MWh energy saving. This amounts to an R 5.7 Million costs saving opportunity per annum.

The upper SFA prediction and lower SFA prediction generated a savings estimation bandwidth of 0.65 MWh to 1.86 MWh. This results in an annual cost savings bandwidth of R 2.96 Million to R 8.42 Million.

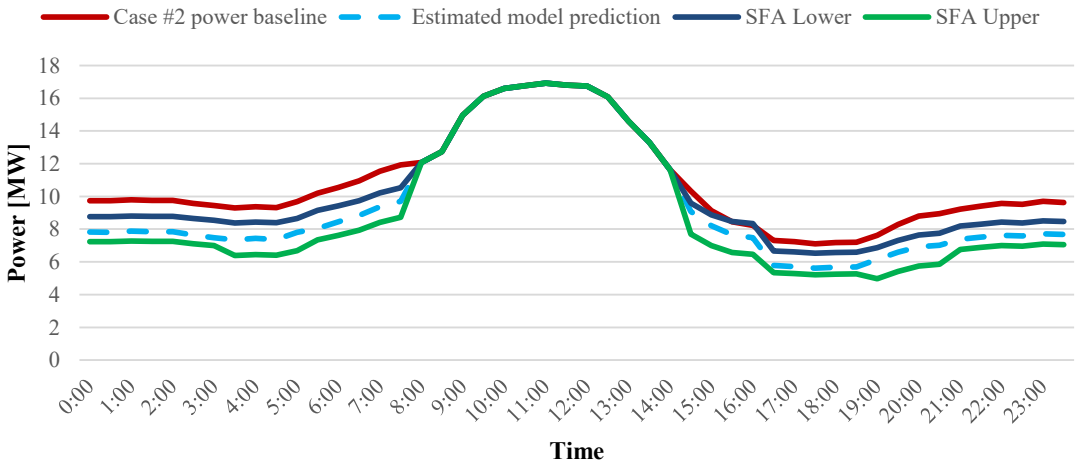

Figure 57 - Case #2 compressed air power baseline

4.3.3 Implementation of energy savings initiatives

After determining the estimated scope that existed on the compressed air network, a complete compressed air audit of the compressed air system was conducted. The compressed air audit included:

1. Characterisation of compressors at compressor house #1
2. Inspection of distribution pipes that connected shaft #1 and shaft #2
3. Stocktaking of control instrumentation on surface and underground
4. Individual-level inspections at shaft #1
5. Inspection of underground distribution pipes on shaft #1
6. The measuring of compressed air flow and pressure for all levels and pipe branches
7. Construction of a compressed air simulation using the necessary parameters

Process ToolboxTM (PTB) was used to develop a complete compressed air simulation of the compressed air network within the limits of the parameters made available by the mining group. Figure 58 displays a piece of the simulation constructed for case study #2. The thermal and compressed air parameters used in the simulation are also visible. The full simulation layout is attached in Appendix U. By comparing the estimation results with the simulation results, the relationship between fundamental engineering calculations and statistical analysis was determined.

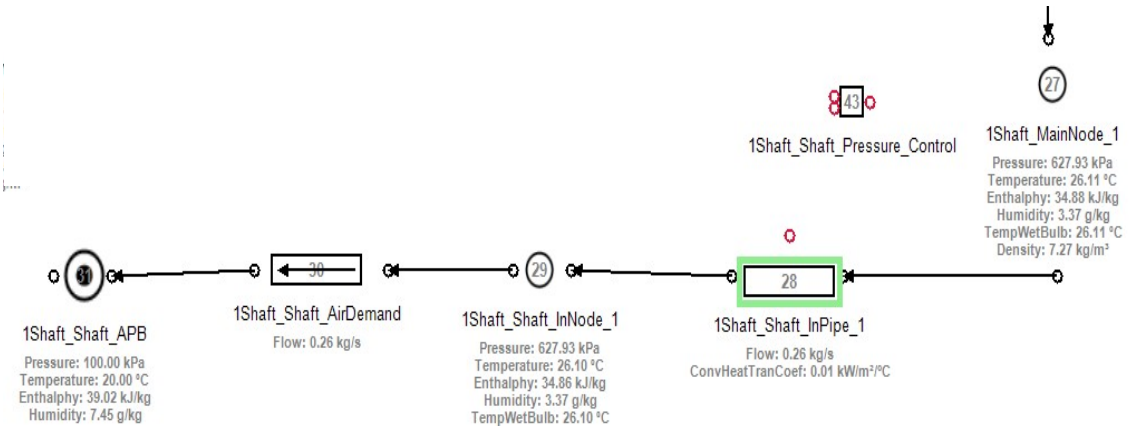

Figure 58 - Case #2 simulation snippet with parameters

The compressed air measuring instrumentation consists of power loggers connected to the compressor motors, flow and pressure loggers connected at specific nodes and valve-positioners installed with the compressed air control valves. The compressed air simulation for case #2 was constructed using the measurement data provided by the Information Management System (SCADA).

Figure 58 and Figure 59 show the simulation results vs the actual baseline power from the motor of the compressors. The average positive difference in power is 2.06% and the average negative difference is 4.54 %. Therefore, the difference bandwidth is smaller than 7%.

Due to the accuracy of the simulation results, the simulations were used to determine the impact of specific energy-saving initiatives on the system, regarding power consumption, flow and pressure. The simulations will be used to validate estimated profile provided by the proposed statistical model. As the simulations are based on fundamental thermodynamic and fluid calculations, it will validate if the statistical approach adheres to the variables influencing power consumption.

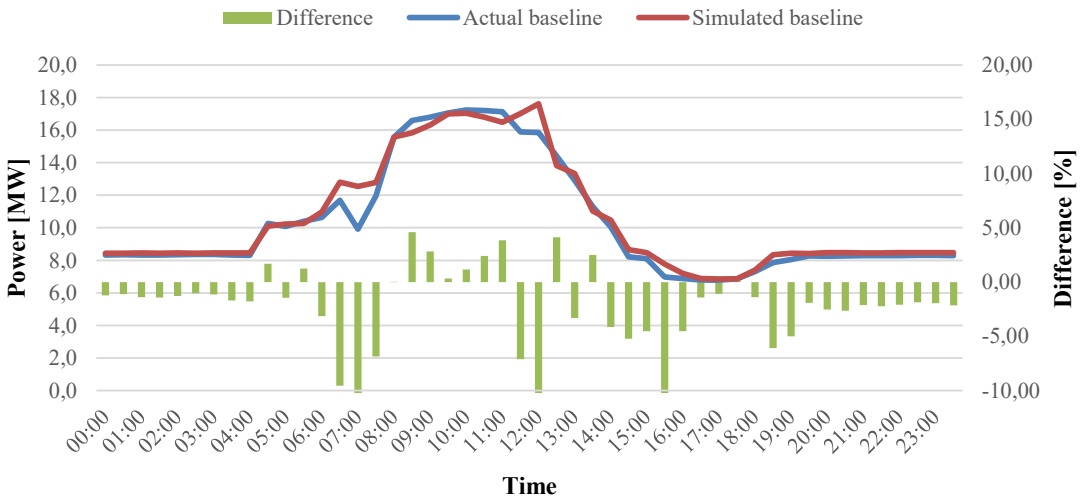

Figure 59 - Case study #2 baseline simulation results

During the compressed air investigation process, and after the simulations were constructed, specific projects were identified and implemented. These projects were all according to the most common compressed air initiatives discussed in section 1.4. Table 21 shows a summary of the energy-saving initiatives that were implemented in case study #1. The specific area where an initiative was implemented, or which was affected, is shown in green; the colour red is assigned to where an initiative was not implemented due to the scope or other logistical reason.

Table 21 - Case study #2 implemented energy savings initiatives summary

Energy Saving Initiative	Reference	Compressors	Shaft #1	Shaft #2
Compressor setpoint control (reduction)	[21]	X	X	X
Compressed air pipe leak identification and repair	[27], [28]	X	X	X
Surface main control valve scheduling	[32]	X	X	X
Underground compressed air valve installation and scheduling	[21]			
Temporary closure of inactive mining levels and sub-levels	[34]		X	
Optimisation of compressed air pipe configurations and pipe sizing.	[30], [31]			

An investigation work breakdown analysis for case study #2 is given in Table 22. Project certainty, project complexity and the resources used are the most critical variables. Table 22 shows the total implementation time for each subsection, yet the total amount of time is not equal to the total amount of time of the project, due to specific tasks that coincided. A total of 29 weeks (sum of the red numbers) spent obtaining data, doing audits and simulating the effect of energy savings initiatives.

Table 22 - Case #2 Compressed air investigation work breakdown

ESCO Action Item	**Required Time**	**Required Resources**	**Number of Personnel**	**Complexity [0 - 10]**	**Project Certainty [0 -10]**
Contact client	**3 Week**	**Senior Engineering Personnel**	**2**	**4**	**0**
Obtain permission to investigate	**4 Weeks**	**Multiple Engineering Personnel**	**2**	**5**	**1**
Access objections	1 Week	Senior Engineering Personnel	2	4	1
Propose alternative solutions	1 Week	Senior Engineering Personnel	2	5	1
Arrange site visits	1 Week	Junior Engineer	2	2	1
Obtain layouts	1 Weeks	Junior Engineer	2	2	1
Obtain data	**9 Weeks**	**Junior Engineering Personnel**	**4**	**4**	**4**
Compressor data	4 Weeks	Junior Engineering Personnel	4	4	3
Valve data	4 Week	Junior Engineering Personnel	4	3	3
Mining level compressed air data	1 Week	Junior Engineering Personnel	4	4	4
Compressed air audits	**12 Weeks**	**Junior Engineering Personnel**	**3**	**4**	**5**
Level investigations	9 Weeks	Junior Engineering Personnel	3	4	5
Surface investigations	3 Weeks	Junior Engineering Personnel	2	3	4
Simulate	**8 Weeks**	**Multiple Engineering Personnel**	**2**	**8**	**9**
Formulate a baseline simulation model	3 Weeks	Senior Simulation Personnel	1	7	6
Validate the baseline simulation model	2 Week	Simulation Personnel/ Project Engineer	2	4	7
Implement simulation scenarios	1 Week	Simulation Personnel & Project Engineer	2	7	8
Annalise simulation scenario results	1 Week	Simulation Personnel & Project Engineer	2	8	8
Verify simulation scenario results	1 Week	Simulation and Project Engineers	2	4	9
Summary	**36 Weeks**	**Multiple Engineering Personnel**	4	8	9

4.3.4 Comparative results and validation

The weekday profiles of three months were taken and averaged to determine the effect that the energy-saving initiatives had on the power consumption of the compressors' motors. Figure 60 shows that the peak drilling shift of case study #1 is from 08:00 to 14:00.

Due to production targets, the mine only allowed for projects that did not affect the peak drilling shift. During the early morning period from 0:00 – 06:00, the average difference between the estimated value (light blue) and the actual performance (orange) result was **5.66%**.

During the evening period, the average difference between the estimation model and performance results are **11.96%**. The difference between the SFA boundary and the performance results were **2.36%**. The SFA boundary predicted a minimum of 0.605 MWh energy-saving potential. The actual savings exceeded the SFA predicted minimum by 0.117 MWh.

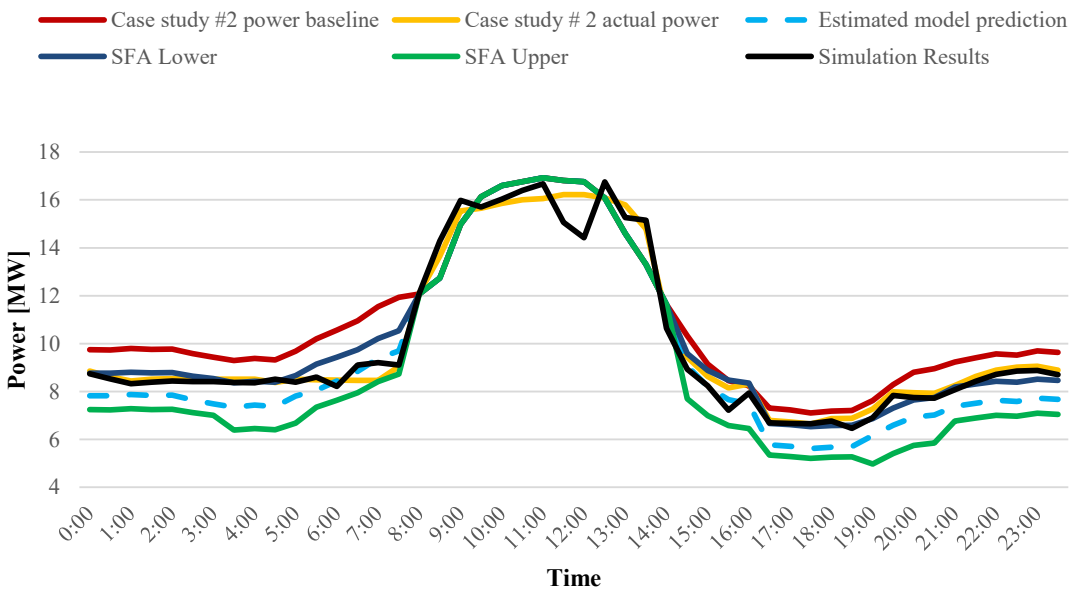

Figure 60 - Case study #2 performance measurement results vs model estimation

The total estimated daily profile energy savings was 1.28 MWh and the total actual energy savings was 0.722 MWh. Thus, a **56.14%** accuracy was achieved by the estimation model. Constraints limiting the energy efficiency initiatives were identified, and a test was conducted to determine the savings if the constraints have been mitigated. The results indicated that the model estimation was **78%** accurate, predicting a 1.007 MWh saving.

Two significant constraints limited the energy savings potential of the compressed air system of case study #2. The first was a compressed air configuration restriction which only allowed for the VK100 (8.3 MW) compressor to be used during off-peak periods. The compressor power usage could not be decreased further than 6.6 MW using the guide vane controller, as the risk for a surge condition increased.

The second constraint was the actuating control valve which controlled the opening and closing of the skip doors on shaft #1. The valve is restricting exhaust flow from the actuator, creating a back-pressure. The opening force of the actuating arm is reduced resulting in an ineffective operation of the skips. This error resulted in a higher-pressure demand during non-peak drilling shift, leading to higher power consumption by the compressor motors. Case study #1 and #2 have different loading box and skip door mechanisms. A business case was submitted to mitigate the error but has not yet been enforced.

A pressure reduction test was conducted which decreased the operating pressure until normal operations were negatively affected by the pressure decrease. Figure 61 displays the average performance (red) with a comparison to the pressure reduction test profile (yellow). A significant decrease in power is shown in the evening period from 19:00 – 00:00. This indicates that further scope for energy savings exists once the actuating control arms are replaced. The energy savings estimation increased from 56% to 78% of the actual energy saved during the drop test. This increase was from 0.772 MWh to 1.007 MWh.

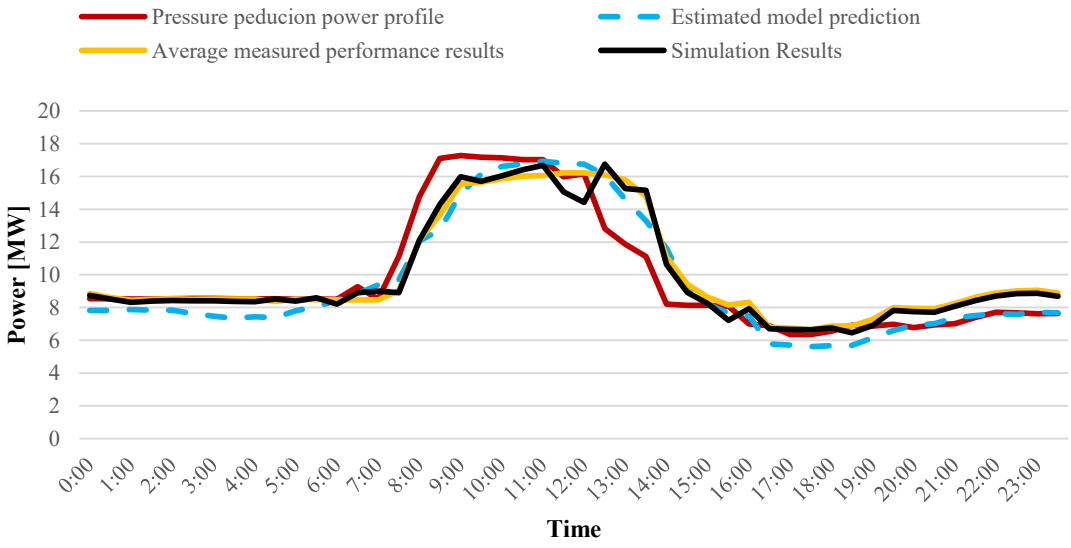

Figure 61 - Case study #2 drop test comparison results

4.4 Resource comparison

Table 23 - ESCo - resource comparrison

Normal Methodology			**Statistical Method**	
Action	Time	Resources	Time	Resources
Contact client	7	8 Engineers	2	2 Engineers
Obtain permission to investigate	10		2	
Obtain data	29		1	
Compressed air audits	30		-	
Simulate	15		-	
Determine Feasibility	91 Weeks		5 Weeks	

The decrease in time spent to determine the feasibility of compressed air energy savings initiatives also had multiple indirect effects.

1. It ensures that an ESCo can determine the scope of compressed air projects before contracts can be negotiated with the client mines.
2. It decreases the time that mining clients need to wait to see the potential impact that an ESCo can have. (40 weeks in this case as investigation were conducted simultaneously).
3. It ensures that mines can submit budgets for necessary infrastructure which will be required. As business units and departments are collaborating on a single compressed air ring, budgets need to be proposed by and approved beforehand, sometimes being a year in advanced. This ensures that capital can be made available at the appointed time – reducing the implementation time of the initiatives. (In this case the ESCo needed to wait 11 months to submit a budget proposal.

If energy saving initiatives were not feasibility, the time spent on these non-feasible projects could be spent elsewhere – saving the personnel cost of 8 engineers for 91 weeks. Implementation of projects on locations were the feasibility of compressed air energy savings

initiatives were determined can be fast-tracked. According to PayScale.com [17] the personnel cost which could have been saved in this case is averaged at R 1.14 Million, while cost for using the statistical method only amounted to R88,000.00. This would have saved R 1.05 Million in personnel costs.

4.5 Limitations and constraints

During the identification of compressed air energy savings potential and the implementation of compressed air energy-saving initiatives, two significant constraints were identified. These include capital and control constraints. Each of these constraints is discussed in the following sections.

Capital expenditure

Some of the projects required capital to either upgrade or install new infrastructure. This process is subject to multiple role-players who need to approve the release of capital from the client mine. Because of budgeting and time constraints, individual projects could not be implemented. For case study #1, a pipe-replacement project was delayed. This project can further reduce energy consumption in the evening period. For case study #2, the actuating valves configuration needs to be replaced, also increasing the scope for energy savings.

Control of compressed air network

Irregular control of compressed air network caused inconsistent results. Multiple operators and multiple personal managing compressed air systems do not always adhere to suggested operating procedures or schedules.

Therefore, the performance of the compressed air network does not always stay consistent. Intricate systems like compressed air networks require skilled and disciplined personnel/managers.

4.6 Conclusion

The most common energy-saving initiatives on compressed air systems were implemented in two different case studies which varied in power consumption, topology and operating schedules. In both cases, an estimation model was used to estimate the achievable energy savings if the most common energy-saving initiatives were to be implemented. The estimated results were 83% and 78 % accurate, respectively. Also, the time it took to obtain data, do compressed air audits and simulate the effects of energy savings initiatives took 49 and 36 weeks respectively. By using the cost savings estimation model, the action to implement the energy savings initiatives could be approved more than half a year earlier.

To obtain the estimated results, a typical/monthly averaged 24-hour profile was used as an input parameter. Typically compressed air simulations, and other prediction methods, require multiple complex parameters as inputs. The investigated estimation results can be obtained within a day, where-as conducting sophisticated compressed air investigations can take several months, as shown in each case study.

Table 19 and Table 22 summarise the resources that a typical ESCo spent on determining the feasibility of a compressed air energy savings initiatives on two compressed air rings. Although the two compressed air rings had different levels of compressed air optimisation infrastructure, advanced compressed air audits and simulations was required to determine feasibility of said initiatives. Table 23 summarises the time and human resources it took an ESCo to present a feasibility study using the normal engineering process as stated by Joubert [18], as well as the statistical method suggested by this study. Table 23 displays the decrease of 91 weeks to five weeks and the decrease of personnel from eight engineers to two. A potential of R 1.05 Million could also have been saved in the event that the compressed air energy savings initiatives were not proven feasible.

The developed cost-saving estimation model provided the following results:

- The time required to estimate the saving potential of the compressed air systems accurately was significantly reduced.
- Accurate predictions were obtained, which correlated with real-world results.
- The resource required to apply the model was only one junior engineer.

- The results obtained by implementing compressed air initiatives were acceptable to the mining group. Thus, the project certainty as predicted by the estimation model is also regarded as acceptable. The survey mentioned in Chapter 1 showed that an average of 7 out of 10 project certainty was obtained after simulations have been constructed. The project certainty presented by the estimation model is 83% and 78 % respectively.
- This model provided a mining group with a valuable benchmarking method to evaluate the energy-saving potential of multiple mines in the group. This also ensures the robustness of the estimation model.

CHAPTER 5. CONCLUSION & RECOMMENDATIONS

5.1 Conclusion

The past decade has witnessed a South African electricity tariff increase of 403%, with a further 15% annual increase submitted to the National Energy Regulator of South Africa for approval. This dramatic increase in electricity cost has made it crucial for industries to rethink how they implement and manage their infrastructure.

This study aimed to investigate the feasibility of a cost-saving identification model which aims to determine the cost-saving potential of a mine's compressed air system. Three study objectives were identified which would ensure that the study aim was met.

The first objective was to complete research on compressed air power profiles, operating schedules and compressed air management techniques. The tools previous researchers have used to estimate the cost-saving potential of compressed air systems were also investigated and evaluated. Within the literature study, a new parameter "Energy Reduction Ratio" (ERR) was identified to hold the most significant promise for accurate estimations. Thus, the first objective was successfully met.

The second objective was met by developing a cost saving identification model in chapter 3.4 – 3.6 which:

- Decreased the time to make an accurate potential cost-saving estimation for compressed air systems.
- Provided accurate estimations compared to detailed simulations.
- Used fewer resources (personnel, equipment and time) to obtain the estimation than previous methods.
- Provided an acceptable level of certainty that the most common compressed air initiatives will produce the estimated results.
- Provided a dynamic benchmarking method for a 24-hour compressed air power profile.

The third objective was to validate the cost saving identification model by implementing it on multiple case studies to test its robustness. Chapter 4 implemented the cost savings identification model in two case studies. The estimated savings for case study #1 was R 9.4 Million, while the actual savings were R 7.8 Million. The estimated savings for case study #2 were R 5.7 Million, and the actual savings were R4.4 Million. This is based on the three-month average profiles of the two case studies. Both mines' compressed air systems still have on-going projects, which indicate that there is still scope to increase the actual savings.

The study objectives were addressed by investigating tools previously used by researchers in the same field and using these tools to construct a customised solution. Chapter 2 determined the complexity of the factors influencing compressed air power profiles. Chapter 3.2 provided a statistical investigation which determined whether a correlation exists between the power profiles of compressed air systems. The actual compressed air power profiles of 29 mines were used to investigate possible relationships. The information used was verified by M&V teams and the results verified by Eskom.

Chapter 3.3 indicated that the larger the system, the higher the scope for energy saving opportunities. However, it could not be used to show precisely how much can be saved. Maximum, average and minimum values summarising the 24-hour profiles were used, but no significant correlation could be determined. The Energy Reduction Ratio (ERR) parameters were identified as the best statistical parameter to be used in the development of a cost saving identification model.

In Chapter 3.4 the data for 29 mines was used to create a regression formula with good regression coefficients ranging between 70% and 80% over nine periods. Together these periods formed a 24-hour regression model which could estimate the energy-saving scope present on a deep-level mine.

The primary objective of mines is to extract ore, and therefore mines are less prone to allow for energy-saving initiatives to be conducted during peak drilling shifts. The data for this period was very distorted, and no significant correlation (R^2 < 70%) was found. Therefore, the estimation model was restricted to non-peak drilling shifts, from 00:00 – 09:00 and 13:00-23:59.

In Chapter 3.5 the estimation model was refined when outliers in the regression model were identified. This led to an adjustment of the base power estimation model. Previous researchers' results validated the refined model, and the dynamic ERR operating range of the model was also verified. The model is thus suitable for any compressed air system on a deep level mine which has a baseline ERR lower than 50% in the morning and lower than 60% in the evenings. The model was constructed for nine different periods and, therefore, individual periods can be used to determine the potential energy savings for a system during a specific time.

In Chapter 4 the implementation of the energy-saving initiatives was conducted by mining personnel and a third party ESCo. The model was used by the ESCo to determine the scope of the energy savings on the compressed air systems. The normal compressed air investigation process was followed as a reference procedure. The implementation of the most common compressed air energy savings initiatives resulted in cost savings being achieved. A junior engineer gathered the baseline data and used the model, which provided acceptable results in comparison to the typical compressed air investigation outputs.

The cost savings estimation model proved 83% and 78% accurate in predicting the cost-saving potential of two case studies. The cost estimation model was implemented by a junior engineer and only required the power baseline as input for the entire case study. Significant time could have been saved, and engineering resources spared by implementing the cost savings identification model in both case studies. This successfully validated the cost savings identification model.

Section 4.6 summarises the time and human resources it took an ESCo to present a feasibility study using the normal engineering process as stated by Joubert [18], as well as the statistical method suggested by this study. Section 4.6 displays the decrease of 91 weeks to five weeks and the decrease of personnel from eight engineers to two. A potential of R 1.05 Million could also have been saved regarding personnel costs in the event that the compressed air energy savings initiatives were not proven feasible.

As a result, all objectives were met and the primary objective to construct a compressed air cost savings identification model was successfully achieved.

5.2 Shortcomings and recommendations

It was found that the constructed model satisfied the study objective. Nevertheless, key areas where limitations were identified or where improvements can be made need to be mentioned. This will ensure that energy-saving identification processes can continue to become more accurate, useful and robust.

Firstly, there are more than 29 deep-level mines in South Africa which use compressed air for the mining operations. It is impossible to collect reliable data from all mines due to privacy constraints, limited infrastructure and the accessibility of data. Therefore, the more data sets that can be acquired, the greater the understanding of the relationship between the compressed air power profiles will be. It is proposed to continually add data and data sets to the statistical model to expand the number of cases used in the model generation. A greater data set will allow for better and more realistic statistical calculations.

Secondly, it is recommended to separate the summer and winter month samples. This is due to the thermodynamic effects that the temperature differences have on compressed air over specific seasons of the year. A more extensive variety of data sets are required to do this. Thus, the first recommendation should be prioritised.

Thirdly, energy-saving initiatives are becoming more feasible and therefore the instrumentation of mines will be upgraded to ensure the sustainability of these initiatives. As a result, more mines are installing better monitoring equipment. As the resolution of data becomes higher, more in-depth studies can be conducted. Using well-instrumented mines/compressed air systems to conduct studies is advised, as this limits the scope for error.

Fourthly, using mines with the same operating schedule will present better results. Due to the nature of mines, labour laws and unions, these schedules are not always strictly followed, nor are the schedules like other mines. With the development of centralised blasting practice, mines are becoming more structured and stricter with their schedules, which will prove advantageous for future studies.

Fifthly, the designed model was built using the data of other mines which had unique time schedules. The operational schedules of a mine should be consulted before implementing this model on their data. Minor deviations (1-hour shifts) are acceptable but if the order of mining

shifts is different to those used in the model – the results will not be accurate. However – because the shifts have been broken down into blocks – an investigator can still use the specific function produced by the estimation model for that shift.

Sixthly, major upgrades, large section closures and irregular infrastructure collapses have not been considered. The proposed model will be most accurate for mines which do not plan major infrastructure changes in the preceding 2 years. This is due to the payback period of the optimisation methods usually being less than 2 years.

Lastly, the study only focusses on determining feasibility of saving opportunities and is does give guidance regarding which procedure to follow to obtain these results. A list of common compressed air optimisation methods has been mentioned and research explaining how these projects were implemented can be found in references [17-30].

The recommendations listed will positively contribute to future studies in this area of investigation. One of the most significant challenges is to ensure that energy savings and production increases co-exist. By making mines aware of optimising systems, energy savings and production increases can be the future for mines in South Africa.

BIBLIOGRAPHY

[1] N. Singh, "Weathering the 'perfect storm' facing the mining sector," *Journal of the Southern African Institute of Mining and Metallurgy*, vol. 117, pp. 223–229, 2017.

[2] A. Lane, J. Guzek, and W. van Antwerpen, "Tough choices facing the South African mining industry," *Journal of the Southern African Institute of Mining and Metallurgy*, vol. 115, pp. 471–479, 2015.

[3] M. Motiang and R. Nembahe, "Energy price report 2016." Department of Energy South Africa, Pretoria, pp. 20–26, 2016.

[4] Eskom Holdings SOC Ltd, "Integrated Annual Financial Report 31 March 2017," edition 31 March. Eskom Holdings SOC Ltd, Johannesburg, South Africa, pp. 1–132, 2017.

[5] "Tradingeconomics." [Online]. Available: https://tradingeconomics.com. [Accessed: 03-Mar-2019].

[6] PricewaterhouseCoopers, "Highlighting trends in the South African mining industry," *SA Mine*, edition 9, p. 58, 2017.

[7] J. I. G. Bredenkamp, "Reconfiguring mining compressed air networks for cost savings," M.Eng Dissertation, Centre for Research and Continuing Engineering Development, North-West University, Pretoria, 2013.

[8] S. Mousavi, K. Sami, and B. Kornfeld, "Energy Efficiency of Compressed Air Systems," in *Conference on Life Cycle Engineering Energy*, vol. 21, pp. 313–318, 2014.

[9] Eskom Holdings SOC Ltd, "The Energy Efficiency series." Eskom Holdings SOC Ltd, Johannesburg, South Africa, p. 2, 2010.

[10] R. Saidur, N. Rahim, and M. Hasanuzzaman, "A review on compressed-air energy use and energy savings," *Renewable and Sustainable Energy Reviews*, vol. 14, edition 4, pp. 1135–1153, May 2010.

[11] F. Benedetti, Miriam; Bonfa, "Explorative study on Compressed Air Systems' energy efficiency in production and use: First steps towards the creation of a benchmarking system for large and energy-intensive industrial firms," *Applied Energy*, vol. 227, pp. 436–448, 2018.

[12] F. Doyle and J. Cosgrove, "An approach to optimising compressed air systems in production operations," *International Journal of Ambient Energy*, vol. 39, edition 2, pp. 194–201, 2018.

[13] R. Christie, *"Electricity, Industry and Class in South Africa,"* 1st ed. New York, USA: State University of New York Press, 1984.

[14] Darling Peter, "SME Mining Engineering Handbook (3rd Edition)," *Society for Mining, Metallurgy, and Exploration (SME)*, pp. 705–710, 2011.

[15] H. Joubert, J. van Rensburg, and R. Pelzer, "Energy efficiency opportunities resulting from splitting a compressed air ring," *2011 Proceedings of the 8th Conference on the Industrial and Commercial Use of Energy (ICUE)*, pp. 75–81, 2011.

[16] A. J. M. Van Tonder, "Automation of compressor networks through a dynamic control system," Ph.D Thesis, Centre for Research and Continuing Engineering Development, North- West University, Pretoria, 2014.

[17] Payscale, "Mechanical Engineer Salary." [Online]. Available: https://www.payscale.com/research/ZA/Job=Mechanical_Engineer/Salary/. [Accessed: 03-Mar-2019].

[18] H. P. R. Joubert, "Improved risk management processes for South African industrial ESCos," Ph.D Thesis, Centre for Research and Continuing Engineering Development, North-West University, Pretoria, 2016.

[19] C. J. R. Kriel, J. H. Marais, and M. Kleingeld, "Modernising underground compressed air DSM projects to reduce operating costs," in *2014 Proceeding of the 11th Conference on the Industrial and Commercial Use of Energy, (ICUE)*, 2014.

[20] G. D. Bolt, J. Venter, and J. F. Van Rensburg, "Dynamic compressor selection," in *2012 Proceedings of the 9th Conference on the Industrial and Commercial Use of Energy, (ICUE)*, pp. 75–80, 2012.

[21] J. Jonker, "Automated mine compressed air control for sustainable savings," M.Eng Dissertation, Centre for Research and Continuing Engineering Development, North- West University, Pretoria, 2016.

[22] M. H. P. Van Niekerk, S. W. Van Heerden, and J. F. Van Rensburg, "The implementation of a Dynamic air Compressor Selector system in mines," in *2015 Proceedings of the 12th Conference on the Industrial and Commercial Use of Energy, (ICUE)*, pp. 129–132, 2015.

[23] J. Venter, "Development of a dynamic centrifugal compressor selector for large compressed air networks in the mining industry," M.Eng Dissertation, Centre for Research and Continuing Engineering Development, North- West University, Pretoria, 2012.

[24] R. A. Stanley and W. R. Bohannan, "Dynamic Simulation of Centrifugal Compressor Systems," *1977 Proceedings of the sixth Turbomachinery Symposium*, pp. 123–132, 1977.

[25] S. Sapmaz, "Selection of Compressors for Petrochemical Industry in Terms of Reliability, Energy Consumption and Maintenance Costs Examining Different Scenarios.," *Energy Exploration & Exploitation*, vol. 33, edition 1, pp. 43–62, 2015.

[26] H. Fengyou, B. Weining, Z. Bing, and T. Yang, "Research of an unattended intelligentized control system of air compressor for supplying constant-pressure air," *2009 2nd International Conference on Intelligent Computing Technology and Automation, ICICTA 2009*, pp. 838–841, 2009.

[27] S. P. Dudić, I. M. Ignjatović, D. D. Šešlija, V. A. Blagojević, and M. M. Stojiljković, "Leakage quantification of compressed air on pipes using thermovision," *Thermal Science*, vol. 16, pp. 555–566, 2013.

[28] A. J. M. van Tonder, "Sustaining compressed air DSM project savings using an air leakage management system," M.Eng Dissertation, Centre for Research and Continuing Engineering Development, North- West University, Pretoria, 2011.

[29] K. Taheri and R. Gadow, "Industrial compressed air system analysis: Exergy and thermoeconomic analysis," *CIRP Journal of Manufacturing Science and Technology*, vol. 18, pp. 10–17, 2017.

[30] J. I. G. Bredenkamp, L. F. Van Der Zee, and J. F. Van Rensburg, "Reconfiguring mining compressed air networks for cost savings," in *2014 Proceedings of the Conference on the Industrial and Commercial Use of Energy, (ICUE)*, 2014.

[31] G. P. Heyns, "Challenges faced during implementation of a compressed air energy savings project on a gold mine," M.Eng Dissertation, Centre for Research and Continuing Engineering Development, North- West University, Pretoria, 2014.

[32] B. Pascoe, H. J. Groenewald, and M. Kleingeld, "Improving mine compressed air network efficiency through demand and supply control," in *2017 Proceedings of the 14th Conference on the Industrial and Commercial Use of Energy, (ICUE)*, 2017.

[33] L. F. van der Zee, "Modelling of electricity cost risks and opportunities in the gold mining industry," Ph.D Thesis, Centre for Research and Continuing Engineering Development, North-West University, Pretoria, 2014.

[34] S. J. Fouché, "Improving efficiency of a mine compressed air system," M.Eng Dissertation,

Centre for Research and Continuing Engineering Development, North-West University, Pretoria, 2016.

[35] H. P. R. Joubert, G. Bolt, and J. F. Van Rensburg, "Energy savings on mining compressed air networks through dedicated process plant compressors," in *2012 Proceedings of the 9th Conference on the Industrial and Commercial Use of Energy, (ICUE)*, pp. 99–102, 2012.

[36] J. H. Marais, "An integrated approach to optimise energy consumption of mine compressed air systems," Ph.D Thesis, Centre for Research and Continuing Engineering Development, North-West University, Pretoria, 2012.

[37] S. W. van Heerden, "A dynamic optimal control system for complex compressed air networks," Ph.D Thesis, Centre for Research and Continuing Engineering Development, North- West University, Pretoria, 2016.

[38] P. C. Hanlon, *Compressor handbook*. New York, USA: McGraw-Hill, 2001.

[39] D. H. Robison and P. J. Beaty, "Compressor types, classifications, and applications," in *21st Turbomachinery Symposium*, pp. 183–188, 1992.

[40] L. B. Vigdal and L. E. Bakken, "Variable Inlet Guide Vane Effect on Centrifugal Compressor Performance in Wet Gas Flow," in *ASME Turbo Expo 2016: Turbomachinery Technical Conference and Exposition*, pp. 13–17, 2016.

[41] C. Cilliers, "Benchmarking electricity use of deep-level mines," Ph.D Thesis, Centre for Research and Continuing Engineering Development, North- West University, Pretoria, 2016.

[42] R. Saidur, "A review on electrical motors energy use and energy savings," *Renewable and Sustainable Energy Reviews*, vol. 14, edition 3, pp. 877–898, Apr. 2010.

[43] J. I. G. Bredenkamp, "An integrated energy management strategy for the deep-level gold mining industry," Ph.D Thesis, Centre for Research and Continuing Engineering Development, North-West University, Pretoria, 2016.

[44] Lawrence Berkeley National Laboratory and C. Berkeley, *Improving compressed air system performance: A sourcebook for industry*, Third. Berkley: U.S Department of Energy, 2016.

[45] D. Seslija, I. Milenkovic, S. Dudic, and J. Sulc, "Improving energy efficiency in compressed air systems - practical experiences," *Thermal Science*, vol. 20, pp. 355–370, 2016.

[46] F. W. Schroeder, "Energy Efficiency Opportunities in Mine Compressed Air Systems," M.Eng Dissertation, Centre for Research and Continuing Engineering Development, North- West

University, Pretoria, 2009.

[47] E. A. Abdelaziz, R. Saidur, and S. Mekhilef, "A review on energy saving strategies in industrial sector," *Renewable and Sustainable Energy Reviews*, vol. 15, pp. 150–168, 2011.

[48] S. Cox, "Predicting electricity consumption and cost in South African mines," M.Eng Dissertation, Centre for Research and Continuing Engineering Development, North-West University, Pretoria, 2013.

[49] D. S. Moore, G. P. McCable, and B. A. Craig, *Introduction to the practice of statistics*, 6th ed. New York, NY: W.H Freeman and Company, 2009.

[50] W. Booysen, L. A. Botes, and W. Hamer, "A practical methodology for the systematic identification of outliers," in *2017 International Conference on the 14th Industrial and Commercial Use of Energy (ICUE)*, pp. 1–6, 2017.

[51] G. Shuttleworth, "Benchmarking of electricity networks: Practical problems with its use for regulation," *Utilities Policy*, vol. 13, pp. 310–317, 2005.

[52] A. B. Haney and M. G. Pollitt, "International benchmarking of electricity transmission by regulators: A contrast between theory and practice?," *Energy Policy*, vol. 62, pp. 267–281, 2013.

[53] J. Vermeulen, "Simplified high - level investigation methodology for energy saving initiatives on deep - level mine compressed air systems," Ph.D Thesis, Centre for Research and Continuing Engineering Development, North-West University, Pretoria, 2017.

[54] L. A. Botes, "Objective evaluation of industrial energy efficiency models for the RSA Section 12L tax incentive," M.Eng Dissertation, Centre for Research and Continuing Engineering Development, North-West University, Pretoria, 2017.

[55] W. Cai, F. Liu, J. Xie, P. Liu, and J. Tuo, "A tool for assessing the energy demand and efficiency of machining systems: Energy benchmarking," *Energy*, vol. 138, pp. 332–347, 2017.

[56] A. L. Meek, "A systems engineering approach to improve the measurement and verification process of energy services companies," M.Eng Dissertation, Centre for Research and Continuing Engineering Development, North-West University, Pretoria, 2013.

[57] Efficiency Valuation Organization, "International Performance Measurement and Verification Protocol." U.S Department of Energy, pp. 1–48, 1997.

[58] International Performance Measurement and Verification Protocol, "SANS 50010 : 2011 South African national standard for measurement and verification of energy savings," Pretoria, 2011.

[59] B. V Liengme, *A guide to microsoft excel 2013 for scientists and engineers*, 1st ed. London: Academic Press, 2016.

[60] D. S. Wilks, "Sampling distributions of the Brier score and Brier skill score under serial dependence," *Quarterly Journal of the Royal Meteorological Society*, vol. 136, pp. 2109–2118, 2010.

[61] S. C. Kumbhakar and C. a. K. Lovell, *Stochastic frontier analysis*, 1st ed. Cambridge: Cambridge University Press, 2000.

APPENDIX A: ESCO SURVEY

A.1 Survey Example

ESCo Compressed Air Survey

The aim of the survey is to determine what resources are required to do a typical compressed air project, audit or investigation on a deep-level mine in South Africa.

Email address *

ccilliers@rems2.com

Name and Surname *

Charl Cilliers

Highest Degree Obtained *

- ○ B.Eng
- ○ M.Eng
- ◉ PhD.Eng

Have you obtained an PR.Eng accreditation *

- ○ Yes
- ◉ No
- ○ In the process

How many years have you spent working for an ESCo *

- ○ 0-1
- ○ 1-2
- ○ 2-5
- ◉ 5-10
- ○ 10+

Current Job Title *

Project Engineer

How many compressed air system projects/investigations/audits have you been a part of? *

- ○ 0-5
- ◉ 6-10
- ○ 10-20
- ○ 20+

Attached Sheets

Please fill in these sheets like the examples posted below. The first table requires the minimum and maximum data.

Table 1

ESCO Action Item	Required Time [Weeks]	Required Resources	Number of Personnel	Complexity [0 - 10]	Project Certainty after completion [0 -10]
Contact client	1	Senior Engineer	2	0	0
Obtain permission to investigate	2	Senior Engineering Personnel	2	2	1
Obtain data	4	Junior Engineering Personnel	4	4	4
Compressed Air Audits	8	Multiple Engineering Personnel	4	5	6
Simulate	21	Multiple Engineering Personnel	2	8	8
Determine Feasibility	2	Project Engineers	2	5	8
Compile Findings Report	1	Project Engineers	1	5	8
Compile Project Proposal	1	Project Engineers	1	6	8
Client Sign Off on Project Proposal	2	Senior Engineer Personnel	1	4	9

Table 2

Initiatives	Description	Used / participated	Complexity [0-10]
Static Compressor Schedules	Create/update static compressor running schedules to ensure most efficient compressors are operating at specific times	Yes	2
Dynamic Compressor Selection	Install control software which automatically uses the most efficient compressors at any given time to supply compressed air	Yes	8
Manual Compressor Selection	Designated compressor operator controls compressor pressure setpoints and running statuses.	No	6
Master pressure setpoint reduction	Average pressure profile is used to control the total pressure of compressed air ring.	Yes	2
Leak Reduction	Repairs of damaged compressed air piping	Yes	3
Pipe Re-configuration	Re-configure compressed air pipe segments to ensure less line losses.	Yes	4
Surface valve control	Control the pressure setpoint for each surface point of delivery (POD)/ shaft.	Yes	6
Peak-Clip Initiatives	Decrease pressure setpoints of compressed air control valves during ESKOM peak periods.	Yes	5
Stope-isolation valves	Closing of manual compressed air valves which connects the stopes to the main level pipelines.	No	2
Ring-feed clearance	Close ring feeds that bypass planned compressed air reticulation plans.	No	1
Close inactive sections	Close valves which lead to inactive mining sections.	No	1
Isolate compressed air components	Install dedicated compressors underground to isolate compressed air consumers from the main compressed air supply pipeline.	No	5

11/19/2018 ESCo Compressed Air Survey

Sheet Location

Please fill the sheets as per example stated above

https://drive.google.com/open?id=1RLJfErzlaqkM4kJhCZ1Uwy73fqFb9Ek-

Please upload the answer sheets *

ESCO Survey_ccilli...

Comments

A.2 Survey Results

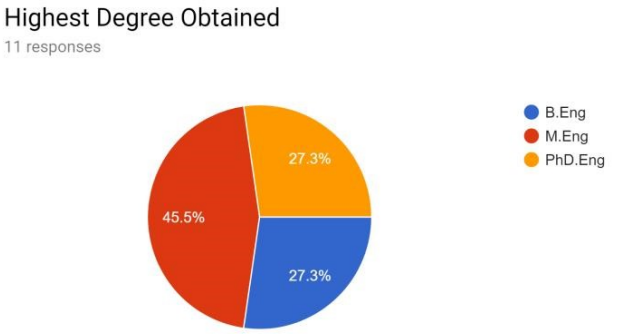

Figure 62 - Survey Results - Degrees

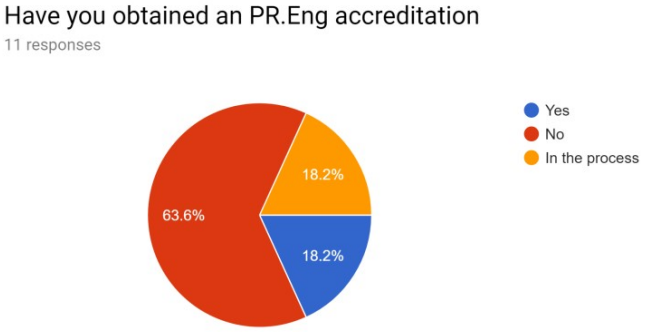

Figure 63 - Survey Results - PR.Eng Registration

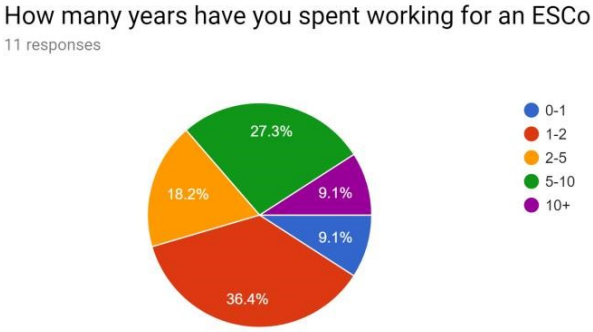

Figure 64 - Survey Results - Number of years working for ESCo

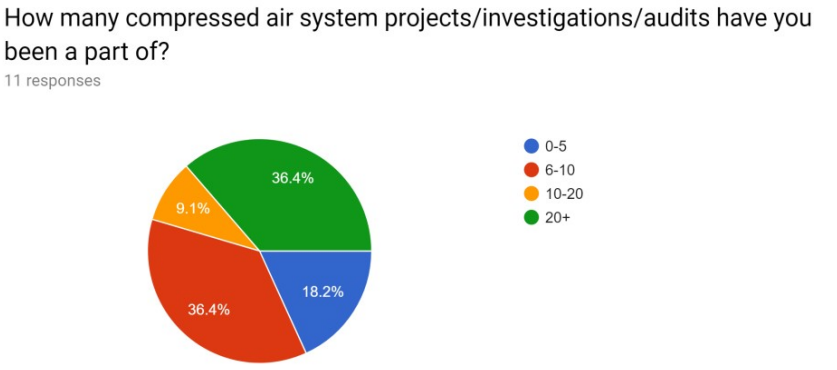

Figure 65 - Survey Results - Number of compressed air systems investigated

APPENDIX B: MATHEMATICAL EXPRESSION OF MINING PROCESSES

Equation 16 - Base process energy consumption vector

$$y=F(x)$$

$$y^{(b)}=F^{b}(x^{b})$$

$\mathbf{x}$ = $(x_1,x_2,\dots,x_m)$ = vectors which influence energy consumption

$\mathbf{x}^{(b)}$ = $\left(x_1^{(b)},x_2^{(b)},\dots,x_m^{(b)}\right)$ = vectors which influence energy consumption (benchmarked)

$\mathbf{y}$ = vectors that represent the energy consumption of the base process

$\mathbf{y}^{(b)}$ = vectors that represent the energy consumption of the base process (benchmarked)

Equation 17 - Base process energy consumption

$$E=K(y)$$

$$E^{(b)}=K^{(b)}(y^{(b)})$$

$\mathbf{E}$ = Energy consumption for base process

$\mathbf{E}^{(b)}$ = Energy consumption for base process (benchmarked)

$\mathbf{y}$ = Vectors that represent the energy consumption of the base process

$\mathbf{y}^{(b)}$ = Vectors that represent the energy consumption of the base process (benchmarked)

$\mathbf{K}$ = Function of calculated energy consumption

Equation 18 - Total energy consumption

$$E_{Total}=E_1+E_2+\ldots+E_N=\sum_{i}^{N} E_i$$

$$E_{Total}^{(b)}=E_1^{(b)}+E_2^{(b)}+\ldots+E_N^{(b)}=\sum_{i}^{N} E_i^{(b)}$$

E = Energy consumption for base process

$E^{(b)}$ = Energy consumption for base process (benchmarked)

APPENDIX C: STATISTICAL TECHNIQUES USED BY PREVIOUS RESEARCHERS

C.1 Brier Score

D. Wilks [60] stated in an article in the Quarterly Journal of Royal Meteorological Society that the Brier Score is one of the most widely used probability forecasts for scalar summary of accuracy in dichotomous events. The Brier Score evaluates the correctness of a scalar forecast given by Equation 19. The Brier Score is, therefore, the mean-squared error over the total forecast observation pairs.

Equation 19 - Brier score

$$BS=\frac{1}{n}\sum_{i=1}^{n}(y_i-x_i)^2$$

BS = Brier Score

n = number of events in the forecast

i = 1, … , n = counter integer

x_i = The i^{th} actual occurrence in a series of n events

y_i = The i^{th} probability forecast in a series of n events

C.2 Regression and Correlation

The purpose of a regression line is to summarise the relationship between two variables (data sets) where it is suspected that one variable influences the other [49]. This summary can also be expressed in a mathematical relation. Figure 66 displays the degree of correlation that exists between different datasets. Multiple data processing software packages exist that automatically determine the necessary variables required for statistical analysis. Therefore, only the most prominent variables will be discussed in this section.

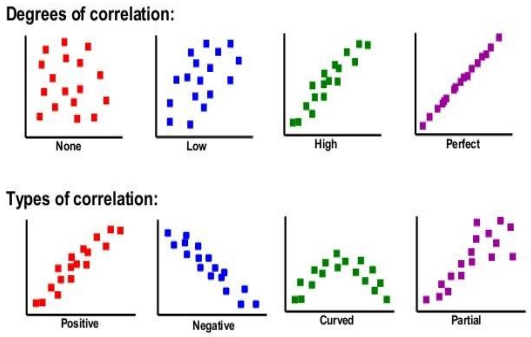

Figure 66 - Regression examples

The correlation of that the relationship between two sets of variables measures the direction and strength of the variables and is denoted by ***r*** [49].

Equation 20 - Correlation coefficient

$$r = \frac{1}{n-1}\sum_{i=1}^{n}\left(\frac{x_i-\bar{x}}{s_x}\right)\cdot\left(\frac{y_i-\bar{y}}{s_y}\right)$$

r = Variable correlation

n = Number of events in the forecast

i = 1, … , n = event iteration

x_i = The i^{th} data variable of the first data set

y_i = The i^{th} data variable of the second data set

$S_{x,y}$ = The standard deviation for x and y data set respectively

$\bar{x}, \bar{y}$ = Mean value of the x and y data set respectively

C.3 Ordinary Least Square Regression

The ordinary least square regression method is a regression-based technique that yields an average best fit function [41], [49]. The regression line output is a first-degree polynomial which produces a relational output (y) for any discreet input variable (x). This method is ideal for determining possible relationships for intervals that are not necessarily part of the original data sets.

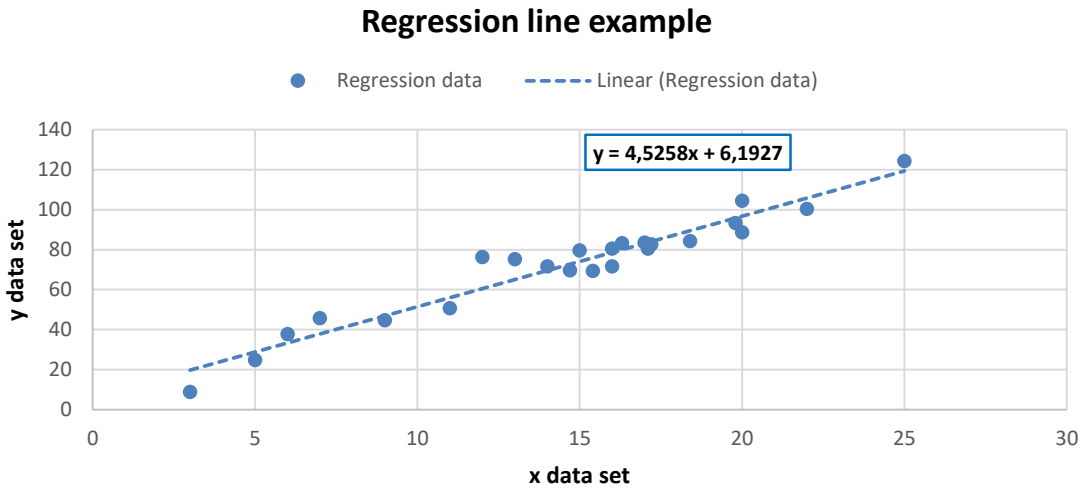

Figure 67 - Ordinary Least Square Regression

The regression line can be expressed using the following notation.

Equation 21 - Regression line equations

$$y_{\_1} = m \cdot x + c$$

$$y_{\_n} = a + m_1 x_1 + \ldots + m_n x_n$$

$$y_{\_k^{the}\ order} = \varepsilon + m_1 x^1 + \ldots + m_k x^k$$

$y_{\_1}$	= Single variable first order polynomial output
$y_{\_n}$	= Multiple variable first order regression model
$y_{\_k^{th}\ order}$	= k^{th} order polynomial output
m	= Gradient for respective x value iteration
x	= Input
a	= y-axis intercept (multi-variable regression)
ε	= y-axis intercept (k^{th} order polynomial)

C.4 Corrected ordinary least square

The ordinary least square (OLS) method determines the best fit average determination of the regression line. Due to multiple factors that influence the energy consumption of compressed air networks the (OLS) method does not necessarily mean the best practice or even average performance of a system like compressed air [41], [51].

To reduce the effort of inspecting multiple variable sets to validate the OLS regression, benchmarking regulators have implemented a corrected ordinary least square model (COLS) to ensure that the benchmarks do not exclude certain processes due to factors which have not been investigated (frontier analysis) [51]. In practical terms, it means shifting the OLS regression line up or down to ensure that all data points are on the same side of the regression line.

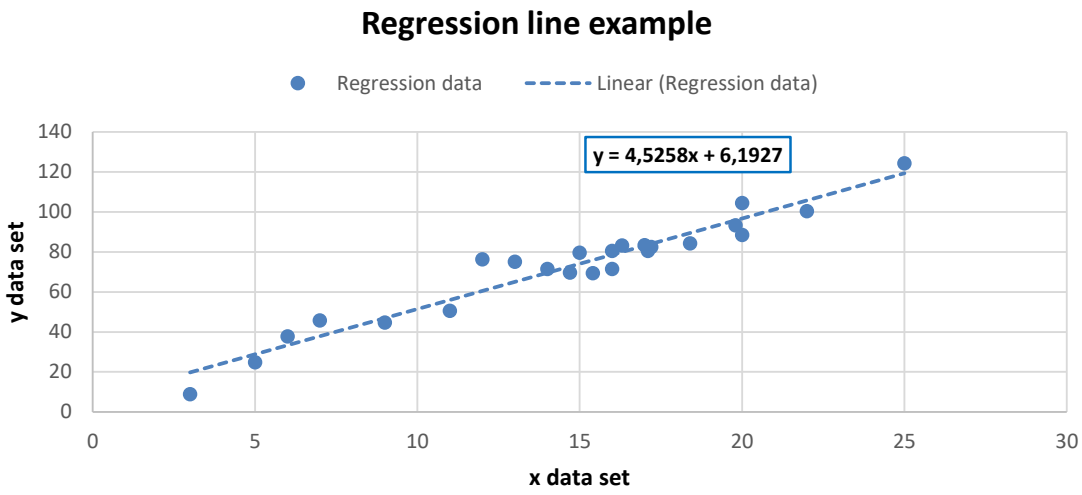

Figure 67Figure 68 shows the translation of OLS to COLS. The red the line represents the upward shifting of the OLS regression line, ensuring that all data elements are beneath it. Similarly, the orange line is the downward shifting of the OLS line, ensuring that all data points are above the regression line. Shifting the regression line ensures the relational parameters (gradient) are kept while creating a minimum or maximum benchmarking curve. The possible increase in margin of error due to outliers and error data points leads to the COLS method over-correcting certain data sets [41]. The COLS system does not omit stochastic factors (randomly distributed data points).

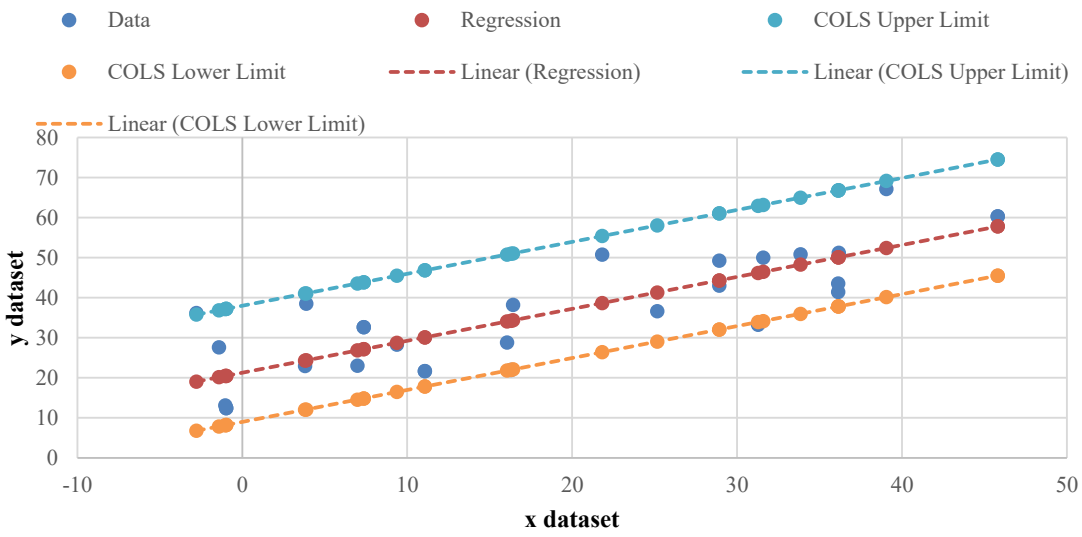

Figure 68 - Corrected ordinary least square implementation

C.5 Stochastics Frontier Analysis

To address the stochastic factors found in the COLS system, a stochastic frontier analysis (SFA) method has been developed [52], [61]. The SFA method lowers or increases the regression line towards the upper or lower quartile of data groupings. Therefore, it is an estimation method, as it is too complex to accurately differentiate the error data sets from the non-error data sets.

The estimation nature of this method has caused regulatory bodies to ignore its application in many cases [51]. It can still be used to eliminate some stochastic factors and thus increase the estimation accuracy with regard to the COLS method.

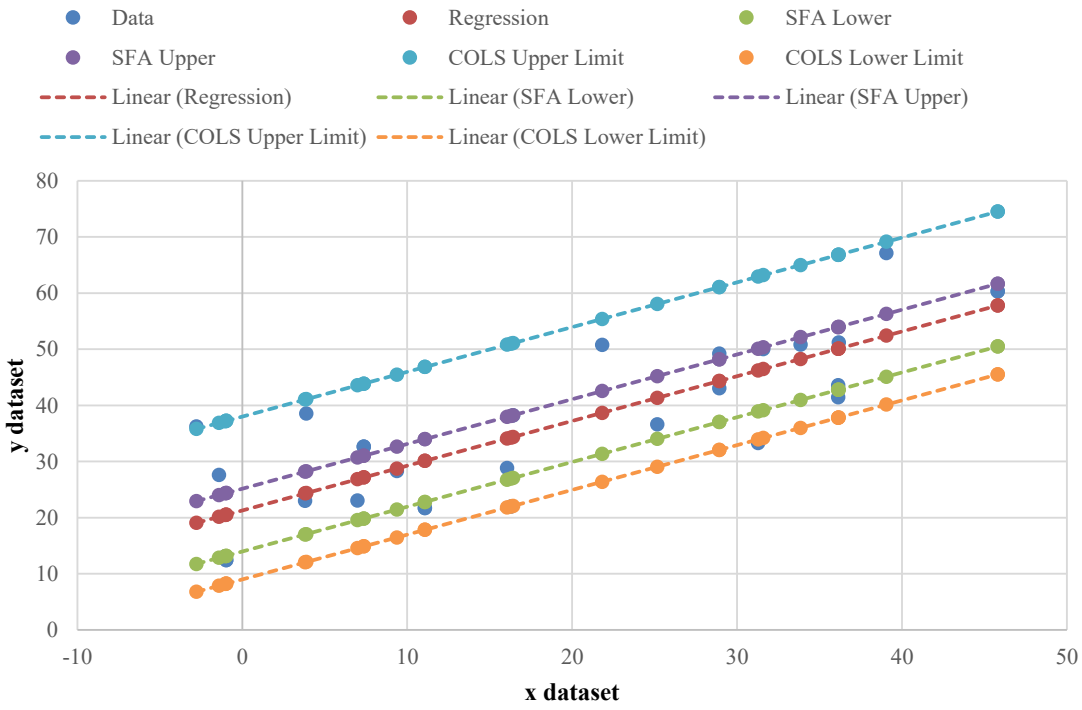

Figure 69 - SFA Application

C.6 DEA (Data envelopment analysis)

The last statistical investigation model is the DEA technique. The DEA method can be classified as an non-parametric technique, which does not aim to identify the parameters that influence the data sets, but rather employs linear programming to dynamically “envelop” (surround) the given data structure [61].

This method can be used to construct dynamic maximum or minimum. The Dutch energy regulator has employed this method but has not been widely used by other European countries. Figure 70 displays the applied DEA method to a data set.

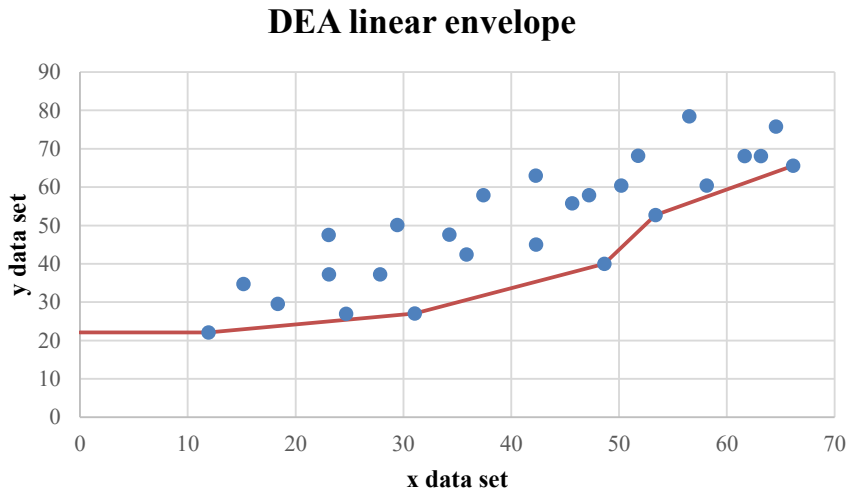

Figure 70 - DEA application example (Adapted from [39])

APPENDIX D: COMMON STATISTICAL PARAMETERS USED BY M&V TEAMS

Equation 22 - Residual sum of squares (adapted from [34],[40])

$$SSResid = \sum_{i=1}^{n} (r_i)^2 = \sum_{i=1}^{n} (y_i - \bar{y})^2$$

SSResid = Residual sum of squares

y_i = Actual y data value

$\bar{y}$ = Predicted y value due to a regression model

r_i = i^{th} correlation parameter = $(y_i - \bar{y})$

Equation 23 - F Statistic

$$\mathbf{F} = \frac{MS_{reg}}{MS_E}$$

Where $\mathbf{MS_{reg}} = SS_{reg}$.

$\mathbf{MS_E}$ can be derived using:

$$\mathbf{MS_E} = \frac{SS_E}{df_E} = \frac{S_{yy} - \beta_1 S_{xy}}{N-2}$$

S_{xy} = $\sum_{j=1}^{N} (x_j - \bar{\bar{x}})(y_j - \bar{\bar{y}})$

S_{yy} = $\sigma_y^2 (N-1)$

$\bar{\bar{x}}, \bar{\bar{y}}$ = Averages of x and y respectively

σ_y = Sample sigma of y values.

SS_{Reg} = $\sum (y' - \bar{y}')^2$

Equation 24 - Coefficient of determination

$$R^2 = \frac{SS_{reg}}{SS_{Total}} = 1 - \frac{SS_E}{SS_{Total}}$$

R^2 = Coefficient of determination

$SS_{Total} = \sum (y-\bar{y})^2$

$SS_{Reg} = \sum (y'-\bar{y}')^2$

$SS_E = \sum (y-y')^2$

APPENDIX E: M&V REPORT DATA

4. Average baseline and actual demand data for: March 2012

Project name: [redacted]
Project number: 2010069
Project Type: Industrial Energy Efficiency
Report period: March 2012

Time	Weekday		Saturday		Sunday	
	Base kW	*Actual kW*	*Base kW*	*Actual kW*	*Base kW*	*Actual kW*
0:00	6 183.7	5 628.6	6 169.1	5 323.2	5 319.5	5 462.8
0:30	6 294.8	5 628.6	6 209.9	5 323.2	5 302.5	5 462.8
1:00	6 371.5	5 878.8	6 250.1	6 059.1	5 302.4	5 195.8
1:30	6 404.5	5 878.8	6 269.8	6 059.1	5 302.8	5 195.8
2:00	6 395.7	5 959.2	6 285.0	6 131.0	5 302.7	5 185.5
2:30	6 398.8	5 959.2	6 275.9	6 131.0	5 296.6	5 185.5
3:00	6 397.6	5 960.6	6 274.3	6 106.4	5 294.0	5 109.4
3:30	6 371.1	5 960.6	6 251.3	6 106.4	5 374.0	5 109.4
4:00	6 320.8	5 837.0	6 211.7	5 955.5	5 363.7	5 033.1
4:30	6 261.9	5 837.0	6 180.7	5 955.5	5 295.6	5 033.1
5:00	6 240.0	5 647.3	6 170.8	5 845.2	5 312.0	4 945.7
5:30	6 195.2	5 647.3	6 152.1	5 845.2	5 300.7	4 945.7
6:00	6 139.3	5 577.8	6 129.1	5 804.3	5 299.4	4 923.0
6:30	6 101.3	5 577.8	6 030.0	5 804.3	5 273.5	4 923.0
7:00	6 097.9	5 517.6	5 726.9	5 794.6	5 023.3	4 708.2
7:30	6 108.6	5 517.6	5 620.9	5 794.6	4 607.2	4 708.2
8:00	6 107.2	5 469.5	5 629.5	5 824.3	4 344.2	4 743.1
8:30	6 358.0	5 469.5	5 775.0	5 824.3	4 219.1	4 743.1
9:00	6 632.0	5 617.8	5 925.2	5 892.5	4 121.3	4 408.6
9:30	6 970.5	5 617.8	6 090.4	5 892.5	4 132.2	4 408.6
10:00	7 273.2	6 124.9	6 259.1	6 266.8	4 118.8	4 760.6
10:30	7 356.4	6 124.9	6 364.5	6 266.8	4 106.9	4 760.6
11:00	7 380.5	6 452.2	6 362.5	6 380.5	4 105.3	4 326.3
11:30	7 441.8	6 452.2	6 362.4	6 380.5	4 095.0	4 326.3
12:00	7 320.1	6 327.0	6 299.5	6 316.7	4 083.6	4 172.6
12:30	7 263.7	6 327.0	6 172.8	6 316.7	4 144.4	4 172.6
13:00	7 069.0	6 393.2	6 003.2	6 077.2	4 592.5	4 191.6
13:30	6 803.4	6 393.2	5 875.0	6 077.2	4 554.1	4 191.6
14:00	6 580.3	5 989.5	5 768.0	5 776.1	4 536.5	4 128.6
14:30	6 400.0	5 989.5	5 683.1	5 776.1	4 272.8	4 128.6
15:00	6 305.6	5 568.9	5 654.7	5 567.1	4 390.6	3 699.5
15:30	6 237.7	5 568.9	5 637.1	5 567.1	4 385.7	3 699.5
16:00	6 166.6	5 395.5	5 617.3	5 203.9	4 388.2	3 560.5
16:30	6 127.1	5 395.5	5 616.9	5 203.9	4 388.7	3 560.5
17:00	6 093.0	5 317.9	5 625.1	5 049.0	4 392.0	3 557.6
17:30	6 099.1	5 317.9	5 634.0	5 049.0	4 383.7	3 557.6
18:00	6 108.4	5 327.3	5 616.6	4 801.1	4 538.8	3 845.2
18:30	6 145.6	5 327.3	5 609.1	4 801.1	4 673.0	3 845.2
19:00	6 160.2	5 322.2	5 603.6	5 018.5	4 729.9	4 061.9
19:30	6 161.4	5 322.2	5 597.4	5 018.5	5 348.3	4 061.9
20:00	6 133.3	5 274.1	5 593.1	5 067.1	5 539.8	4 107.6
20:30	6 108.6	5 274.1	5 579.0	5 067.1	5 526.3	4 107.6
21:00	6 072.0	5 235.9	5 755.3	5 221.4	5 518.0	4 394.7
21:30	6 049.9	5 235.9	5 657.8	5 221.4	5 519.3	4 394.7
22:00	6 049.0	5 245.9	5 558.0	5 192.2	5 705.2	4 903.8
22:30	6 082.9	5 245.9	5 561.7	5 192.2	5 939.4	4 903.8
23:00	6 049.1	5 402.3	5 561.4	5 230.9	5 915.5	5 321.4
23:30	6 140.1	5 402.3	5 576.1	5 230.9	5 923.3	5 321.4

Figure 71 - Typical M&V investigation summary

APPENDIX F: MATHEMATICAL ANALYSIS OF AVERAGE 24-HOUR PROFILE

F.1 Constructing mean profiles

The analysis of the 29 compressed air systems contributing to the statistical population yielded multiple compressed air networks ranging from 9 MW – 62 MW peak power consumption.

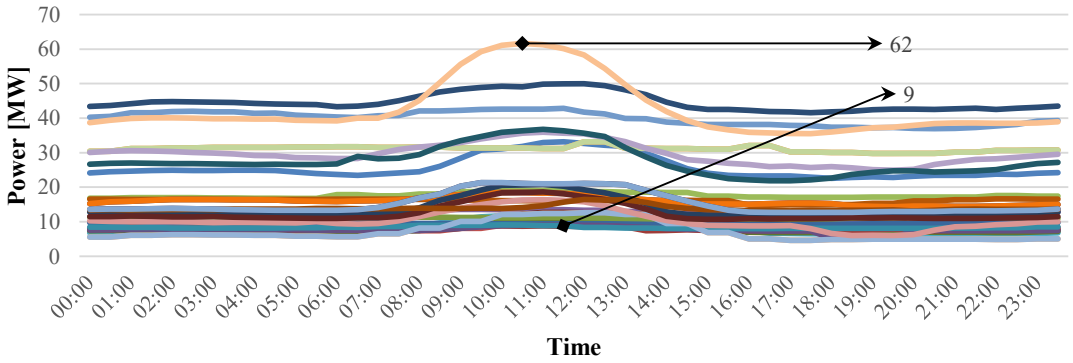

Figure 72 - Average baseline population sample

Equation 25 is based on the equation summary of Table 7 and is the statistical expression of each profile in Figure 72

Equation 25 - 3-month baseline mean expression

If

$$P=\{P_{B1},P_{B2}, \ldots, P_{B29}\} \; ; \; P_B=\{p_{B1},p_{B2},p_{B3}\} \; ; \; p_{Bi}=\{x_1(t)\}$$

Then

$$\mu_{p_B}=\frac{1}{k}\sum_{i=1}^{k} p_{Bi}$$

$P_{B1\text{-}B29}$ = Population proportion

$p_{1\text{-}k}$ = Monthly performance assessment data

x_1 = Baseline vector for weekdays as a function of t

t = 24-hour daily profile containing 48 half hour segments as independent variables

μ_{p_B} = Mean of monthly performance assessment

p_{Bi} = Weekday data of one month for one mine

k = Number of months in performance assessment period

Figure 73 shows the average of 29 power profiles where the performance of these systems were measured after the implementation of compressed air initiatives.

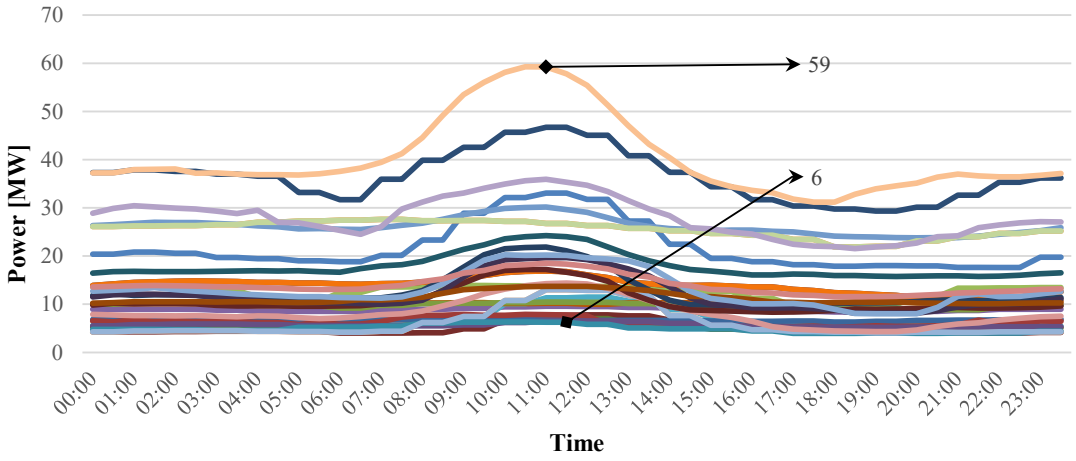

Figure 73 - Average measured population sample

Equation 26 is based on the equation summary of Table 7 and is the analytical expression of each profile in Figure 73.

Equation 26 - 3-month measured performance mean expression

If

$$P=\{P_{M1},P_{M2}, \ldots, P_{M29}\} \; ; \; P_M=\{p_{M1},p_{M2},p_{M3}\} \; ; \; p_{Mi}=\{x_1(t)\}$$

Then

$$\mu_{p_B}=\frac{1}{k}\sum_{i=1}^{k} p_{Mi}$$

$P_{M1\text{-}M29}$ = Population proportion

$p_{1\text{-}k}$ = Monthly performance assessment data

x_1 = Measured vector for weekdays as a function of t

t = 24-hour dialy profile containing 48 half hour segments as independent variables

μ_{p_M} = Mean of monthly performance assessment

p_{Mi} = Weekday data of one month for one mine

k = Number of months in performance assessment period

Figure 74 displays the average (mean) of the 29 baseline and 29 performances assed measurements expressed in Figure 72 and Figure 73 and Equation 25 and Equation 26.

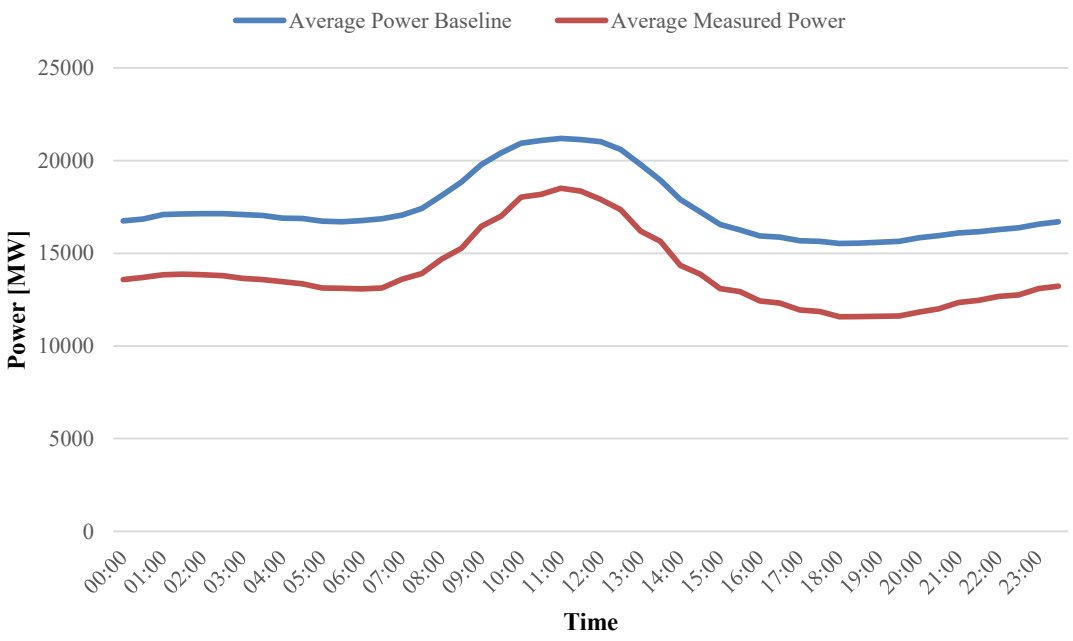

Figure 74 - Average power baseline and performance assessed power profiles

Equation 27 is the mathematical expression of each profile in Figure 74. The population mean of the baselines are denoted at μPB, while the population mean of the performance assessed measurements are denoted by μPM. Equation 25 and Equation 26 are explained above, and therefore the only additional parameter in the mean of the mean values are N. N is the total number of mines in the population proportion.

Equation 27 - Statistical expression for baseline and performances assessed mean profiles

$$\boldsymbol{\mu_{PB}} = \frac{1}{N}\sum_{i=1}^{N}\left(\frac{1}{k}\sum_{i=1}^{k} p_{Bi}\right) ; \boldsymbol{\mu_{PM}} = \frac{1}{N}\sum_{i=1}^{N}\left(\frac{1}{k}\sum_{i=1}^{k} p_{Mi}\right)$$

F.2 Polynomial expression of statistical averages

The averaged population baseline can be approximated by Equation 28. x is the respective half-hour of the day expressed as a number, ranging from 1-48.

Equation 28 - Polynomial expression of μPB (Equation 27)

$$\mu_{PB} = f(x_B) = (-1.7\times10^{-14})x^{14}+(-5.5\times10^{-12})x^{13}+(-7.95\times10^{-10})x^{12}+(6.56\times10^{-8})x^{11}$$
$$+(-3.45\times10^{-6})x^{10}+(1.2\times10^{-4})x^{9}+(-2.83\times10^{-3})x^{8}$$
$$+(-4.37\times10^{-2})x^{7}+(-0.42)x^{6}+(2.16)x^{5}+(-1.63\times)x^{4}$$
$$+(-43.47\times)x^{3}+(198.55)x^{2}+(-158.55)x^{1}+16737.60$$

x = Period interval (1 - 48 for each half hour in a day)

$f(x_B)$ = Polynomial transform of x

The averaged population baseline can be approximated by Equation 29. x is the respective half-hour of the day expressed as a number, ranging from 1-48.

Equation 29 - Polynomial expression of μPM (Equation 27)

$$\mu_{PM} = f(x_M) = (-4.01\times10^{-14})x^{14}+(1.3\times10^{-12})x^{13}+(-1.87\times10^{-10})x^{12}+(1.56\times10^{-8})x^{11}$$
$$+(-8.46\times10^{-6})x^{10}+(3.1\times10^{-4})x^{9}+(-7.72\times10^{-3})x^{8}$$
$$+(1.3\times10^{-1})x^{7}+(-1.56)x^{6}+(11.78)x^{5}+(-56.70\times)x^{4}$$
$$+(153.33\times)x^{3}+(-217.54)x^{2}+(272.33)x^{1}+13417.1$$

x = Period interval (1 - 48 for each half hour in a day)

$f(x_M)$ = Polynomial transform of x

By extrapolating the mean baseline function using the LINEST tool in excel, calculus principles can be used to evaluate the mean baseline function expressed in Equation 27.

F.3 Determine inflection points in averaged profiles

By using the higher order derivates of the mean function f(x) in Equation 27, the localised minima, maxima and inflexion points can be determined. The inflexion point can be used to determine where the function changes course. To determine the localised minima and maxima the n^{th} order (uneven integers: 1, 3 … n) derivates are intersecting the y a-axis at x = 0 can be used.

To determine the inflexion points of the function f(x) the n^{th} order (even integers: 2, 4 … n) derivates intersecting the y a-axis at x = 0 can be used. Because the purpose of evaluating the function is to determine the periods where the functions direction changes, the derivates providing the inflexion points will be investigated.

These derivates are plotted in Figure 75 to indicate where the inflexion points oscillate. The inflexion points are indicated in blue. The differentiated curves are given by the symbol "D" followed by the order number.

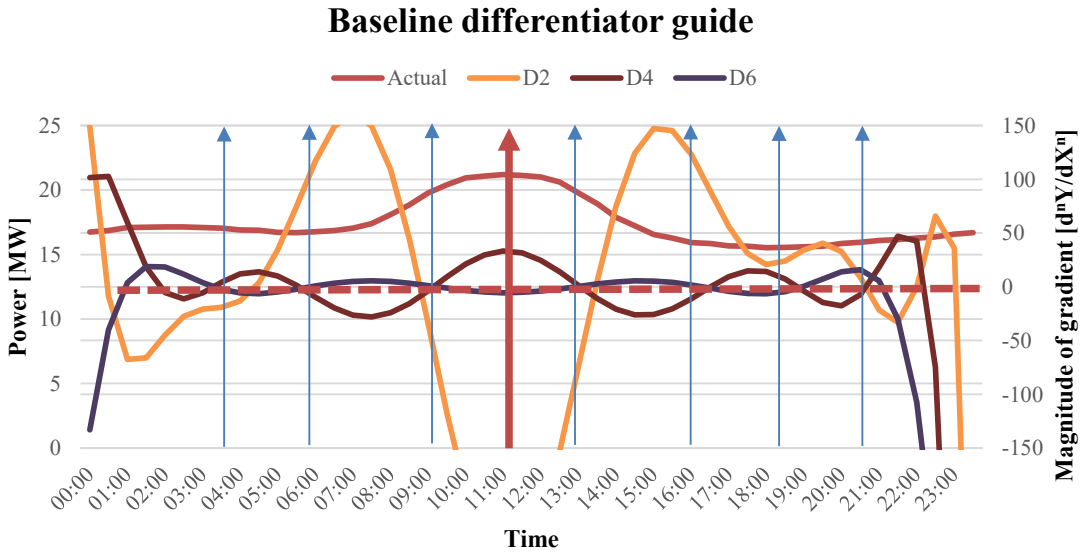

Figure 75 - Inflection points for average baseline power profile

Table 24 displays the inflexion points of the averaged baseline power profiles for 29 mines.

Table 24 - Baseline inflection point summary

Inflection Points	03:30	05:30	09:00	13:00	16:30	19:00	21:00	00:00

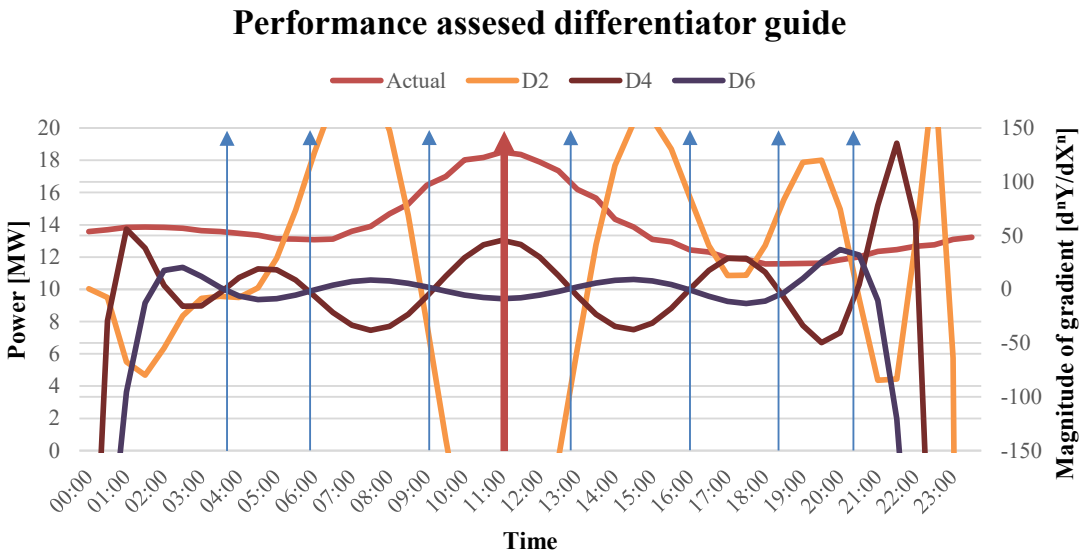

Figure 76 - Inflection points for average performance assessed measured power profile

Table 25 displays the inflection points of the averaged performance assessed power profiles for 29 mines.

Table 25 - Performance assessed measured inflection point summary

Inflection Points	03:30	05:30	09:00	13:00	16:30	19:00	21:00	00:00

APPENDIX G: MAX, MIN AND AVERAGE PROFILES

Figure 78 compares the baselines sample space's average power data points with the performance measured sample space's average power data points. R^2 for the average power data is calculated at 0.949 (as calculated by Microsoft Excel® 2016). A strong linear correlation also exists for this parameter.

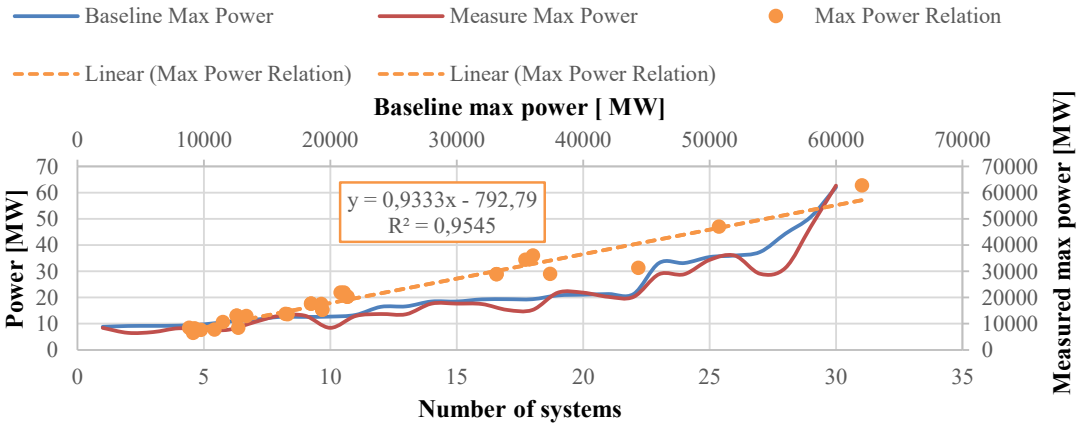

Figure 77 - Figure 27 additional data

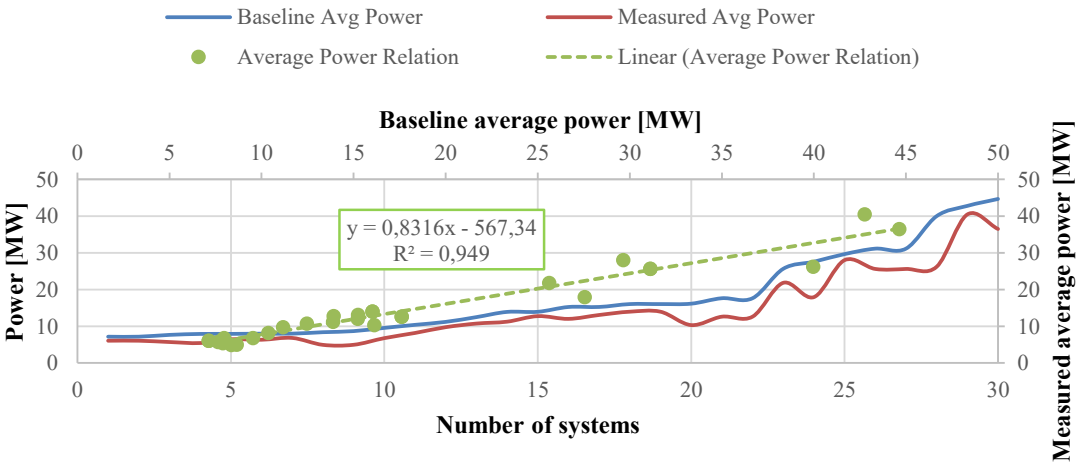

Figure 78 - Average power correlation

Figure 79 compares the baselines sample space's minimum power data points with the performance measured sample space's minimum power data points.

R^2 for the average power data is calculated at 0.949 (as calculated by Microsoft Excel® 2016). A strong linear correlation also exists for this parameter.

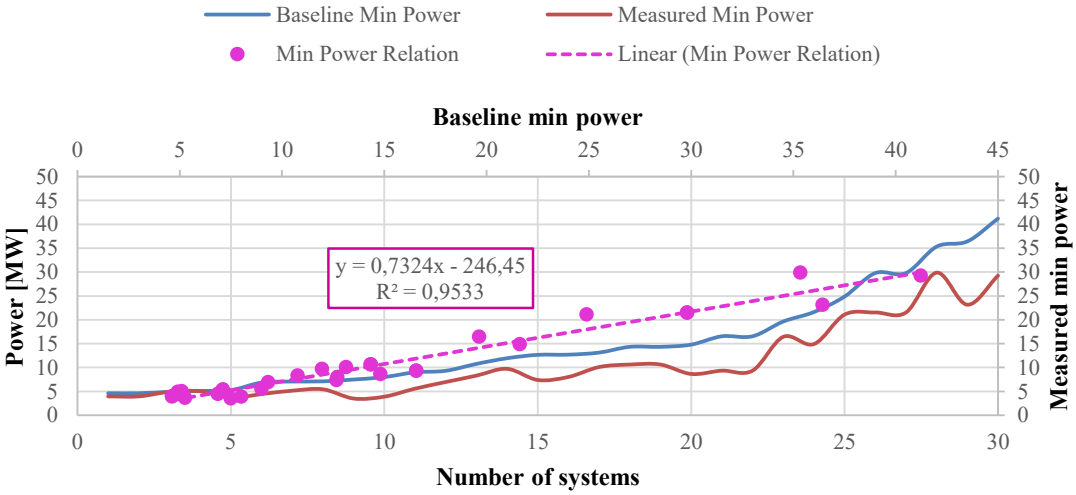

Figure 79 - Minimum power calculations

APPENDIX H: MATHEMATICAL EXPRESSION OF TABULATED DATA

Equation 30 and Equation 31 are mathematical expressions used to indicate how the results were calculated in Table 26.

P_{Peak_B} = Peak baseline power during drilling shift

$P_{no\text{-}Peak_{Zi\_B}}$ = Baseline power for each zone

$P_{no\text{-}Peak_{Zi\_PA}}$ = Performance assessed power for each zone

t = 24-hour dialy profile containing 48 half hour segments

Equation 30 - ERR Pre-Implementation Profile

$$ERR(t)_{Pre\_Profile} = \begin{cases} 1-(P_{no\text{-}Peak_{Z1\_B}} / P_{Peak\_B}), & t<3:30 \\ 1-(P_{no\text{-}Peak_{Z2\_B}} / P_{Peak\_B}), & 03:30<t<05:30 \\ 1-(P_{no\text{-}Peak_{Z3\_B}} / P_{Peak\_B}), & 05:30<t<09:00 \\ 1-(P_{no\text{-}Peak_{Z4\_B}} / P_{Peak\_B}), & 09:00<t<11:00 \\ 1-(P_{no\text{-}Peak_{Z5\_B}} / P_{Peak\_B}), & 11:00<t<13:00 \\ 1-(P_{no\text{-}Peak_{Z6\_B}} / P_{Peak\_B}), & 13:00<t<16:30 \\ 1-(P_{no\text{-}Peak_{Z7\_B}} / P_{Peak\_B}), & 16:30<t<19:00 \\ 1-(P_{no\text{-}Peak_{Z8\_B}} / P_{Peak\_B}), & 19:00<t<21:00 \\ 1-(P_{no\text{-}Peak_{Z9\_B}} / P_{Peak\_B}), & 21:00<t<23:59 \end{cases}$$

Equation 31 - ERR Post-Implementation Profile

$$ERR(t)_{Post\_Profile} = \begin{cases} 1-(P_{no\text{-}Peak_{Z1\_PA}} / P_{Peak\_B}), & t<3:30 \\ 1-(P_{no\text{-}Peak_{Z2\_PA}} / P_{Peak\_B}), & 03:30<t<05:30 \\ 1-(P_{no\text{-}Peak_{Z3\_PA}} / P_{Peak\_B}), & 05:30<t<09:00 \\ 1-(P_{no\text{-}Peak_{Z4\_PA}} / P_{Peak\_B}), & 09:00<t<11:00 \\ 1-(P_{no\text{-}Peak_{Z5\_PA}} / P_{Peak\_B}), & 11:00<t<13:00 \\ 1-(P_{no\text{-}Peak_{Z6\_PA}} / P_{Peak\_B}), & 13:00<t<16:30 \\ 1-(P_{no\text{-}Peak_{Z7\_PA}} / P_{Peak\_B}), & 16:30<t<19:00 \\ 1-(P_{no\text{-}Peak_{Z8\_PA}} / P_{Peak\_B}), & 19:00<t<21:00 \\ 1-(P_{no\text{-}Peak_{Z9\_PA}} / P_{Peak\_B}), & 21:00<t<23:59 \end{cases}$$

APPENDIX I: TOTAL ERR CALCULATION RESULT FOR 29 SYSTEMS

I.1 Tabulated Results

Table 26 - ERR parameters for 30 compressed air

	Maximum power usage kW	Pre-implementation ERR									Post-implementation ERR								
System Nr	Zones	Z1	Z2	Z3	Z4	Z5	Z6	Z7	Z8	Z9	Z1	Z2	Z3	Z4	Z5	Z6	Z7	Z8	Z9
1	35439.20	23.72	23.47	25.15	5.71	-1.10	18.19	28.98	28.55	26.51	36.72	40.05	36.61	5.75	-0.10	30.56	43.73	44.44	43.29
2	9273.50	10.33	10.17	16.05	6.19	-0.81	9.55	20.89	21.14	20.01	28.35	34.23	28.84	18.67	17.13	27.96	36.48	37.48	31.64
3	19361.80	11.12	11.67	7.37	0.74	0.81	5.53	10.42	10.02	8.62	29.43	39.01	32.63	27.26	27.59	32.94	47.52	43.47	29.68
4	13361.50	40.98	41.10	33.85	1.88	2.55	19.67	43.71	45.39	43.27	49.86	50.69	50.81	25.90	1.68	26.95	51.15	52.42	52.83
5	33153.60	0.81	-0.80	-0.97	-0.28	-2.79	0.10	2.50	4.81	2.64	16.10	13.96	12.42	12.87	15.22	19.81	26.56	27.97	21.31
6	50733.30	10.42	10.52	9.37	1.15	-0.68	10.42	15.41	13.96	13.15	24.14	27.54	28.27	10.82	7.19	25.81	38.53	39.87	29.79
7	12723.60	38.23	38.36	39.06	18.39	-1.45	17.48	39.33	38.43	38.22	65.20	64.79	67.14	53.08	37.72	50.57	65.14	66.82	67.31
8	10840.60	31.44	32.77	31.59	5.48	1.00	22.91	36.23	35.08	35.17	52.02	53.27	50.00	33.72	33.75	50.20	57.24	57.57	54.82
9	18485.70	12.53	11.52	11.07	0.61	2.36	14.65	17.41	21.36	20.13	21.01	20.97	21.71	11.67	11.26	23.88	30.17	36.67	36.80
10	16627.40	-2.55	-2.56	-2.78	-1.00	0.13	0.58	7.38	2.25	-2.87	36.89	36.72	36.21	36.16	37.12	35.68	36.19	34.27	34.02
11	44354.40	2.91	2.87	3.87	0.28	1.25	8.97	11.52	12.94	10.58	37.27	38.68	38.51	30.98	31.47	39.63	42.33	44.06	41.94
12	13061.40	50.91	50.49	45.81	9.52	-2.19	27.89	60.84	59.39	59.35	63.73	63.84	60.33	25.47	-5.92	35.77	64.26	66.28	65.30
13	9773.50	-3.15	-2.85	-1.41	-0.33	0.06	1.03	0.97	-0.36	-2.86	26.72	27.22	27.59	26.98	28.28	29.99	31.64	30.59	27.84
14	8840.00	8.36	11.20	6.99	-0.63	0.69	12.52	16.00	13.23	9.31	25.67	29.47	23.03	11.00	17.03	36.23	38.96	37.16	28.54
15	11512.80	-2.36	-1.73	-1.04	-0.22	0.12	3.01	2.85	0.15	0.01	9.08	10.87	13.14	8.11	6.65	13.16	19.08	20.40	16.11

16	9189.20	13.83	14.52	16.42	4.21	0.23	11.89	28.06	29.60	17.57	35.99	35.98	38.24	33.82	27.61	34.29	41.64	41.90	40.85
17	9145.90	7.26	8.37	4.05	-0.86	4.11	9.70	10.07	9.80	7.17	47.30	47.08	38.14	29.83	32.42	45.35	54.44	55.39	53.85
18	17675.40	12.53	11.52	11.07	0.61	2.36	14.65	17.41	21.36	20.13	21.01	20.97	21.71	11.67	11.26	23.88	30.17	36.67	36.80
19	13061.00	50.91	50.49	45.81	9.52	-2.19	27.89	60.84	59.39	59.35	63.73	63.84	60.33	25.47	-5.92	35.77	64.26	66.28	65.30
20	17514.53	38.68	40.14	36.16	6.65	3.52	37.70	52.95	60.34	43.14	53.01	54.49	51.19	23.60	13.94	45.17	71.04	71.30	58.34
21	28882.00	0.81	-0.80	-0.97	-0.28	-2.79	0.10	2.50	4.81	2.64	16.10	13.96	12.42	12.87	15.22	19.81	26.56	27.97	21.31
22	35978.30	15.36	18.61	16.29	3.97	1.13	18.81	27.68	28.84	20.38	16.79	21.60	21.97	3.74	2.67	23.86	37.67	36.61	26.61
23	62682.20	35.40	35.51	31.27	3.37	4.74	33.52	41.64	38.63	37.17	38.87	39.98	33.26	7.73	9.00	36.88	47.89	43.06	40.26
24	21866.30	37.88	39.73	36.12	5.95	4.94	35.57	41.05	40.38	39.88	42.58	45.53	41.42	1.88	2.32	46.13	51.75	49.28	47.11
25	29046.16	26.60	27.24	21.81	4.01	1.93	29.95	38.62	32.90	29.60	54.21	53.71	50.75	37.57	36.02	51.54	55.97	56.71	56.06
27	20270.92	34.73	36.26	28.92	0.04	0.08	22.53	39.48	38.38	36.84	43.64	49.13	49.22	13.99	8.37	40.72	57.56	60.59	51.40
28	13715.30	6.25	4.94	3.81	2.98	-9.52	0.36	7.70	7.56	5.46	27.39	27.38	22.96	7.28	5.16	16.72	27.78	28.16	29.29
29	20258.41	34.73	36.26	28.92	0.04	0.08	22.53	39.48	38.38	36.84	38.53	43.58	43.05	9.27	5.65	34.15	55.17	60.19	43.10

I.2 Statistical Expression

Equation 32 - ERR Data set

$$\mathbf{ERR = \{ P_{Pre} \ , P_{Post}\}}$$

$$\mathbf{P_{pre} \ , \ P_{post} = \{p_1, p_2, p_3 \cdots p_9 \}}$$

$$\mathbf{p_{1\text{-}9} = \{x_1, x_2, x_3 \ldots \ x_{29}\}}$$

ERR	= Total ERR population proportion
$\mathbf{P_{pre}}$ **and** $\mathbf{P_{post}}$	= Population proportion for ERR parameters
x_k	= ERR variable
$\mathbf{p_{1\text{-}9}}$	= ERR for a specific zone
k	= Variable number

APPENDIX J: ERR BANDWITH RESULTS FOR ALL ZONES

Figure 80 displays the collection of results for all zones regarding the bandwidth calculations explained in section 3.3.3. Zone one is enlarged to indicate the legends for all nine figures.

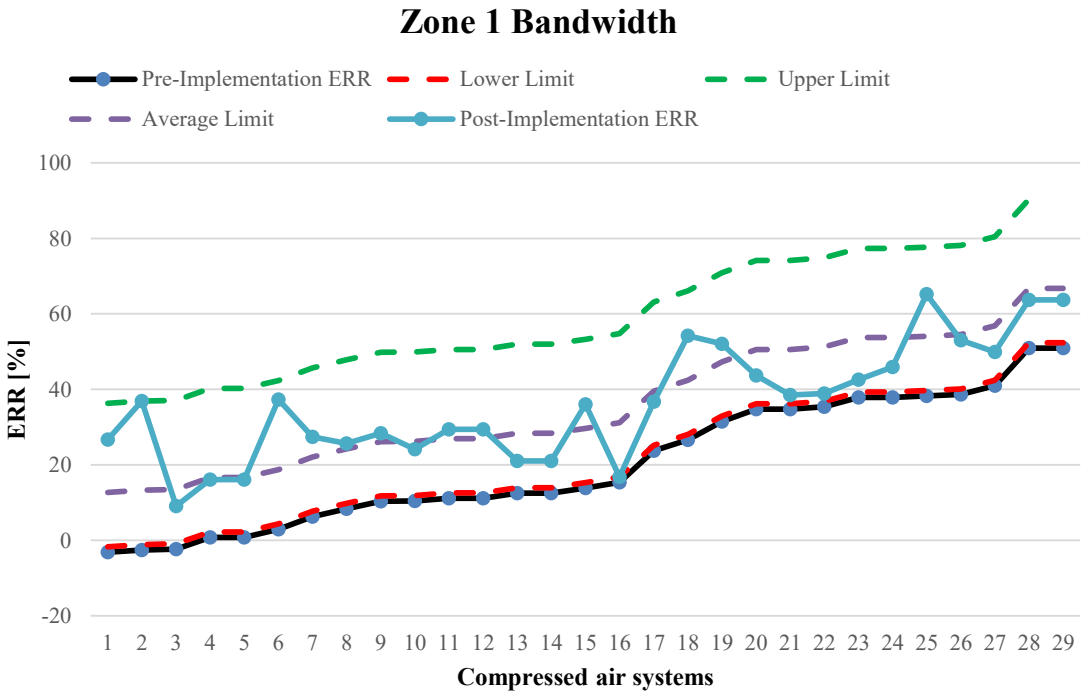

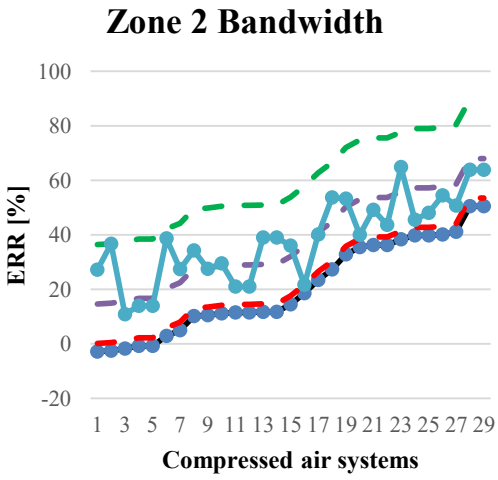

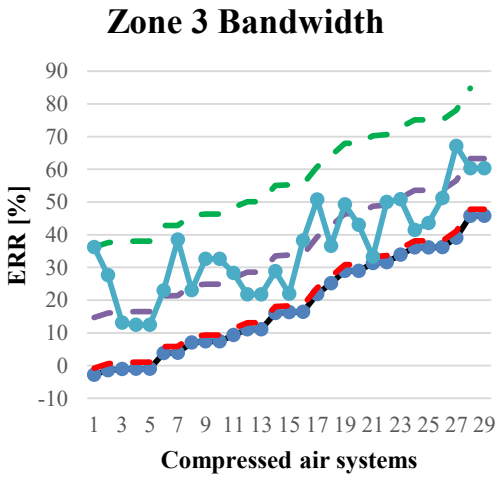

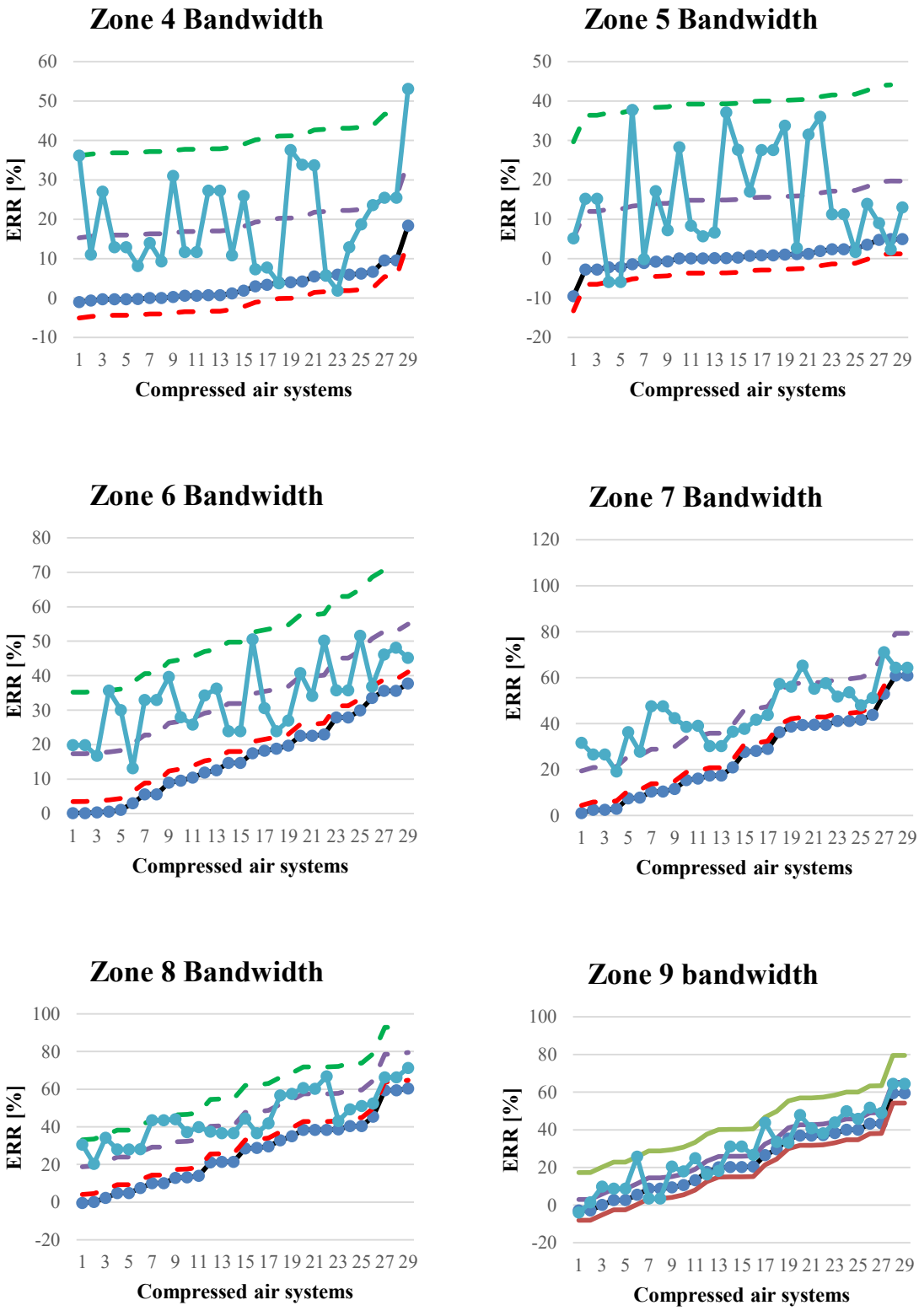

Figure 80 - Collection of ERR bandwidth data for all zones

APPENDIX K: ERR VS POWER CONSUMPTION

Figure 81 displays the collection of results for zone 1 regarding the ERR vs other power consumption parameters explained in section 3.3.3. Similar calculations were conducted for all zones and the results are summarised in section 3.3.3.

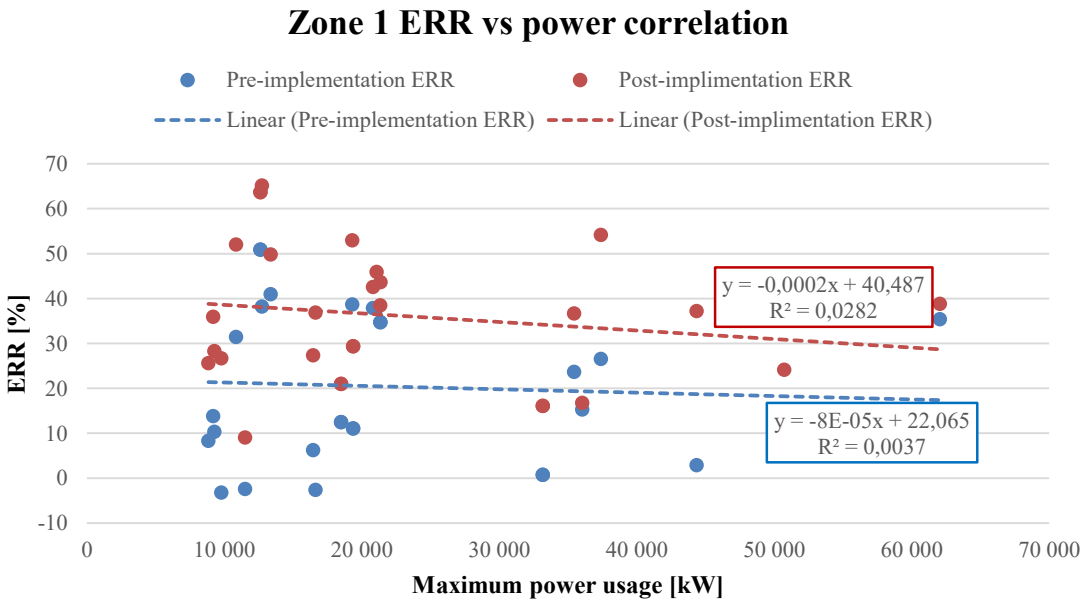

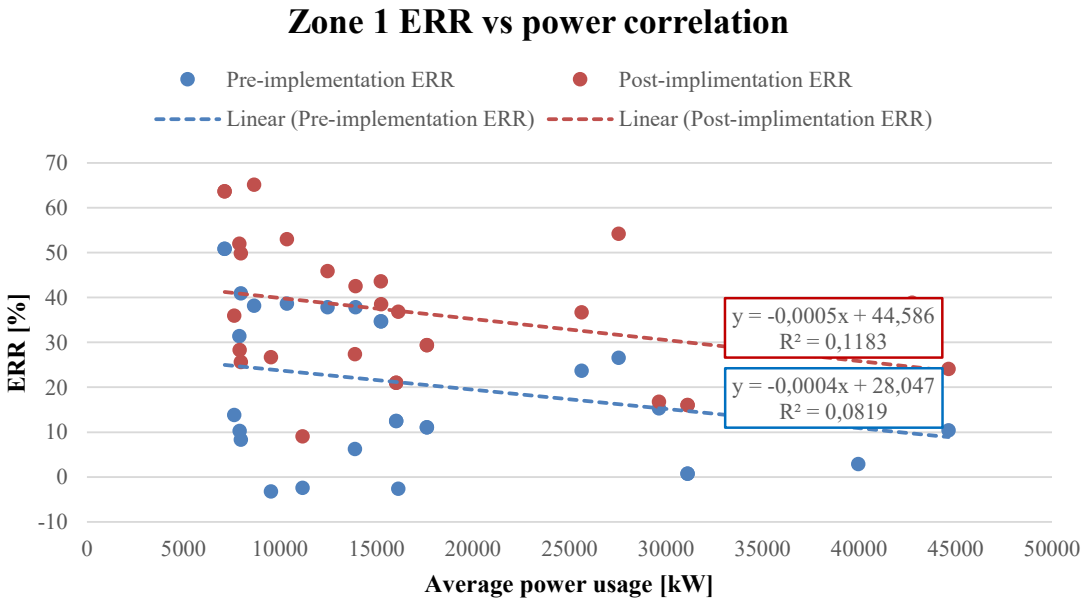

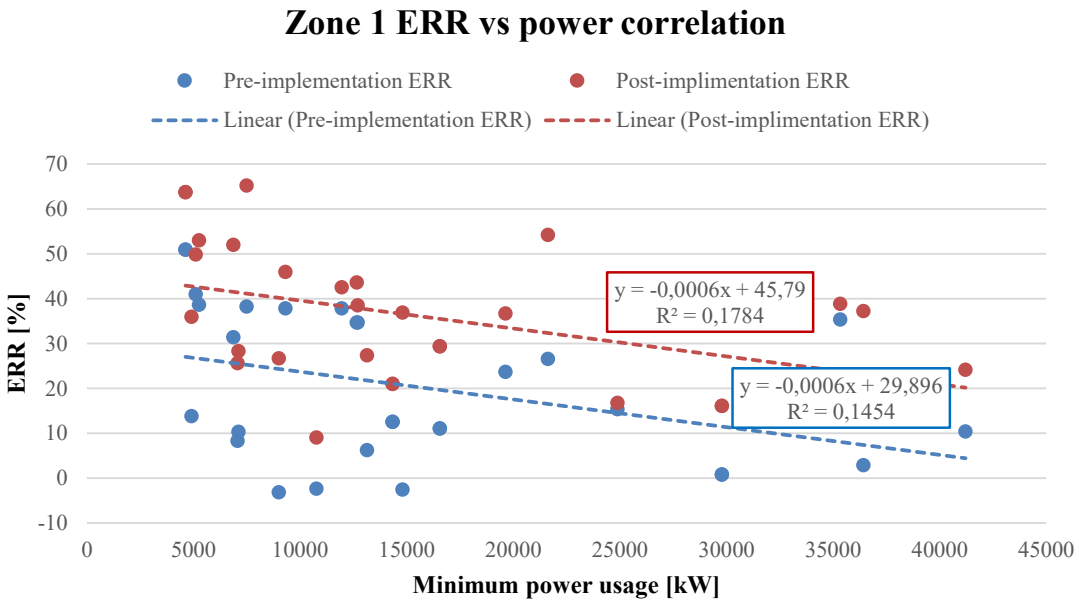

Figure 81 - ERR vs power correlations - Max, Min, and Average

APPENDIX L: TOTAL ERR CALCULATION RESULT FOR 29 SYSTEMS

Figure 82 displays the collection of results for all zones regarding the bandwidth calculations explained in section 3.3.3. Zone 1 is enlarged to indicate the legends for all nine figures.

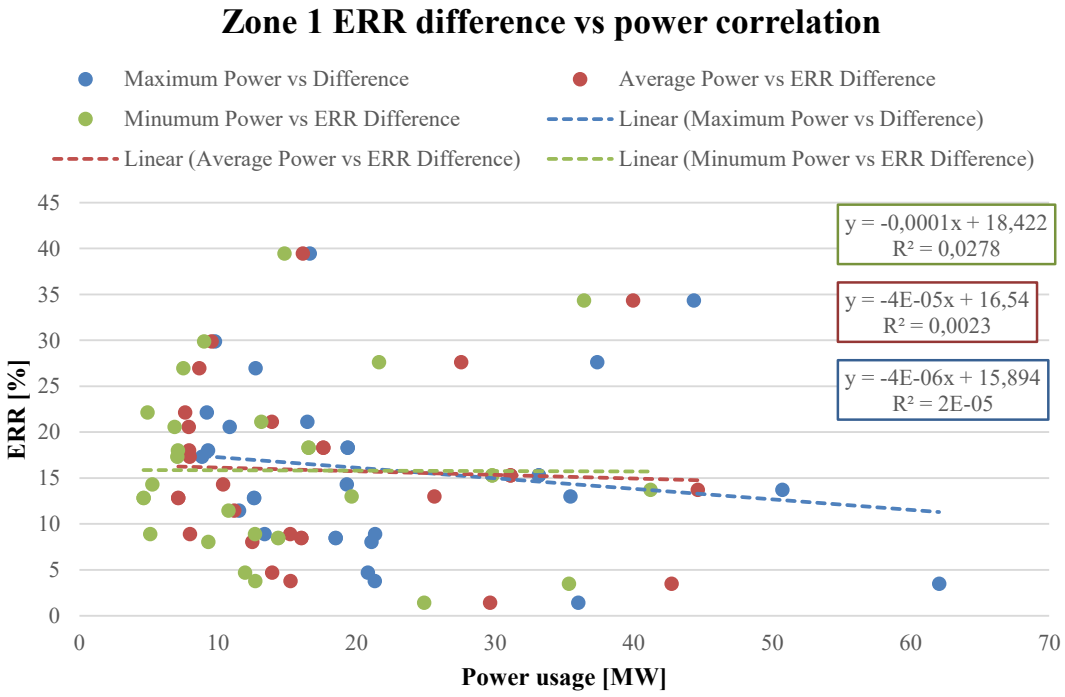

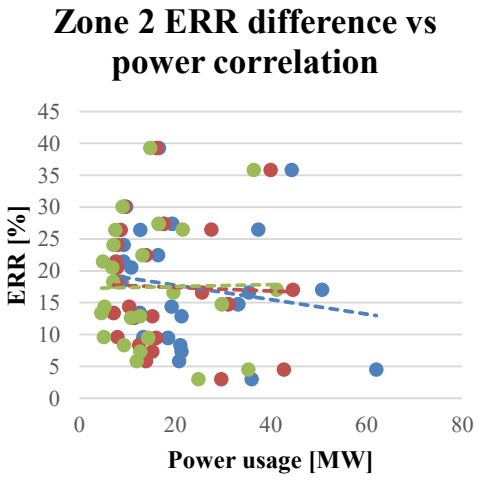

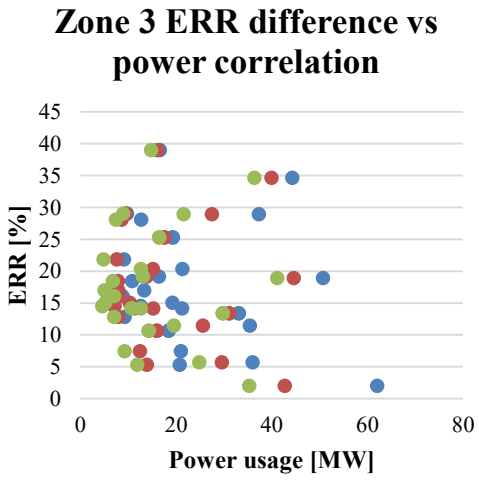

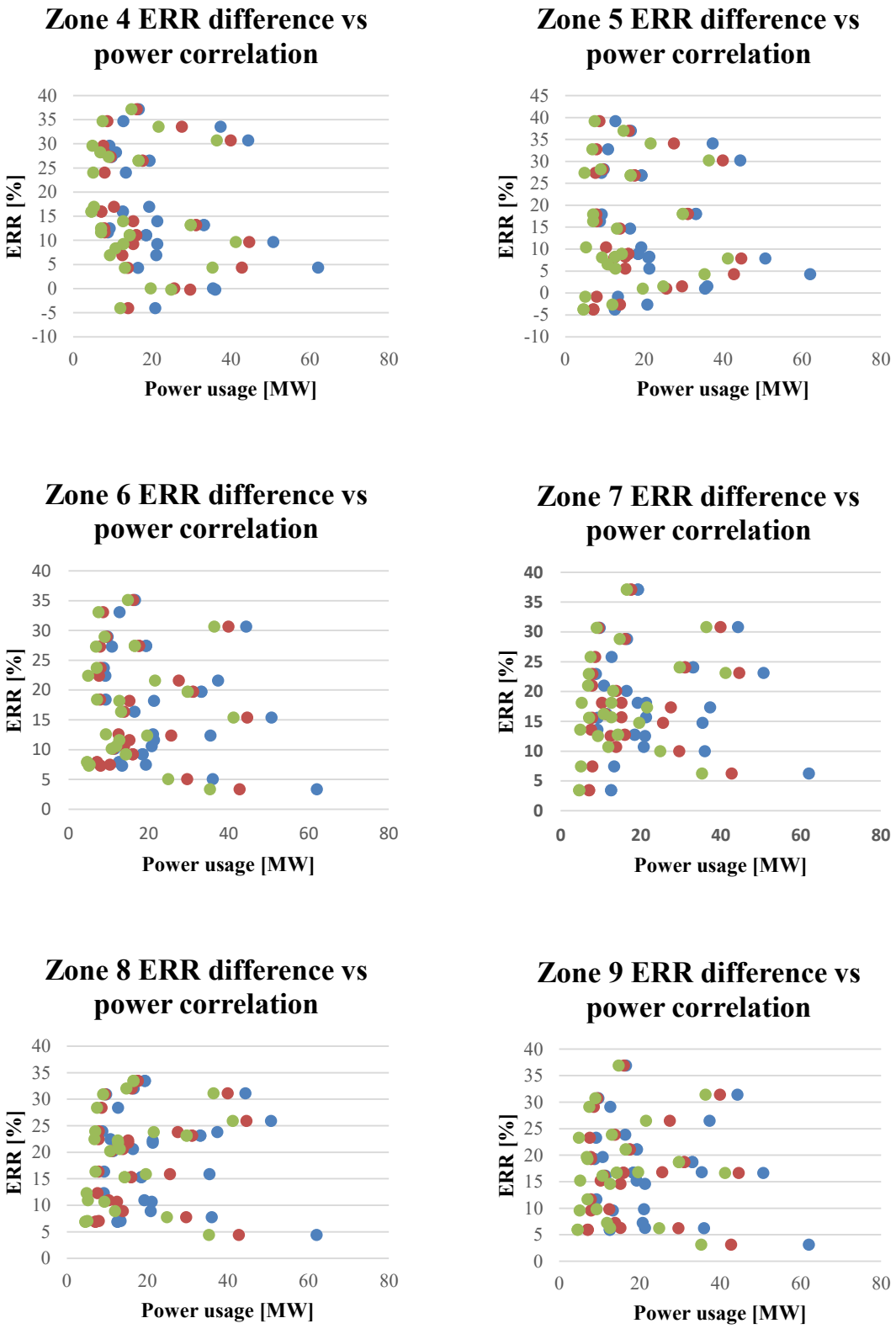

Figure 82 - Collection of ERR difference vs power relations parameters

APPENDIX M: TOTAL ERR CALCULATION RESULT FOR 29 SYSTEMS

Figure 83 displays the collection of results for all zones pre-implementation and post-implementation ERR calculations explained in section 3.3.3. Zone 1 is enlarged to indicate the legends for all 9 figures.

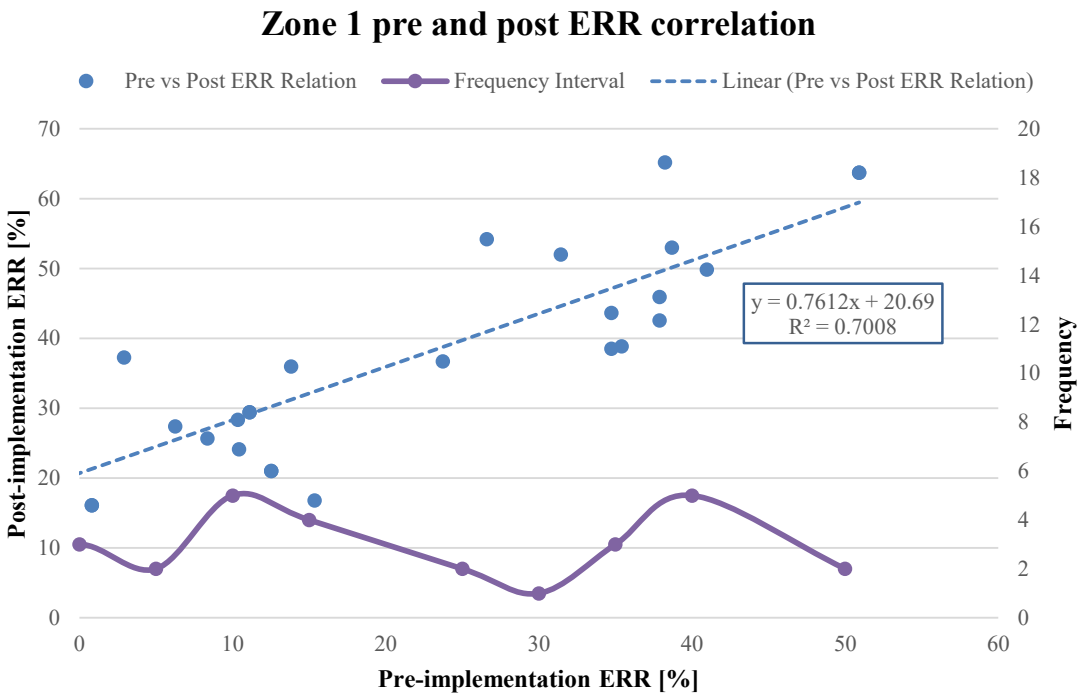

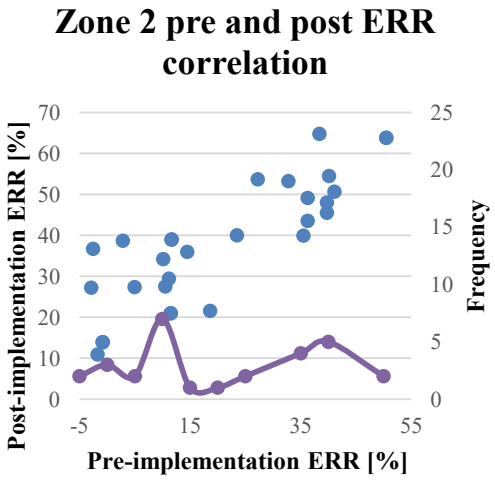

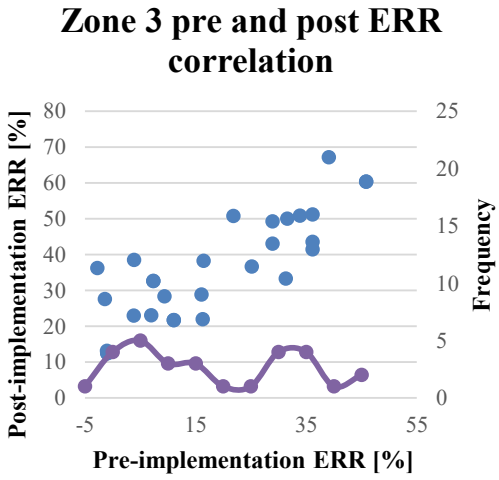

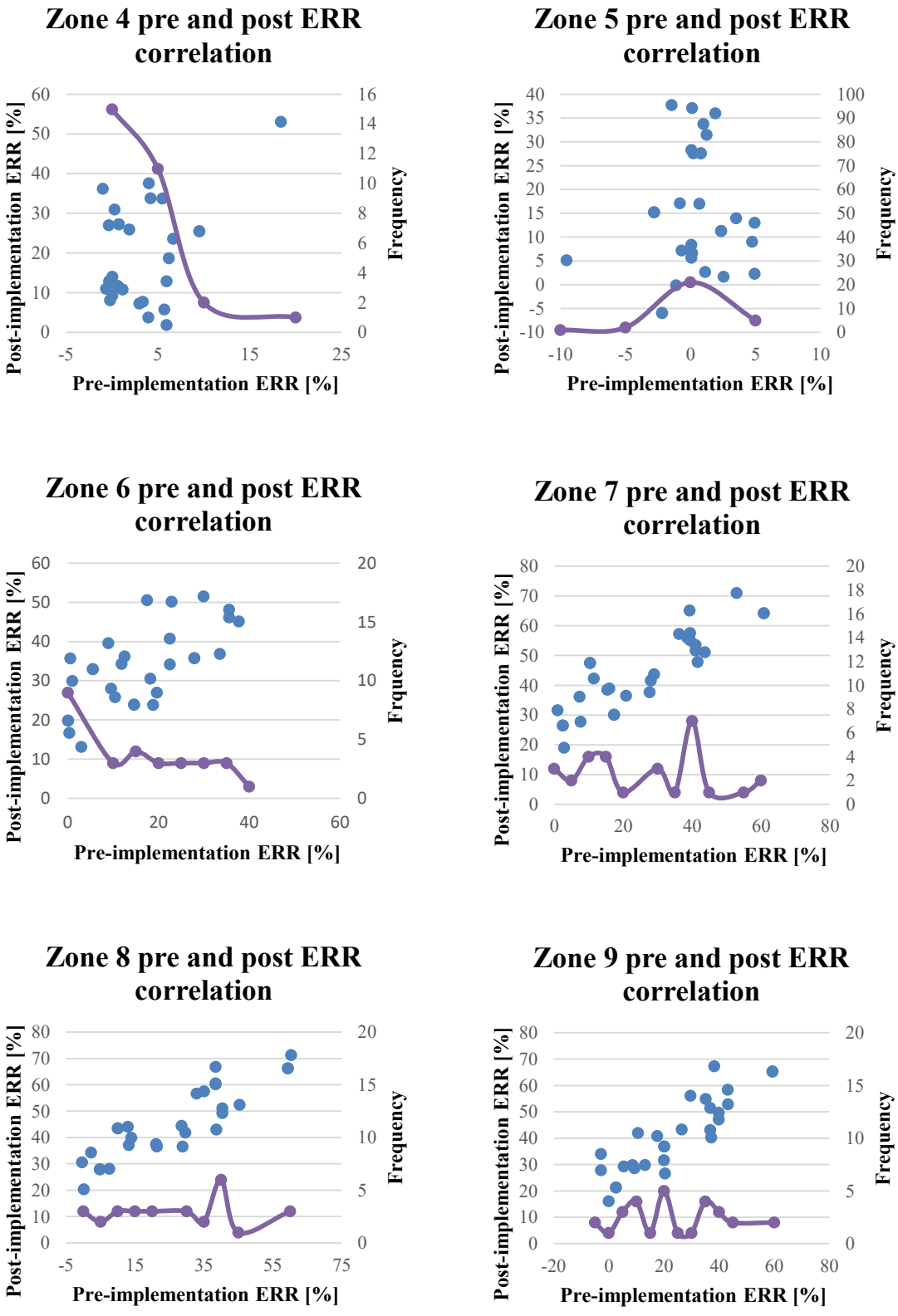

Figure 83 - Collection of pre-implementation vs post-implementation correlations

APPENDIX N: PRIMARY ERR REGRESSION SUMMARY

N.1 Linear Regression summary for pre-implementation ERR vs post-implementation ERR.

Table 27 displays the correlation parameters for all the zones as displayed in Figure 51.

Table 27 - Regression lines and correlation coefficients of all zones

Zones	R^2	Regression line
Z1	0.7008	0.7612X + 20.6897
Z2	0.7096	0.7443X + 22.7731
Z3	0.6943	0.7972X + 21.2756
Z4	0.1654	1.1887X + 15.6637
Z5	0.0104	0.4663X + 14.9394
Z6	0.4541	0.5915X + 23.8503
Z7	0.7607	0.6563X + 27.4698
Z8	0.776	0.6569X + 28.1086
Z9	0.7773	0.6956X + 24.305

N.2 Effect of filtering zone 4, 5, six on data frequency distribution

Figure 84 plots the frequency distribution of the nine district zones. The primary axis at the bottom displays the nine different zones frequency distribution per 5 % pre-implementation ERR interval.

The upper lines display the maximum, average and minimum values parameters of the 9 zones. According to the plotted data, a large sample of systems with low pre-implementation ERR is contained within the investigated sample space. This creates an imbalance in data processing.

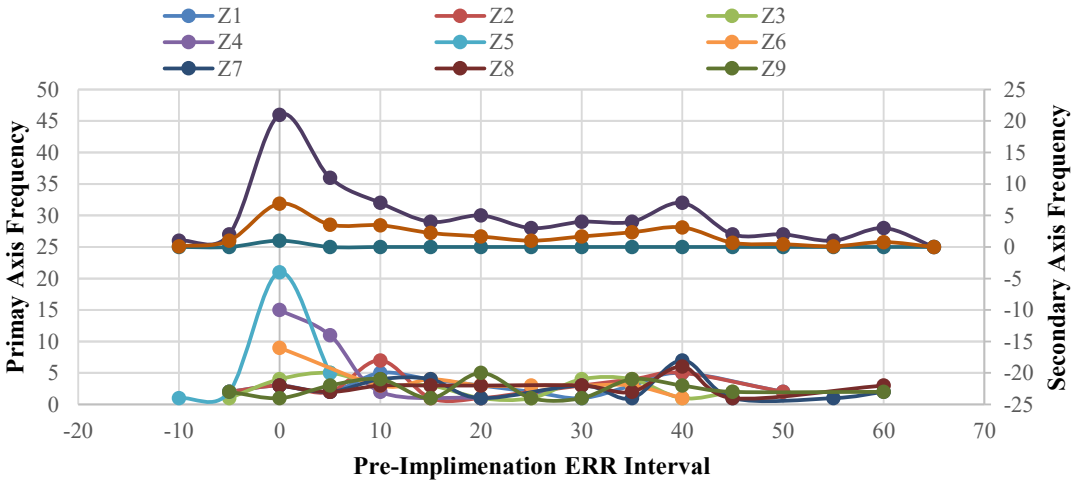

Figure 84 - Frequency distribution analysis

Figure 85 displays the same profile as Figure 84, with zones 4,5 and 6 filtered from the data set. The result is a more balanced frequency distribution across the remaining zones, resulting in the increased validity of the correlation coefficients.

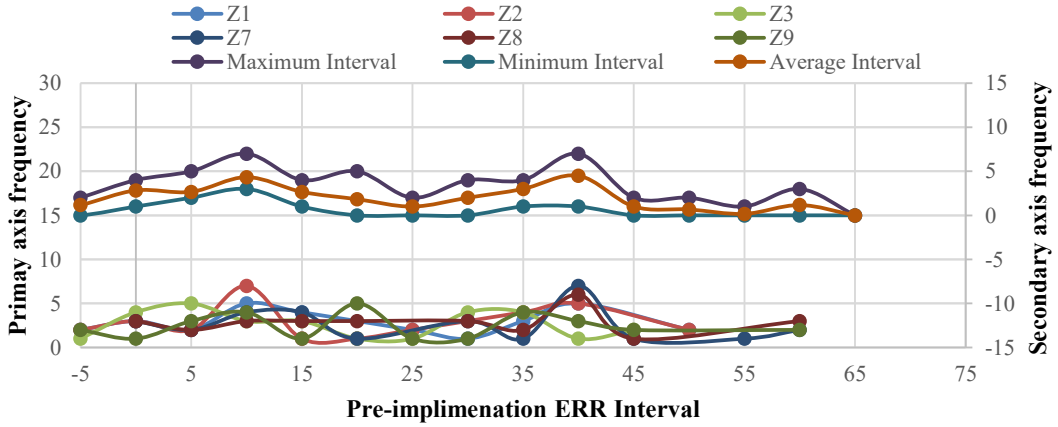

Figure 85 - Filtered frequency distribution

APPENDIX O: ADJUSTED ESTIMATION MODEL #1 REGRESSIONS

Figure 86 displays the collection of results for all zones adjusted model #1 calculations explained in section 3.5. Zone 1 is enlarged to indicate the legends for all 9 figures.

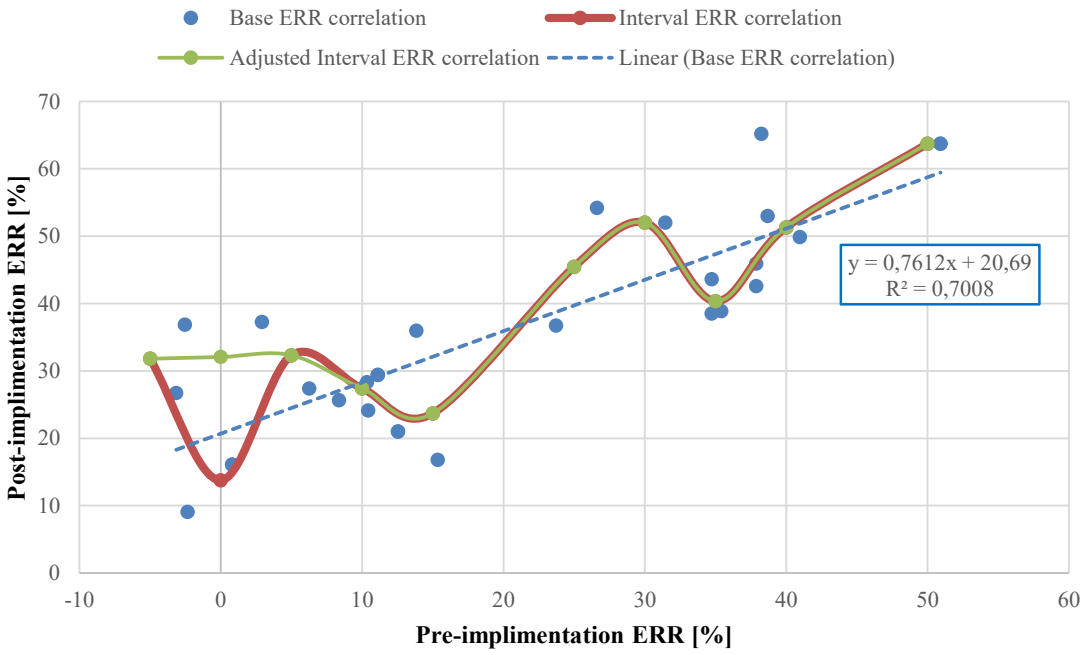

Zone 2 adjusted model #1 regression

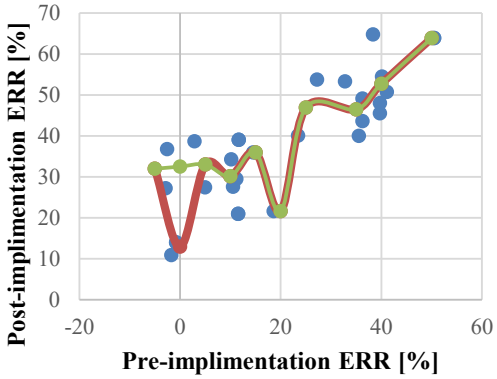

Zone 3 adjusted model #1 regression

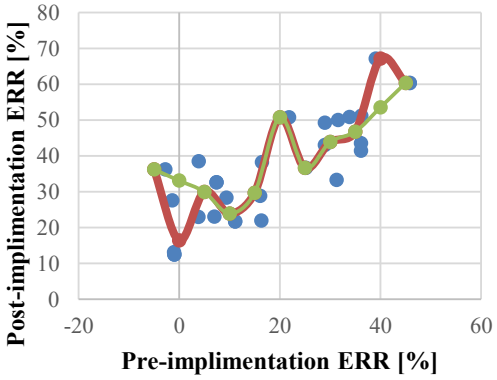

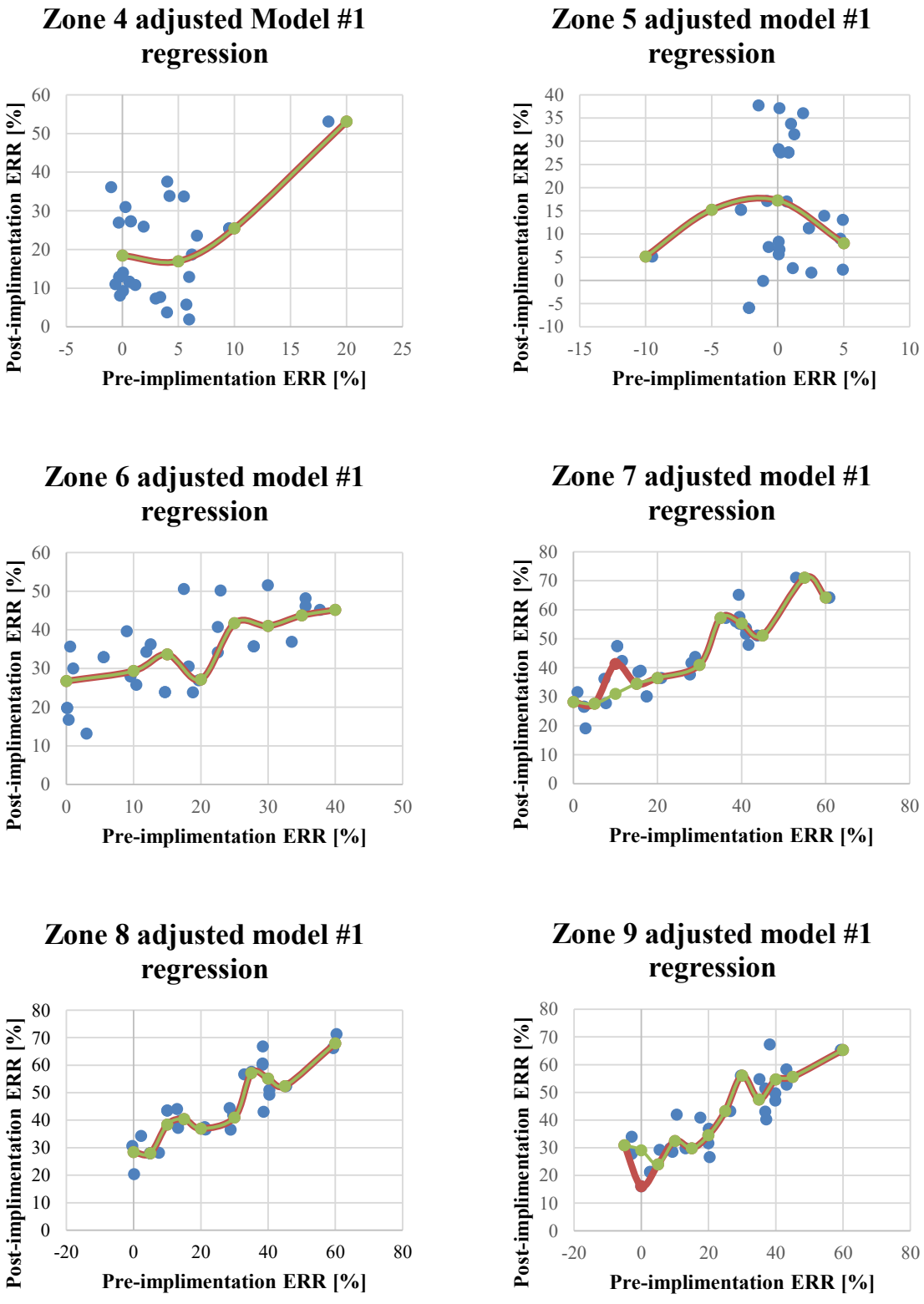

Figure 86 - Collection of adjusted models #1 regression analysis

APPENDIX P: ADJUSTED ESTIMATION MODEL #2 REGRESSIONS

Figure 87 displays the collection of results for all zones adjusted model #2 calculations explained in section 3.5. Zone 1 is enlarged to indicate the legends for all 9 figures.

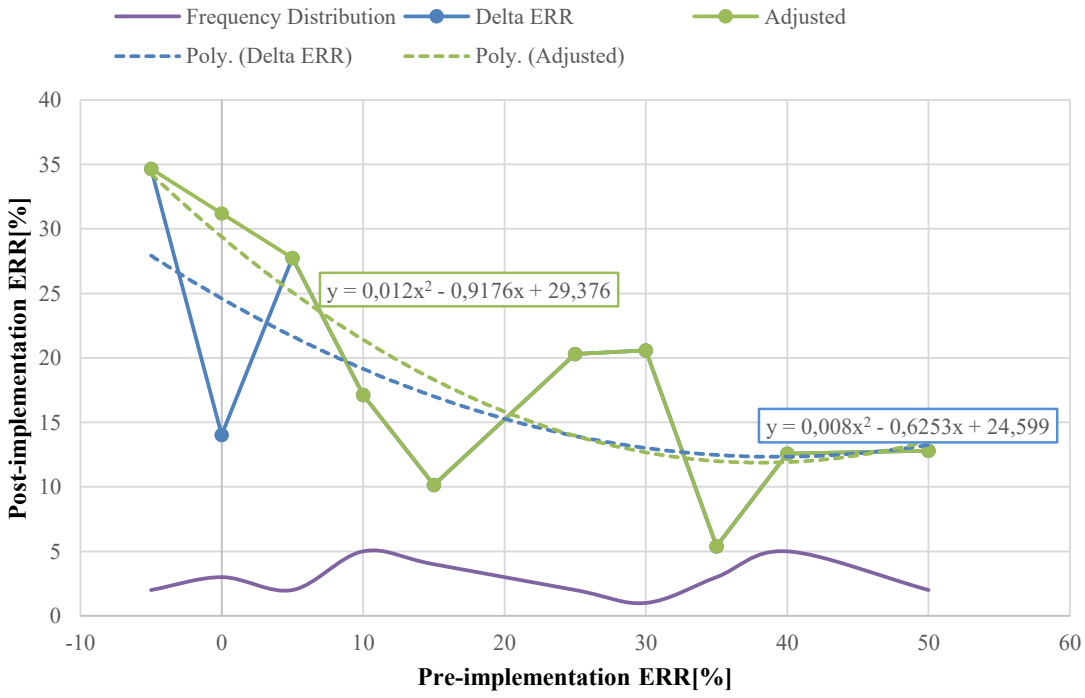

Zone 2 adjusted model #2 regression

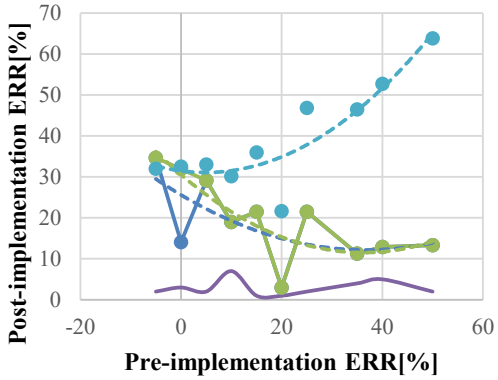

Zone 3 adjusted model #2 regression

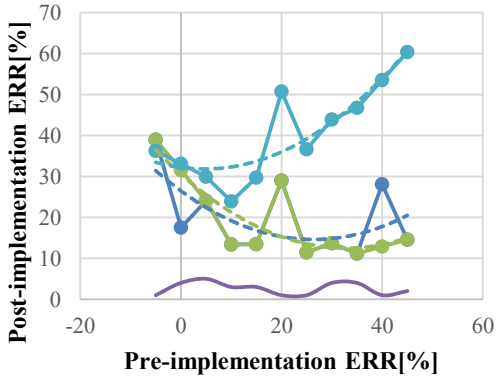

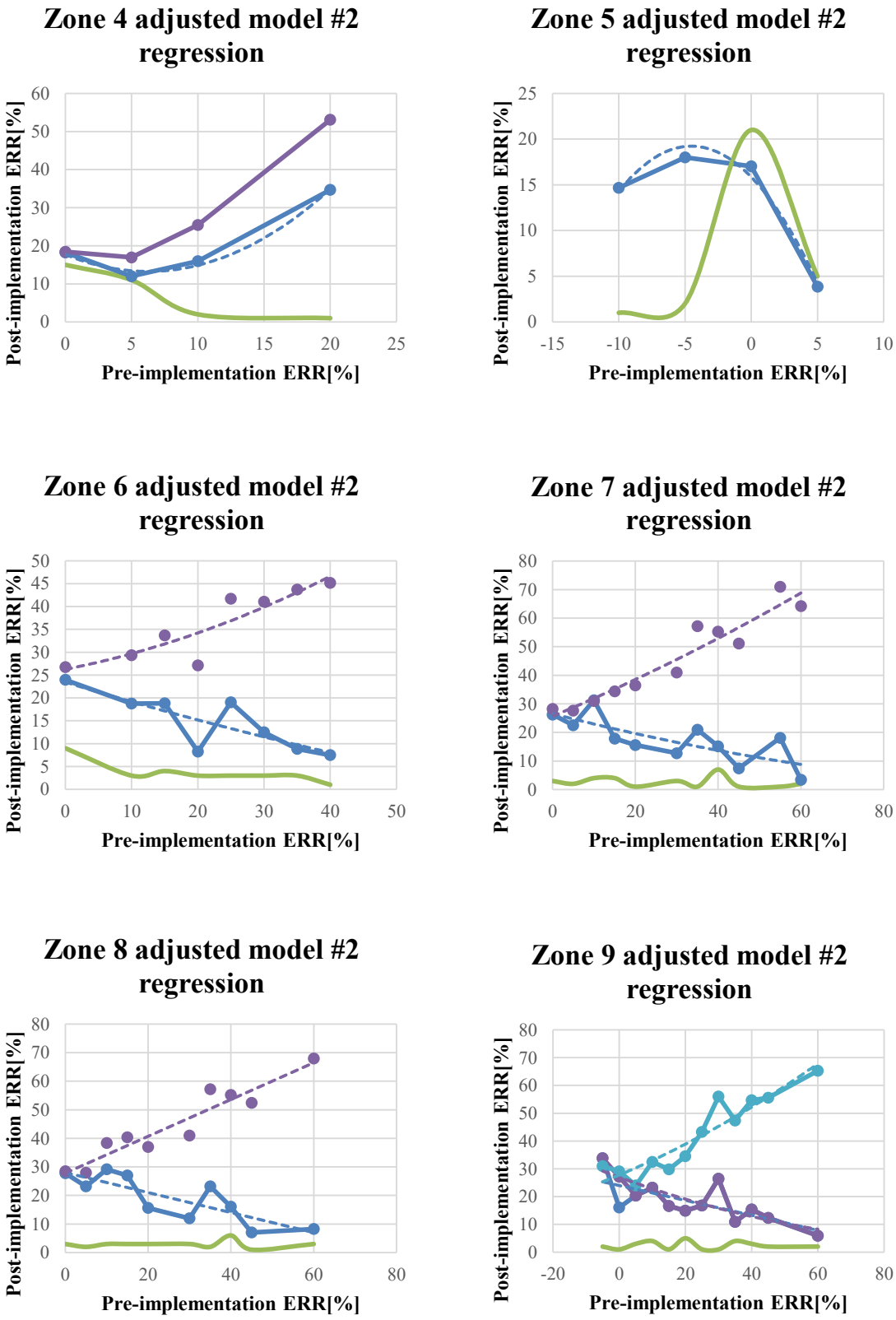

Figure 87 - Collection of adjusted models #2 regression analysis

APPENDIX Q: GUIDANCE ESTIMATION REGRESSIONS

Q.1 Input quantification of adjusted models

Figure 88 displays the collection of results for all zones adjusted model #2 calculations explained in section 3.5. Zone 1 is enlarged to indicate the legends for all 9 figures.

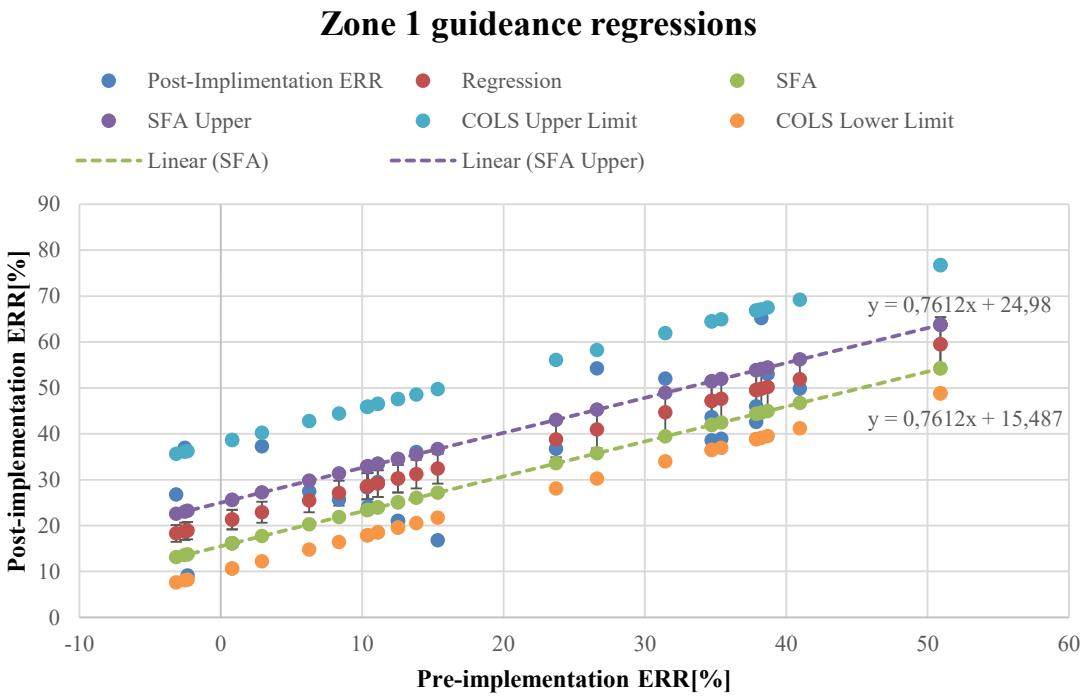

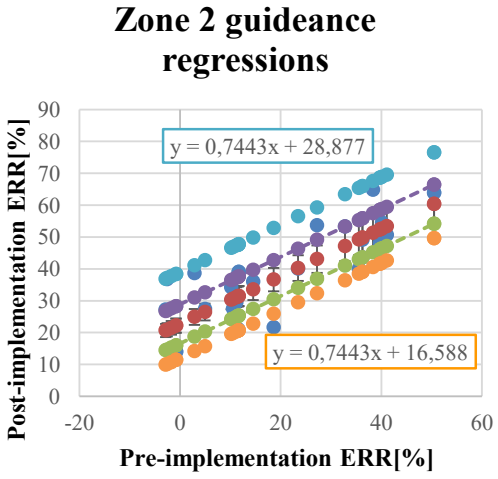

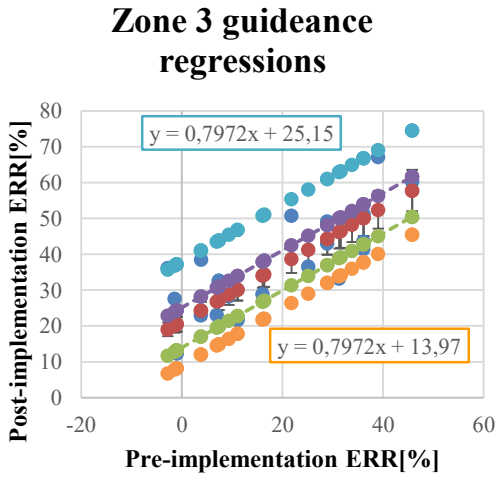

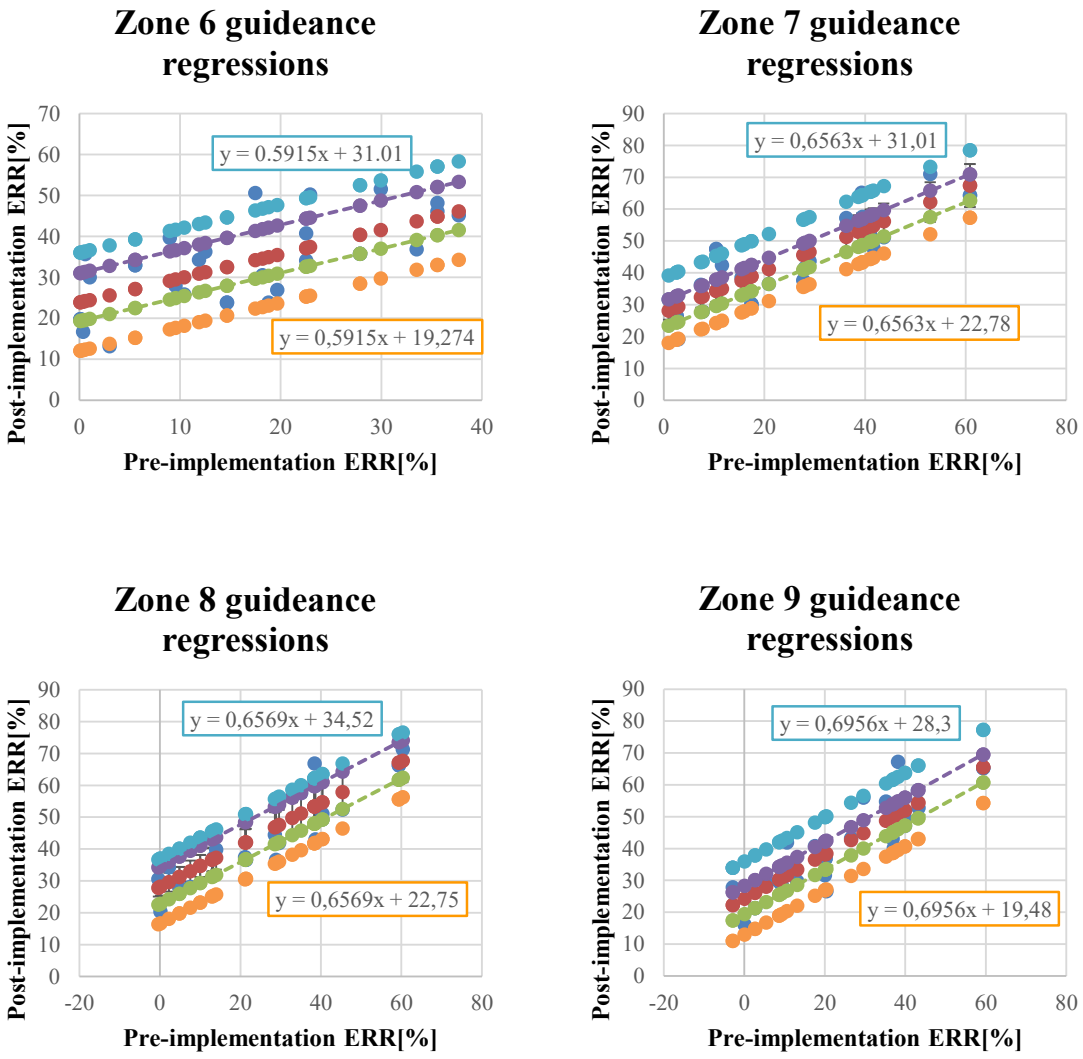

Figure 88 - Collection of guidance regressions

Q.2 Input quantification of adjusted models

The input variables for the adjusted models are the same as the input variables for the original model shown in section 3.4.1 as equation 27.

Q.3 Calculation of adjusted model parameters

The ERR calculation method for the adjusted models are the same as the ERR calculation method for the original model shown in section 3.4.2 as equation 28.

Q.4 Calculation of adjusted model parameters

The difference between the models exists in the transformation of the pre-implementation ERR to the post-implementation ERR. The proposed transformation equations are given below in Equation 33 and Equation 34.

Equation 33 - Adjusted method #1 post-implementation vector

$$\overline{ERR_{post}} = \bar{y} = \bar{C} \cdot \overline{ERR_{pre}}^{2} + \bar{D} \cdot \overline{ERR_{pre}} + \bar{e}$$

$$\overline{ERR_{post}} = \bar{y} = \begin{bmatrix} 0.0140 \\ 0.0166 \\ 0.0177 \\ 0 \\ 0 \\ 0.0055 \\ 0.002 \\ 0 \\ 0.0028 \end{bmatrix} \overline{ERR_{pre}}^{2} + \begin{bmatrix} -0.0190 \\ -0.1610 \\ -0.1640 \\ 0 \\ 0 \\ 0.2875 \\ 0.5518 \\ 0.6440 \\ 0.5004 \end{bmatrix} \overline{ERR_{pre}} + \begin{bmatrix} 30.2730 \\ 31.4610 \\ 32.1840 \\ 0 \\ 0 \\ 26.2510 \\ 27.9830 \\ 27.8250 \\ 27.7590 \end{bmatrix}$$

$\overline{ERR_{post}}$	= Post-implementation ERR vector	[-]
$\overline{ERR_{pre}}$	= Pre-implementation ERR vector	[-]
$\bar{C}$	= Second order gradient vector	[-]
$\bar{D}$	= First order gradient vector	[-]
$\bar{e}$	= Constants vector	[-]

Equation 34 - Adjusted method #2 post-implementation vector

$$\overline{ERR_{post}} = \bar{y} = \bar{C} \cdot \overline{ERR_{pre}} + \bar{d}$$

$$\overline{ERR_{post}} = \bar{y} = \begin{bmatrix} 0.0120 \\ 0.0145 \\ 0.0167 \\ 0 \\ 0 \\ 0.0014 \\ 0.0013 \\ 0.0004 \\ 0.0021 \end{bmatrix} \overline{ERR_{pre}}^{2} + \begin{bmatrix} -0.918 \\ -1.0510 \\ -1.0980 \\ 0 \\ 0 \\ -0.4420 \\ -0.3720 \\ -0.3720 \\ -0.4350 \end{bmatrix} \overline{ERR_{pre}} + \begin{bmatrix} 29.376 \\ 30.559 \\ 30.582 \\ 0 \\ 0 \\ 23.4560 \\ 26.5390 \\ 28.2000 \\ 26.9690 \end{bmatrix}$$

$\overline{ERR_{post}}$	= Post-implementation ERR vector	[-]
$\overline{ERR_{pre}}$	= Pre-implementation ERR vector	[-]
$\bar{C}$	= Gradient vector	[-]
$\bar{d}$	=Constants vector	[-]

Q.5 Calculation of guidance regression lines

Table 28 displays the data tables which is used to create the guidance regression lines.

Table 28 - Guidance regression data tables

SFA Lower

	Slope								
	Z1	Z2	Z3	Z4	Z5	Z6	Z7	Z8	Z9
M_weights	0.761198	0.744316	0.797167	1.188653	0.466347	0.591512	0.656261	0.656945	0.69563
	Intercept								
	Z1	Z2	Z3	Z4	Z5	Z6	Z7	Z8	Z9
C_Constants	15.487	16.588	13.97	0	0	19.274	22.78	22.75	19.48

SFA Upper

	Slope								
	Z1	Z2	Z3	Z4	Z5	Z6	Z7	Z8	Z9
M_weights	0.761198	0.744316	0.797167	1.188653	0.466347	0.591512	0.656261	0.656945	0.69563
	Intercept								
	Z1	Z2	Z3	Z4	Z5	Z6	Z7	Z8	Z9
C_Constants	24.98	28.877	25.15	0	0	31.01	31.01	34.52	28.3
SFA Bandwidth	Z1	Z2	Z3	Z4	Z5	Z6	Z7	Z8	Z9
	9.493	12.289	11.18	0	0	11.736	8.23	11.77	8.82

COLS Lower

	Slope								
	Z1	**Z2**	**Z3**	**Z4**	**Z5**	**Z6**	**Z7**	**Z8**	**Z9**
M_weights	0.761198	0.744316	0.797167	1.188653	0.466347	0.591512	0.656261	0.656945	0.69563
	Intercept								
	Z1	**Z2**	**Z3**	**Z4**	**Z5**	**Z6**	**Z7**	**Z8**	**Z9**
C_Constants	10	12	9	0	0	12	17.4	16.6	13

COLS Upper

Slope

	Z1	Z2	Z3	Z4	Z5	Z6	Z7	Z8	Z9
M_weights	0.7611	0.7443	0.7971	1.1886	0.4663	0.5915	0.6562	0.6569	0.695

Intercept

	Z1	Z2	Z3	Z4	Z5	Z6	Z7	Z8	Z9
C_Constants	38	39	38	0	0	36	38.5	37	36
COLS Bandwidth	Z1	Z2	Z3	Z4	Z5	Z6	Z7	Z8	Z9
	28	27	29	0	0	24	21.1	20.4	23

APPENDIX R: CASE STUDY #1 BASELINE REPORT

ESCo Company

5.2 BASELINE POWER DEMAND VALUES

The actual baseline half-hourly values in kW are shown in Table 5, Table 6 and Table 7 below.

Table 5: Baseline data – Normal periods

Time	Weekdays	Saturdays	Sundays	Time	Weekdays	Saturdays	Sundays
00:30	16957	17095	15581	12:30	22012	20418	11844
01:00	16929	16986	14173	13:00	21556	19593	11837
01:30	16865	16897	13911	13:30	20525	18634	11863
02:00	16835	16745	13861	14:00	18497	17414	11776
02:30	16532	16670	13854	14:30	16839	16343	11798
03:00	16301	16574	13878	15:00	16039	16225	11843
03:30	16129	16568	13879	15:30	16199	16693	11899
04:00	16066	16632	13891	16:00	16278	16700	11875
04:30	16065	16666	13955	16:30	16004	16472	11845
05:00	16509	17239	14070	17:00	15286	15375	12216
05:30	16550	17234	14175	17:30	14775	14533	12729
06:00	16997	17805	14397	18:00	14884	14440	12925
06:30	18692	18590	13226	18:30	15817	14635	13088
07:00	20488	19322	12600	19:00	16875	16171	13255
07:30	21703	20140	12539	19:30	16907	16618	13405
08:00	22628	20842	12094	20:00	16894	16568	13537
08:30	23533	21774	11785	20:30	17012	16567	13678
09:00	24031	21874	11565	21:00	17065	16569	13773
09:30	24322	21926	11907	21:30	17042	16570	15294
10:00	24549	21948	11989	22:00	16975	16424	16077
10:30	24365	21894	11937	22:30	16896	16564	15976
11:00	23940	21501	11859	23:00	16881	16653	16084
11:30	23202	21201	12113	23:30	16849	16702	16446
12:00	22475	20901	11981	00:00	16742	16596	15985

Figure 89 - Case study #1 baseline data determined by ESCo

APPENDIX S: CASE STUDY #1 RING SIMULATION LAYOUT

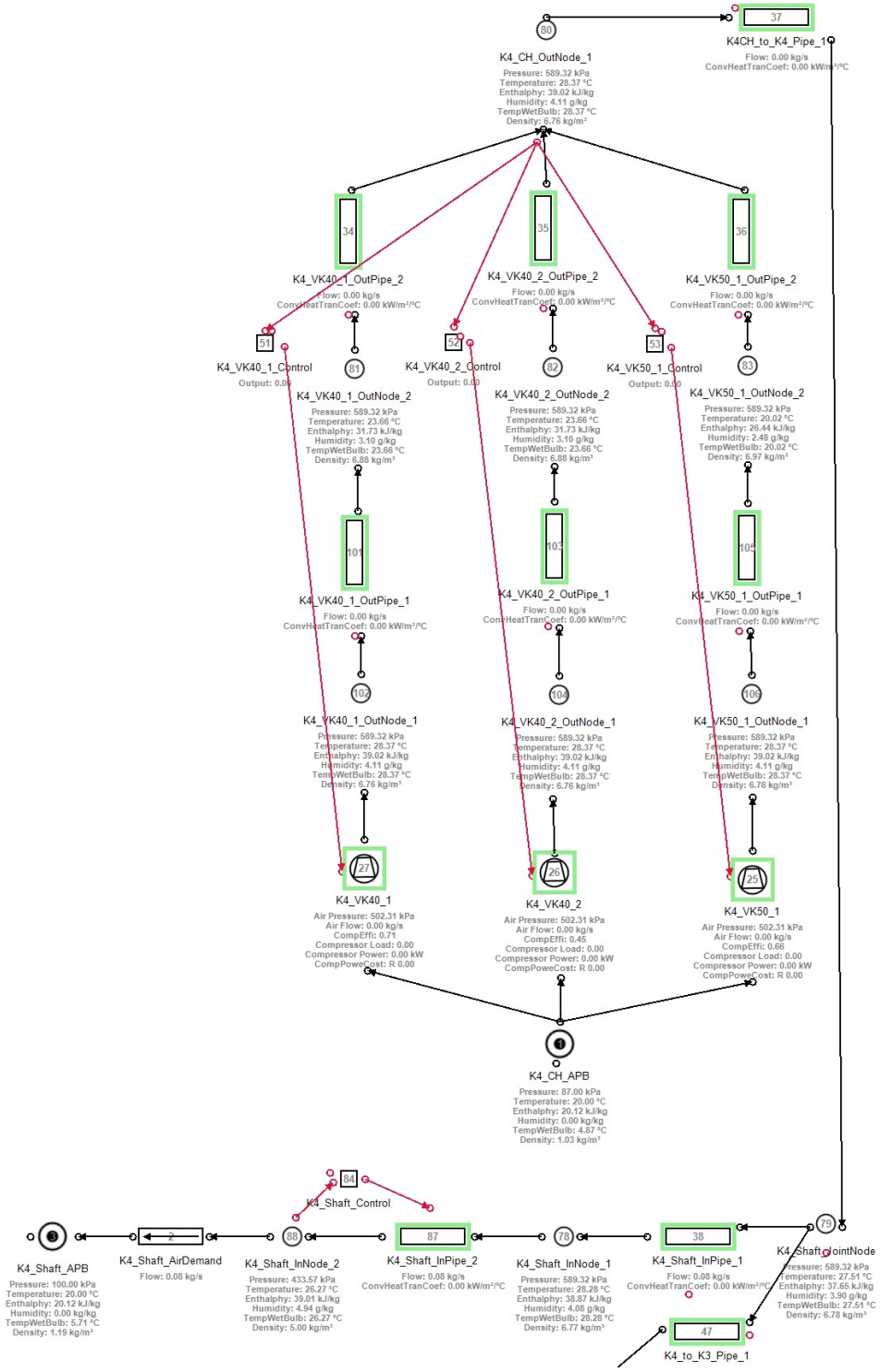

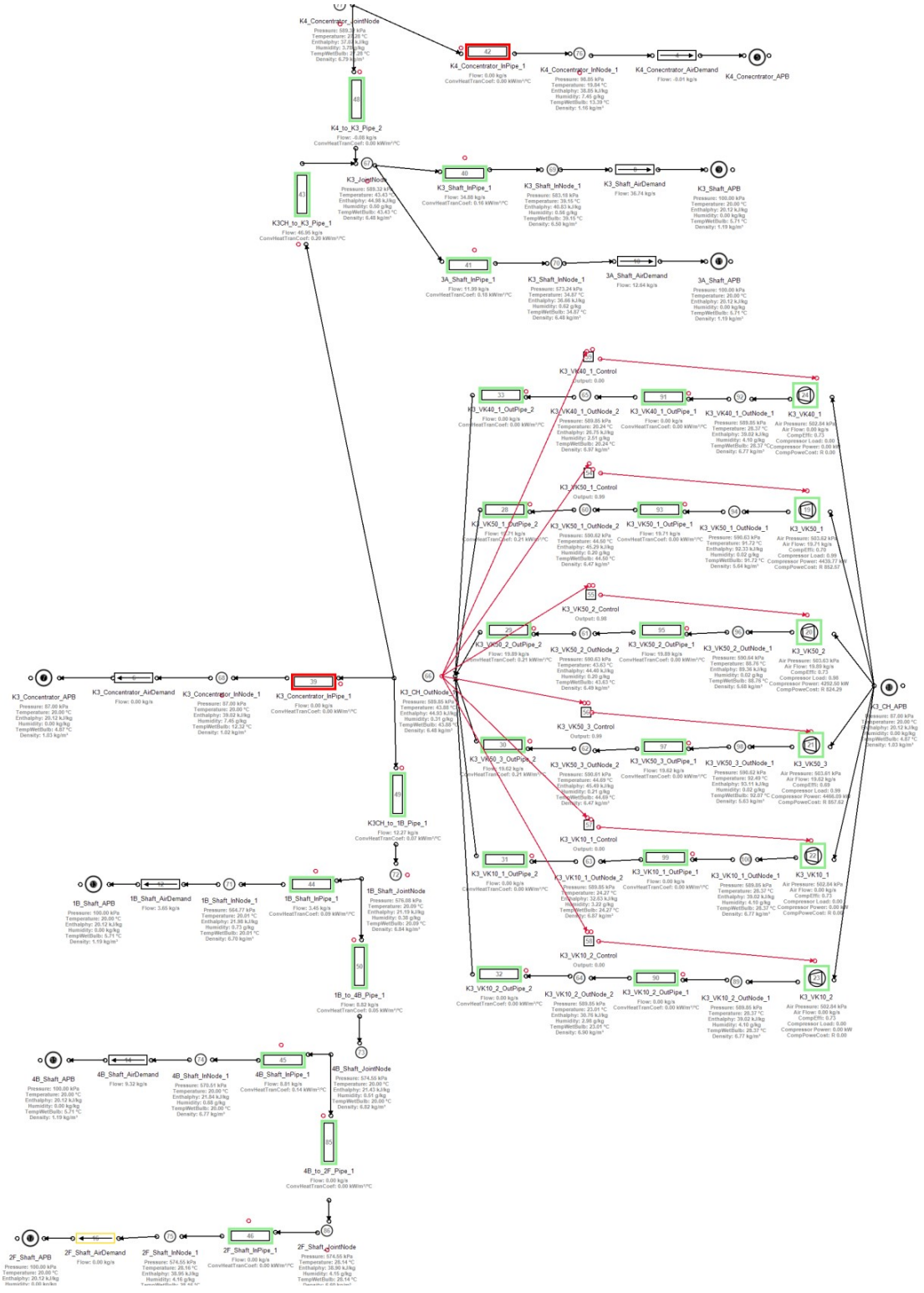

Figure 90 - Case study #1 compressed air simulation

APPENDIX T: CASE STUDY #2 BASELINE REPORT

Table 29 - Case Study #2 baseline as determined by ESCo

Whole year except Dec-Jan

Time	Weekdays	Saturdays	Sundays	*Time*	Weekdays	Saturdays	Sundays
0:30	9735	8895	7966	***12:30***	16081	11617	6118
1:00	9791	8593	7888	***13:00***	14594	11371	6035
1:30	9753	8560	7914	***13:30***	13298	11292	5993
2:00	9764	8558	8056	***14:00***	11626	10888	5937
2:30	9578	8554	8096	***14:30***	10328	10684	6033
3:00	9435	8520	8101	***15:00***	9135	10162	6196
3:30	9297	8520	8153	***15:30***	8443	9818	6399
4:00	9373	8449	8169	***16:00***	8231	9568	6677
4:30	9322	8532	8143	***16:30***	7311	9561	6722
5:00	9687	8686	8224	***17:00***	7227	9109	6762
5:30	10198	8770	8127	***17:30***	7102	8978	6695
6:00	10555	9469	8034	***18:00***	7176	8870	6805
6:30	10946	10050	8025	***18:30***	7200	8411	7529
7:00	11538	10840	7796	***19:00***	7616	7227	8340
7:30	11935	11569	7341	***19:30***	8282	7486	8917
8:00	12065	12974	6817	***20:00***	8803	7821	8542
8:30	12734	14284	6361	***20:30***	8951	8066	9048
9:00	14972	14484	6328	***21:00***	9228	8023	8836
9:30	16130	14415	6513	***21:30***	9401	8053	9080
10:00	16599	14334	6415	***22:00***	9571	7949	9170
10:30	16762	14176	6305	***22:30***	9513	7913	9260
11:00	16923	13785	6162	***23:00***	9693	8172	9724
11:30	16805	13018	6215	***23:30***	9629	7961	9823
12:00	16754	12445	6267	***0:00***	9740	7831	9857

APPENDIX U: CASE STUDY #2 RING SIMULATION LAYOUT

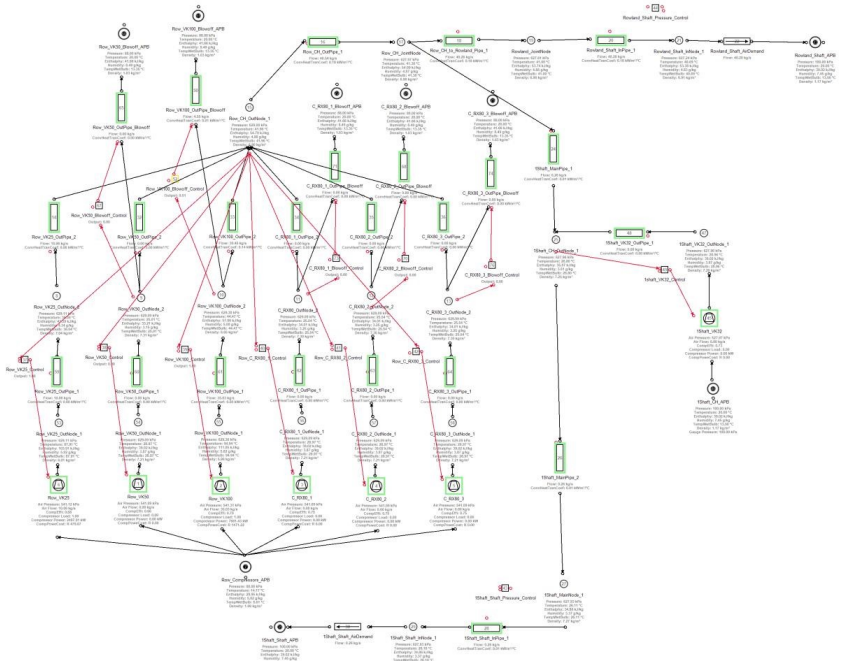

Figure 91 - Case study #2 compressed air simulation layout